FUSION TECHNOLOGY

Annual Report of the Association EURATOM/CEA 2001

Compiled by : Ph. MAGAUD and F. Le VAGUERES

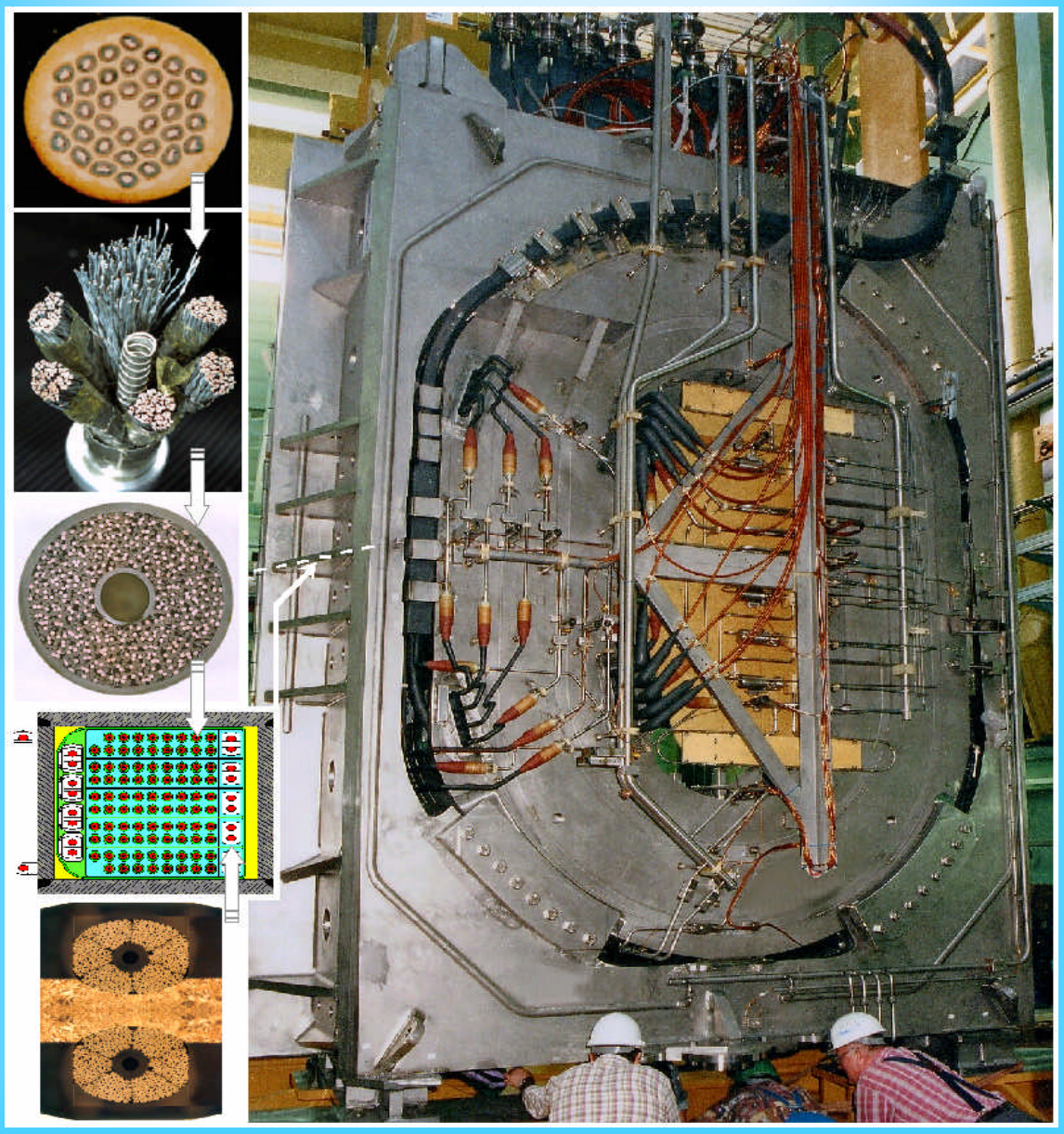

ASSOCIATION EURATOM/CEA
DSM/DRFC
CEA/CADARACHE
13108 Saint-Paul-Lez-Durance (France)

FUSION TECHNOLOGY

Annual Report of the Association CEA/EURATOM

2001

Compiled by : Ph. MAGAUD and F. LE VAGUERES

ASSOCIATION CEA/EURATOM
DSM/DRFC
CEA CADARACHE
13108 Saint-Paul-Lez-Durance (France)

Tél. : 33 - 4 42 25 46 59
Fax : 33 - 4 42 25 64 21
e-mail : dirdrfc@drfc.cad.cea.fr
Web : http://www-fusion-magnetique.cea.fr

This report is also available on-line at : http://www-fusion-magnetique.cea.fr

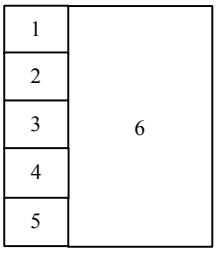

Cover : Toroidal Field Model Coil (TFMC) installation and test
1 – Superconducting strand (courtesy of ENEA)
2&3 – Superconducting conductor (courtesy of ENEA)
4 – Cross section of the TMFC
5 – Superconducting joint
6 – TFMC at FZK (courtesy of FZK)

CONTENTS

Vessel/Blanket

Remote Handling

Magnet Structure

Cryoplant

Magnets

Tritium Breeding and Materials

Breeding Blanket

Water Cooled Lithium Lead (WCLL) Blanket

Helium Cooled Pebble Bed (HCPB) Blanket

Structural materials development

Advanced materials

Reduced Activation Ferritic Martensitic (RAFM) steels

Socio-economic studies

JET Technology

UNDERLYING TECHNOLOGY PROGRAMME 349

Physics Integration

Diagnostics

Vessel/In Vessel

Plasma Facing Components

Remote Handling

Tritium Breeding and Materials

Breeding Blanket

Materials development

Structural materials

Fuel cycle

Safety and Environment

System studies

Task Title : TEST BLANKET MODULE - ADAPTATION TO NEXT STEP MACHINE

INTRODUCTION

The water-cooled lithium-lead (WCLL) DEMO blanket [1] is one of the two European blanket lines to be further developed with the aim, in the short term, of manufacturing a DEMO blanket mock-up, named the Test Blanket Module (TBM), to be tested in ITER-FEAT. This line is based on the principles of using the well-established PWR-technology for the power conversion cycle (water coolant at 15.5 MPa, outlet temperature 325°C) and of slowly circulating the liquid Pb-17Li for extracting the tritium outside the reactor.

The WCLL TBM, whose main body is quite similar to the equatorial part of an inboard segment of the corresponding DEMO blanket, is expected to use all technologies required for that concept: martensitic steel as structural material, liquid Pb-17Li as breeder and neutron multiplier, and light water at typical PWR conditions as coolant.

The evolution of the ITER-FEAT specifications [2] with respect to ITER-FDR [3] in terms of neutron wall loading, heat flux, dimension of test ports, space availability for ancillary circuits, and safety have led to various design evolutions of the WCLL TBM System. Conceptual studies were aimed at demonstrating that ITER-FEAT requirements for TBM and DEMO relevant testing conditions can be simultaneously met with a unique reference WCLL TBM design by properly adjusting the thermal-hydraulic conditions in the two separate cooling systems. A preliminary WCLL TBM fabrication sequence had already been established in 2000 [4] but had to be revised in 2001 according to the latest dimensional requirements in ITER and R&D results.

2001 ACTIVITIES

The WCLL TBM (figures 1 & 2) is essentially formed by a directly cooled steel box having the function of Pb-17Li container and by a double-walled C-shaped tube-bundle, immersed in the liquid metal, in which the water coolant circulates.

The module box is reinforced by radial and toroidal stiffeners to whistand the disruption-induced forces and the full water pressure under faulted conditions. Two independent water-coolant circuits are present, one cooling the module box and one cooling the breeder region.

The Pb-17Li circuit conveys the Pb-17Li to the detritiation unit outside the Test Blanket Module. The main characteristics of the WCLL TBM are reported in Table 1.

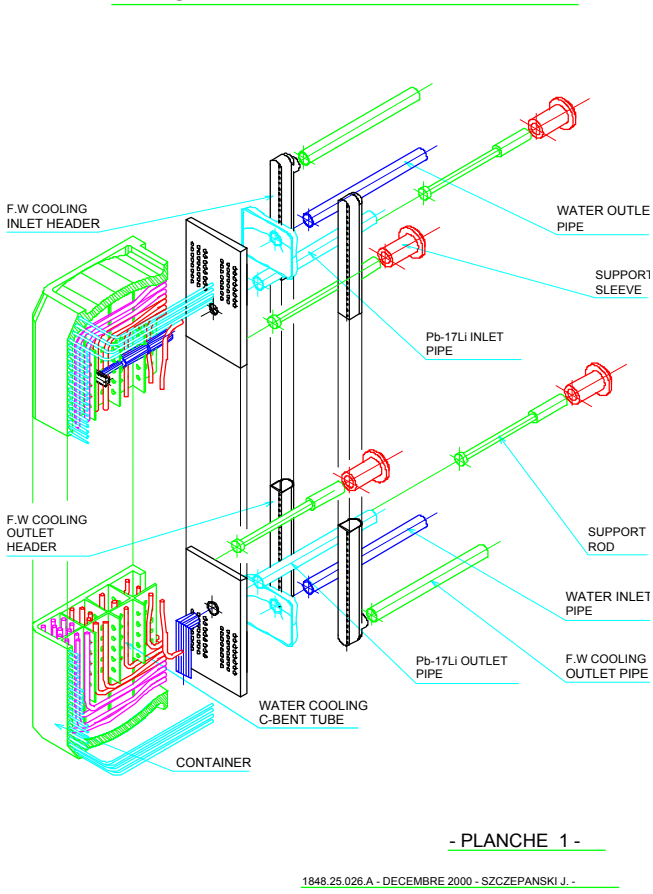

Figure 1 : Exploded 3d view of the WCLL TBM

Table 1 : Main characteristics of the EU WCLL-TBM to be tested in ITER-FEAT (HF = 0.25 MW/m^2, NWL = 1.1 MW/m^2)

Dimensions	1.72 m high x 0.514 m wide x 0.585 m deep
Mass in operation	Be 8.75 kg, steel 950 kg, water 60 kg, Pb-17Li 3385 kg, total 4404 kg
Deposited power in the whole TBM	1.07 MW (assuming 0.25 MW/m^2 surface heat flux and 1.1 MW/m^2 neutron wall loading)
Tritium production	36 mg/day (22 % duty cycle, 90% ^{6}Li enrichment; 1.1 MW/m^2 NWL)
Breeder zone water cooling circuit	Pressure 15.5 MPa, inlet/outlet temperatures 315/325 °C, mass flow rate 7.8 kg/s, extracted power 0.48 MW, number of cooling tubes 35
Segment box water cooling circuit	Pressure 15.5 MPa, inlet/outlet temperatures 303/325 °C, mass flow rate 4.4 kg/s, extracted power 0.58 MW, number of cooling tubes 65
Maximum temperatures	Pb-17Li/steel interface 450°C, Be armor 458 °C, FW steel 449 °C, Pb-17Li 459°C
Maximum stress levels	FW steel 290 MPa

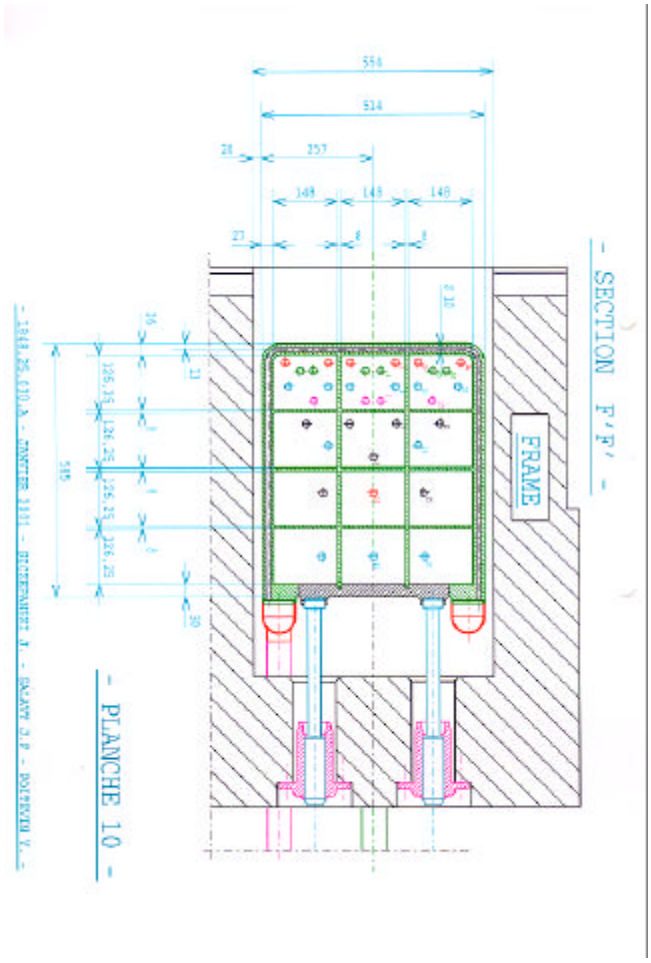

Figure 2 : Equatorial section of the WCLL TBM for ITER-FEAT

Conceptual studies have shown (Table 2) that, under the range of the foreseen heat flux and neutron wall loading in ITER-FEAT, relevant testing conditions could be reached with a unique reference TBM design by properly adjusting the water cooling conditions in the breeder zone and segment box. So, it is intended to use the same WCLL TBM in place from the first day of ITER operation until the end of the BPP.

The only exceptions are however:

i) long maintenance periods in which the TBM might be removed from the VV if required;

ii) the insertion for a limited duration of a specifically instrumented TBM for neutronic measurements,

iii) in case of TBM failure where the TBM has to be removed and replaced; and

iv) if a newly developed preferred technology has to be tested.

Assuming a 90% ^{6}Li enrichment and a 22% duty cycle in ITER (400 s burn, 1400 s dwell), the expected TBM tritium production per day of pulsed full power has been evaluated to 26 mg/day at 0.8 MW/m^2 neutron wall loading (respectively 36 mg/day at 1.1 MW/m^2).

Table 2 : WCLL TBM thermal-mechanical performances in operating conditions

	Most-likely ITER operation value	Nominal design value
Neutron Wall Loading [MW/m^2]	0.8	1.1
Heat Flux [MW/m^2]	0.1	0.25
Segment Box Tmax/Tmin [°C]	409/324	449/324
Breeder Zone Tmax/Tmin [°C]	428/331	459/333
PbLi/DWT interface Tmax/Tmin [°C]	418/333	450/335
Max stress level (von Mises) in Segment Box [MPa]	220	290

Due to the reduced space available in the ITER test port area, the cooling water systems are located in the Tokamak Cooling Water System Vault where a limited space has been allocated for both water loops (figure 3).

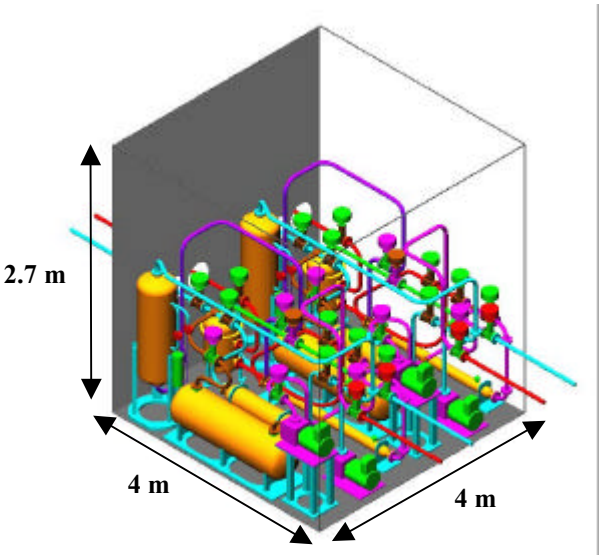

Figure 3 : Layout of the two water-cooling loops inside the TCWS vault

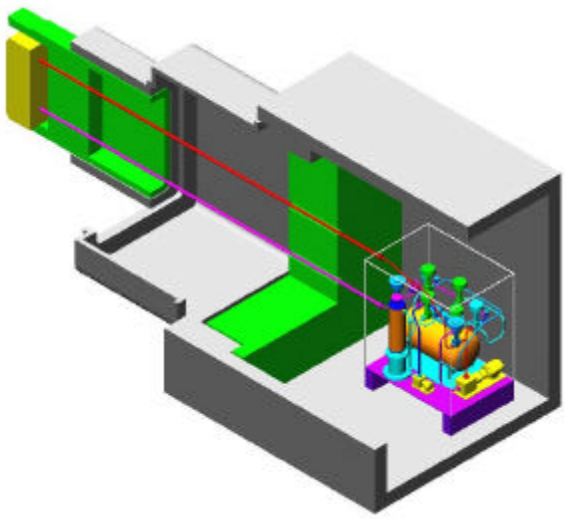

Figure 4 : ITER equatorial port layout showing location of the EU Pb-17Li loop behind the Bioshield Plug

The components of the water loops have been designed and the overall dimensions fit into the ITER space requirement. The Pb-17Li ancillary loop has to be placed in the test port area (Figure 4), as close as possible from the TBM, in order to reduce the tritium permeation along pipework, keeping a measurable concentration in the tritium extraction system. A LOCA in the TBM causes the interaction of the cooling water with the Pb-17Li. The determination of the induced heat and hydrogen generation is currently being investigated within the ongoing EU R&D program. Previous experiments indicate a self-limiting reaction. However, due to the remaining uncertainties in quantifying this effect, the maximum envelope value for reaction enthalpy and hydrogen production are evaluated considering a hypothetically complete reaction of the entire TBM Pb-17Li inventory (0.36 m^3) with water.

The resulting H_2 and enthalpy releases are estimated as 3.3 kg and 727 MJ, respectively. In order to meet the ITER requirement of 2.5 kg H_2 release from TBM, it is proposed to limit the Pb-17Li volume in the TBM to 0.28 m^3. This could be achieved by reducing the depth of the WCLL TBM - and consequently the Pb-17Li inventory – by 25% (the last 25 % of the rear part of the breeder zone contribute to only 6% of the total TBM tritium production). This reduction of Pb-17Li inventory has not been considered in the present TBM design since significant experimental and analytical R&D is underway in the EU to collect more realistic data on Pb-17Li interaction.

In case of In-TBM LOCA, the TBM segment box is subject to 15.5 MPa pressurization, at least for short periods of time.

This situation has been re-examined with the updated TBM design and it has been demonstrated that only a minor design modification (increase of the radii of the steel box) was necessary to guarantee the box integrity with regard to IISDC criteria.

The corresponding maximum von Mises stress level in the segment box is around 400 MPa, ensuring thus a margin of 10 MPa with regard to IISDC criteria (0.7 Rm).

A preliminary WCLL TBM fabrication sequence had already been established [4] but had to be revised according to the latest dimensional requirements in ITER and R&D results. In particular, the fabrication of the TBM segment box cooling system was previously based on the use of powder HIPing. But, recent R&D results have shown that the use of a mixed powder/solid HIPing process may lead to better results in term of positioning and dimensional changes of the tubes. Furthermore, cost consideration about the previous fabrication sequence described in [4] (especially machining of the segment box structure from a large Eurofer steel block) led to explore less costly options which are considered in this study.

The fabrication sequence of the WCLL TBM, as defined in this 2001 task, constitutes the reference solution compatible with the latest design option and R&D results.

CONCLUSION

Considering the specifications of ITER-FEAT, thermo-mechanical analyses of the WCLL Test Blanket Module have shown that, despite the lower heat flux and neutron wall loading in ITER-FEAT, temperature and stress levels relevant to those of DEMO, and tritium permeation tests could be achieved considering minor modifications of the design and by properly adjusting the cooling conditions.

In order to ensure as correctly as possible the determination of the complete T balance, the Pb-17Li ancillary circuit has been located as close as possible to the TBM, behind the bioshield plug.

It has been designed in an integrated leak-tight housing taking into account space and remote handling constraints of the ITER machine. The two coolant circuits have been designed to fit properly in the allocated space in the TCWS vault.

The overall test program of the WCLL TBM has been re-evaluated. It has been shown in particular that a single WCLL TBM design could be considered for all phases of ITER-FEAT operation and test runs considering a proper adjustment of cooling conditions and adapted instrumentation. The same TBM design will be specifically instrumented according to the envisaged test sequence.

REFERENCES

[1] L. Giancarli et al., Development of the EU water-cooled Pb-17Li blanket, Fusion Eng. and Design 39-40 (1998) 639-644.

[2] S. Booth, Minutes of the 7th meeting of the Test Blanket Working Group, ITER JWS Garching, February 22-23, 2000.

[3] M. Fütterer et al., Design Description Document (DDD) for the European Water-cooled Pb-17Li Test Blanket Module, in ITER Final Design Report, DDD 5.6.C (1997).

[4] M. Fütterer et al., Design modifications of the WCLL Test Blanket Module for ITER: Reduction of header space, CEA internal report, SERMA/RT/00-2761/A (2000).

REPORTS

Y. Poitevin et al., « Status of the design and testing programme of the WCLL Test Blanket Module for ITER-FEAT », CEA internal report SERMA/RT/01-3019/A, December 2001.

Y. Poitevin et al., « Fabrication sequence of the WCLL Test Blanket Module for ITER-FEAT », CEA internal report SERMA/RT/01-3020/A, January 2002.

Y. Poitevin et al., "WCLL Blanket concept: synthesis of last R&D results and impact on the Test Blanket Module design", CEA internal report, SERMA/RT/02-3061, March 2002.

TASK LEADER

Yves POITEVIN

DEN/DM2S/SERMA
CEA Saclay
91191 Gif-sur-Yvette Cedex

Tél. : 33 1 69 08 31 86
Fax : 33 1 69 08 99 35

E-mail : ypoitevin@cea.fr

Task Title : TRITIUM BREEDING MODULE ADAPTATION TO NEXT STEP MACHINE
Adaptation of thermal-hydraulic performance to ITER specification

INTRODUCTION

Previous studies on a Water-Cooled Lithium-Lead (WCLL) heat exchanger were performed in nominal case in 2D dimension.

The objective of this activity is to determine the impact of an accidental case when the cooling mass-flow rate of water inside the tubes has a very low value (10 times less). Unstationary calculations were performed in 3D, taking into account the boiling phenomenon and the pressure drop (frictional and singular) inside the cooling tubes.

2001 ACTIVITIES

We have considered a Lithium-Lead block (0.529 m large, 0.46 long and 1.664 m height) cooled with 35 U tubes. The height is divided in 4 meshes; the width and the length are, respectively, divided in 62 and 38 meshes. Each tube has a specific length.

The coolant water is flowing inside (7.8 kg/s in nominal case) with an inlet temperature of 300°C.

We considered both frictional and singular pressure drop inside the tubes.

We used a specific heat deposition profile in the Li-17Pb, due to neutron deposition. An adiabatic condition is imposed to the six sides of the Pb-17Li block.

We have to complete this work by taking more realistic boundary conditions (cooling effect due to the First Wall heat exchanger).

The thermal conduction phenomenon in the tube leads to a constant heat transfer coefficient (5455 $W/m^2/K$).

Inside the tubes, the Dittus-Boelter heat transfer coefficient is used in the pure liquid zone.

We considered a sub-cooled boiling zone and a bubbly zone by using the Jens-Lottes heat transfer coefficient.

Treating the two-phase flow as an equivalent single-phase flow, the frictional contribution to the overall pressure gradient requires a determination of a friction factor and of a two-phase multiplier.

They are, respectively, determined from the Blasius correlation (for smooth tubes) and from the Cicchitti correlation.

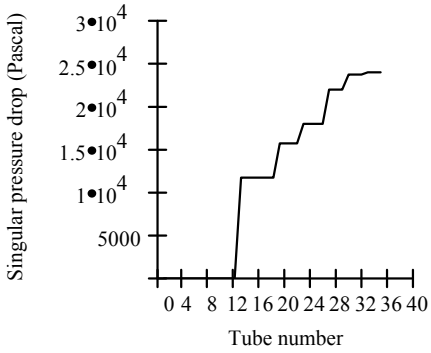

Figure 1 : Singular pressure drop inside each tube

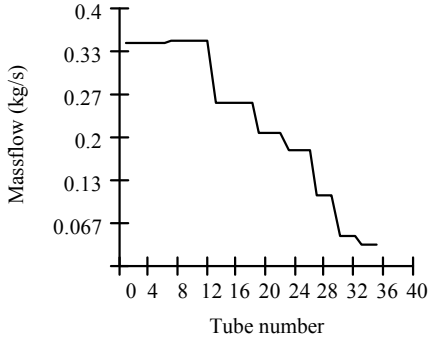

Figure 2 : Water mass flow-rate inside each tube

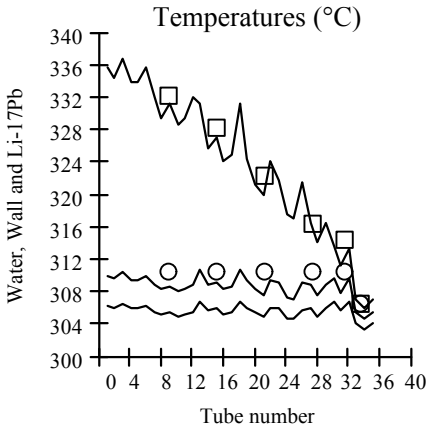

Figure 3 : Temperatures at z = 1.664 m for each tube location

CONCLUSIONS

NOMINAL CASE

We used a total cooling water mass flow-rate of 7.8 kg/s. From Figures 1 to 3 the following conclusions can be drawn:

- Figure 1 : We recommended to used specific singular pressure drop for each tubes. The total pressure drop is then 2.4 10^4 Pa.
- Figure 2 : The water mass-flow rate inside the tubes is the greater in the longer tubes (tubes 1 to 12) and reach 0.33 kg/s than in the shorter tubes (tubes 29 to 35).
- Figure 3 : Consequently the exit water temperature is in a narrow range, between 306 and 308 °C (continuous line with no symbol). Circles and squares note the wall and Li-17Pb temperature respectively.

Like this :

- The power extract from the tubes is in the range 10 kW (tube 1) to 0.8 kW (tube 35).
- The heat transfer coefficient in liquid phase (Dittus-Boelter correlation) inside the tubes is in the range 3.7 10^4 W/m^2/K (at great mass flow-rates) and 0.67 10^4 W/m^2/K (at low mass flow-rates).

ACCIDENTAL CASE

We used a total cooling water mass flow-rate (0.78 kg/s) 10 times smaller than in the nominal case. Thus the total pressure drop inside de cooling tubes is very low (381.8 Pa). The tube number history of the water mass flow-rate is the same as on figure 2. We focus our attention on the tube number 1. The heat flux along this tube is constant (1.4 10^5 W/m^2). From Figures 4 to 6 the following conclusions can be drawn:

- Figure 4 : The subcooled boiling zone begin at 0.7 m approximately. The temperature of the wall (noted with circles) reaches T_{sat}+D_{tsat}, namely 346.5 °C. The bubbly zone appears at 1.7 m where the bulk temperature of the water reaches T_{sat} (345 °C). Squares note the Li-17Pb temperature.
- Figure 5 : The water quality increase from –0.3 to 0.05.
- Figure 6 : The water heat transfer coefficient increase continuously from 6 10^3 W/m^2/K (in pure liquid zone) to 10^5 W/m^2/K (in bubbly zone)

Taking into account the First Wall heat exchanger (to better estimate the temperature, especially in the Li-17Pb) must complete these results on WCLL behaviour.

REPORTS AND PUBLICATIONS

[1] G. AVAKIAN - Modélisation d'un échangeur Eau/Li-17Pb en situation normale et accidentelle - Modelling of a heat exchanger Water/Li-17Pb in normal and accidental situation - CEA report DER/DTP/STH/ LTA/2001-30 - December 2001.

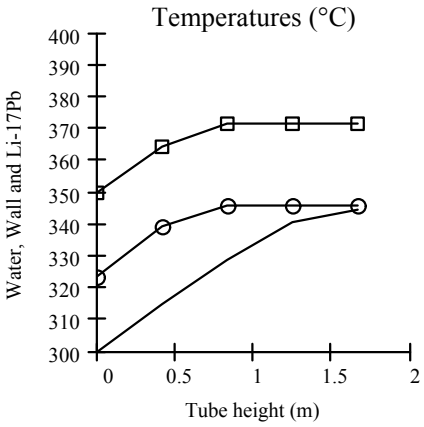

Figure 4 : Temperatures along tube 1

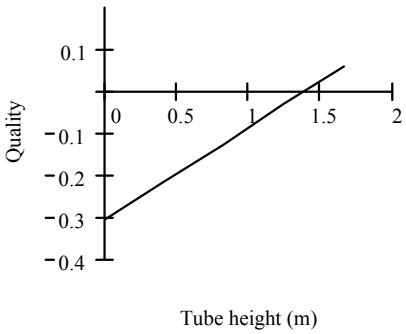

Figure 5 : Quality along tube 1

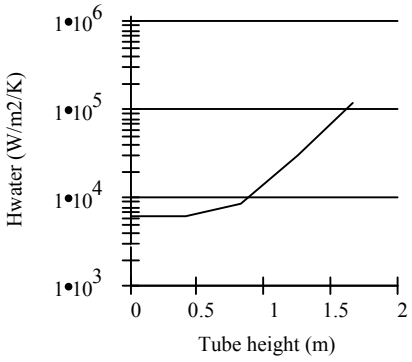

Figure 6 : Water Heat transfer coefficient along tube 1

TASK LEADER

G. AVAKIAN

DEN/DTP/STH/LTA
CEA Cadarache
13108 St Paul Lez Durance Cedex

Tél. : 33 4 42 25 75 12
Fax : 33 4 42 25 77 67

E-mail : gilles.avakian@cea.fr

Task Title : BLANKET MANUFACTURING TECHNIQUES
Definition of specification of a demonstrator

INTRODUCTION

The International Thermonuclear Experimental Reactor in its reviewed version, ITER-FEAT (Fusion Energy Advanced Tokamak), is currently foreseen to be the only intermediate step towards a fusion power reactor [1, 2]. Apart from plasma studies and component testing, the ITER-FEAT shall be used as a test bed for test modules (TBM, Test Blanket Module) of different tritium breeding blankets for which various conceptual design are under developments in view of a fusion power plant. The Water Cooled Lithium Lead (WCLL) [3] is one of the breeding blanket concepts chosen to be tested in ITER.

The analysis of the WCLL project schedule up to ITER-FEAT operation (2015) has shown that future activities has to meet key milestones such as fabrication and pre-testing of a large-scale TBM mock-up (last step before TBM fabrication) around 2006 and TBM design freezing around 2007 [4]. These milestones could be met only if some technical issues are achieved at the end of the 2001-02 period. In this frame, the objective of this task was reoriented in order to provide to the fabrication team a support for definition of mock-ups/demonstrators and to ensure strong consistency between design and fabrication activities and minimize risk of unsuccessful R&D or significant delays.

2001 ACTIVITIES

2001 activities focused on reference all TBM components and provide a standard interface between design and fabrication, which should allow a better consistency between the two teams work. Furthermore, the real thermal operating conditions of the breeder zone (BZ) tubes in a FPR have been furnished to the fabrication team in order to better define the conditions in which crack tests on double walled tubes (DWTs) should be performed.

REFERENCE OF THE COMPONENTS & GEOMETRICAL SPECIFICATIONS

In collaboration both with the design and the fabrication team a standard interface has been defined which should allow a better consistency between the two teams work. A table was compiled, which summarizes all TBM components. Each component is referenced both in the table and in the drawings (for example figure 1) with an item number and a letter describing its last version.

In case of a component modification both the table and the corresponding drawings will be updated, so guarantying as well as possible, the coherence between the design and fabrication activities.

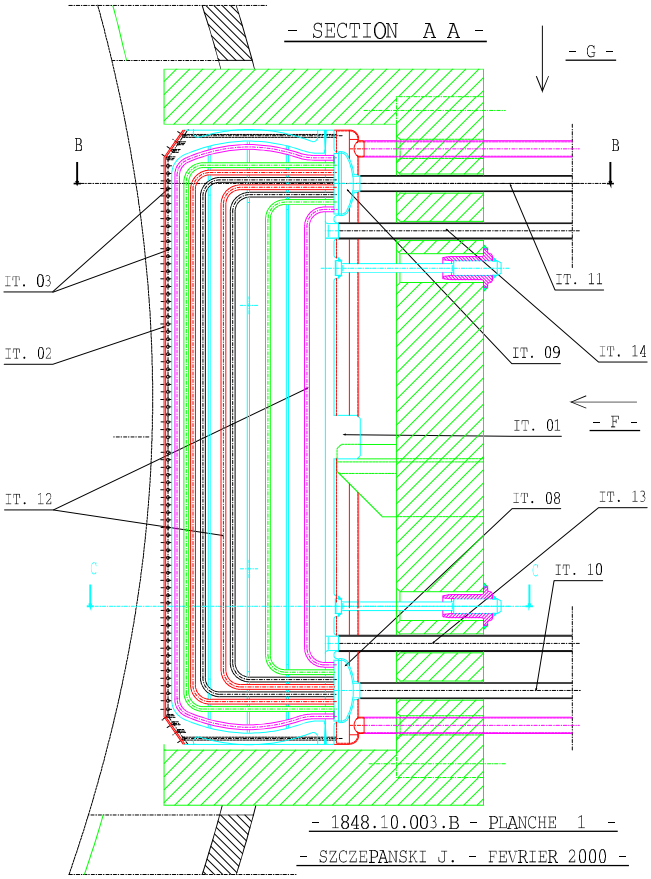

Figure 1 : 2D view of the WCLL-TBM, detail of the items number

Furthermore, a recapitulating table (Tab. 1) highlights TBM critical elements whether in the design and in the fabrication, constituting a guideline for the definition of the different mock-ups and demonstrators needs and planning.

For each component, referenced with its item number, the material, the geometry, the principal constraints and tolerances as well as the envisaged fabrication difficulties or drawbacks are specified.

SUPPORT TO DWT CRACK PROPAGATION TESTS IN BENT REGIONS

Crack propagation test on double walled tubes should be carried out in conditions as similar as possible to those foreseen in the TBM.

Table 1 : Recapitulating table with main items specifications

ITEM	Component	Specifications
1	SB	Eurofer box, external dimensions (r × t × z): (585×554×1720) FW thickness 21 mm; SW thickness 27 mm; corner radius between FW and SW at tube axis 52 mm; corner thickness between 21 and 27 mm. Cooling holes Ø 10, pitch 26 mm. FW ending with a cooled inclined part, height 94 mm, angle 35° (in this region the tubes pitch could be lower than 26 mm). Distance between tube axis and external wall of the SW 14 mm (13 mm) in order to allow the attachment of the SB manifold.
2	Top/bottom caps	Eurofer. Thickness 40 mm. Rounded shape welded to SB.
3	SB Tubes	Eurofer. Cu layer in order to guarantee double confinement between water and Pb-17Li. $Ø_{int/ext}$ 8/10 mm. N_{tubes} = 65.
4	Back plate	Eurofer. Thickness 30 mm. Holes for FW tubes and BZ tubes. Holes for Pb-17Li feed and drain. Attachments to the frame to be defined.
5	SB manifold	Eurofer. Semi-cylinders dimensions depth 32 mm +R_{int} 71 mm, poloidal length 1720 mm. Thickness 4 mm. Welded to BP.
6	BZ stiffeners	Thickness 8 mm, drilled. Welded to SB and between them to form rectangular channels, dimensions: (126.25 × 148 mm).
7	BZ tubes	Eurofer. Double walled tubes $Ø_{int/ext}$ 11/13.4; 13.6/16.5. Tolerance on inner radius ±15%. Tolerance on location ± 2 mm. Cu layer between tubes to stop creaks. 1 spacer grid in the middle plane of the TBM. C shape with two 90° angles. 3D bending in the top and in the bottom (only for the first line of tubes, near the plasma). Welded on BP, minimum pitch 8.5 mm ⇒ θ_{max}[1] = 5.3° (welds have to guarantee double confinement between water and Pb-17Li).
8	BZ cooling headers	Eurofer, external dimensions (56 × 320 × 189). Thickness 5 mm. Inlet outlet pipe $Ø_{int/ext}$ 50/56 mm.
9	Pb-17Li Supply	Tube $Ø_{int/ext}$ 50/56 mm, thickness 3 mm. Distribution system for inlet tube. Outlet tube plunges down in the Pb-17Li.

The thermal conditions (minimum and maximum temperature along the tube) provided to the fabrication team are relevant to the improved WCLL blanket module for a fusion power reactor [5]. These data, obtained with the hypotheses assumed for the Power Plant Availability study, are more conservative because of temperatures and gradients on the tube are higher than those foreseen for the TBM.

SPECIFICATIONS ON BZ TUBES

Number and location of the BZ DWTs in the TBM were chosen in order to minimize their number and uniform, as well as possible, the power extracted from each of them. As far as their diameters are concerned, the TBM tubes are identical to those of a generic DEMO-WCLL blanket module.

[1] Considering a minimum distance between tubes of 3 mm.

Previous experimental campaigns showed that some deformations could appear after fabrication.

An assessment has been carried out in order to evaluate the impact of these deformations on the TBM behaviour and to furnish to the fabrication team needed tolerances. Thermo-mechanical calculations have been performed on a model representative of the equatorial section, assuming the maximum peak surface heat flux (0.5 MWm^{-2}) and the maximum neutron wall load (1.1 MWm^{-2}). A uniform reduction of tubes diameters on the whole length of all tubes has been assumed. Furthermore, tubes have been displaced from their optimized location. Various configurations have been examined, the worst of which is shown in figure 2.

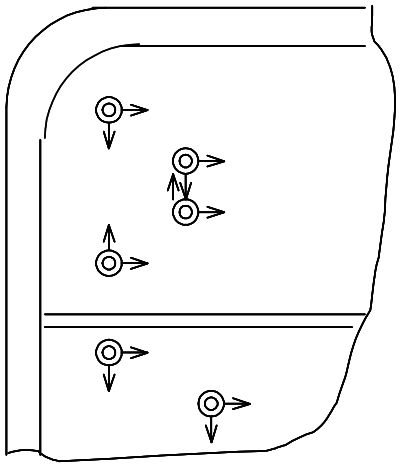

Figure 2 : Detail of the TBM equatorial section, with assumed displacements of the tubes from their nominal position.

In this case, the temperature reaches 537 °C in the steel (T_{lim} = 550 °C), 480 °C in the liquid metal and 471 °C at the interface between the Pb-17Li and the steel (T_{lim} = 480°C). The margin to subcooled boiling is 1 °C, which is low, but acceptable because of very conservative assumptions.

A reduction of 17% on tube cross section and a displacements of ± 2 mm for each tube can, thus, be tolerated. Further reduction in the tube section could produce the sub cooled-boiling in tubes nearest the plasma.

A further margin of 2% has been assumed to take into account the bent zone, leading to a tolerance of 15%, as reported in the table 1.

In the TBM design two tubes have estimated to be the most critical, because of their length and bending. The feasibility of these tubes (figure 3) with previous tolerances should be demonstrated.

WELDS

In the fabrication procedure, six typical weld operations have been identified, the feasibility of which will be checked in material program. Main issues have been pointed out, taking into account the required specifications.

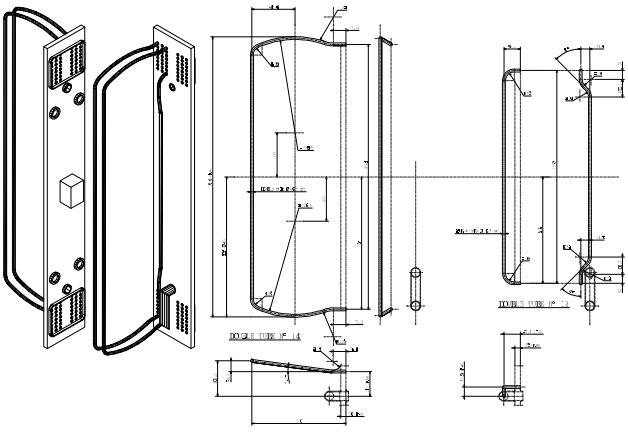

Figure 3 : 3d view and dimensions of two most critical BZ tubes

Case 1: weld between FW and radial stiffeners. Best solution seems to be the one shown in the figure whithwelding of two Eurofer plates of 8.

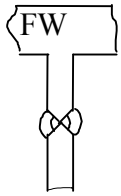

X toe is foreseen with double pass from both sides. Key ponts of this weld are the position and distance, main issues: the mechanical stresses and the accessibility (on one side almost). A solution could be an automatic procedure from one or both sides with automatic check. If well dimensioned, automatic procedure would be more safe.

Case 2: Cup on FW, Eurofer on Eurofer, 40 mm thickness.

Case 3: Tubes of the SB on the back (before HIP). Eurofer/Eurofer. Tubes pitch 26 mm, distance between tubes walls 16 mm.

Case 4: toroidal stiffeners to SWs and to radial stiffeners after positioning of the BZ tubes. This weld is similar to the one described for the case 1, but in this case only one side is accessible, that implies a different welding toe. (V, not X). Main issue of this weld are the deformation and residual stresses. Furthermore, attention must be paid to the tubes behind the weld which could be damaged during the process.

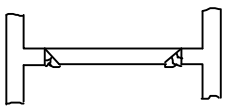

Case 5: Back plate. Eurofer on Eurofer, thickness 30 mm. Accessibility from one side.

Case 6: Stiffeners on BP. In this case, the procedure consists in positioning the stiffeners in grooves on BP and then welding for transparency (electron beam). Main issue is the small stiffener thickness.

Some priorities have been identified in the study, because of the feasibility of these welds could compromise the fabrication procedure.

Case n°1: it is the the most generic. Cumulating deformations could make changes to the foreseen fabrication sequence.

Case n° 6: the feasibility of which could call in question a BP in one block.

Case n° 3: pitch between tubes could not be enough for the bead.

CONCLUSIONS

The main objective of this task was to provide to the fabrication team a support for definition of mock-ups/demonstrators and to ensure strong consistency between design and fabrication activities and minimize risk of unsuccessful R&D or significant delays.

At this scope, a table has been compiled summarizing all TBM components, which will be updated, toghether with corresponding driwings in case of design modification. Furthermore, a recapitulating table (Tab. 1) highlights TBM critical elements whether in the design and in the fabrication, constituting a guideline for the definition of the different mock-ups and demonstrators needs and planning.

An assessment has been carried out in order to evaluate the impact of the deformations of the BZ tubes during the fabrication process on the TBM behaviour. Results showed that reduction of 15% on tube cross section and a displacements of ± 2 mm for each tube can be tolerated.

Typical welding procedures have been identified in the fabrication process the feasibility of which will be checked in material program. Some priorities have been identified in the study, because of the feasibility of these welds could compromise the fabrication procedure.

REFERENCES

[1] R. Aymar, ITER achievements by July 1998 and future prospects, Fus. Eng. Des. 46 (1999) 115-127.

[2] R. Aymar, The ITER Reduced Cost Design, Fus. Eng. Des. 49-50 (1999) 13-25.

[3] L. Giancarli et al., Development of the EU water-cooled Pb-17Li blanket, Fus. Eng. Des. 639 (1998) 39-40.

[4] Y. Poitevin et al., Proposal for a revised work programme for WCLL TTTBA-001 (Design) & -002 (Fabrication) for 2001-2002.

[5] A. Li Puma et al. Potential and limits of WCLL alternative blanket concepts, CEA Report, CEA Saclay, SERMA/LCA/RT/01-3026, September 2001.

REPORTS AND PUBLICATIONS

[1] Li Puma et al., WCLL test Blanket Module Demonstrator: development programme ans specifications, CEA Report, DM2S/SERMA/LCA/RT/01-3026/A (2001).

TASK LEADER

Antonella LI PUMA

DEN/DM2S/SERMA/LCA
CEA Saclay
91191 Gif-sur-Yvette Cedex

Tél. : 33 1 69 08 79 76
Fax : 33 1 69 08 99 35

E-mail : alipuma@cea.fr

TTBA-2.1

Task Title : BLANKET MANUFACTURING TECHNIQUES Definition of specifications for demonstrators

INTRODUCTION

The WCLL Blanket R&D programme foresees, within the following years, the manufacturing of a series of mock-ups which shall demonstrate and qualify the manufacturing technologies. The small-scale mock-ups – currently under development and testing - shall firstly demonstrate the feasibility of the manufacturing and the functionality of individual subcomponents like double-wall-tubes (DWT), first wall, etc. A medium-scale mock-up (called demonstrator) is then intended to demonstrate the ability to assembly subcomponents in a reproducible procedure which could be easily extrapolated to the final TBM prototype. After this demonstration, the manufacturing of a large-scale mock-up to be tested under typical WCLL conditions (out-of-tokamak) shall constitute the last step before the TBM design freezing and the manufacturing of the TBM prototype to be tested in ITER.

These mock-up activities are strongly related to the reference TBM design development and task TTBA-2.1 was aimed at analyzing the main design characteristics of the actual TBM reference design to serve as a basis for the future mock-ups.

2001 ACTIVITIES

TBM DESIGN EVOLUTION AND IMPACT ON DEMONSTRATORS

The 2000-2001 WCLL design activities performed in the framework of task TTBA-1.1 [1] have led to an update of the conceptual design and operating conditions of the Test Blanket Module (TBM) for a testing in ITER-FEAT on the basis of the design previously envisaged for ITER-FDR [2]. Some slight modifications of the TBM design resulted from this activity like overall dimensions of the segment box, thickness of the side walls, number and location of DWTs, Pb-17Li supply system, etc. The work carried out within Task TTBA-2.1 consisted in assessing the possible impact of these modifications on the definition of TBM demonstrators and extract all relevant design data required for the definition of these mock-ups.

Dimensions of the Module Box

The overall dimensions of the WCLL TBM have changed with regard to the previous TBM designed for ITER-FDR (respectively 1.72 m high x 0.514 m wide x 0.585 m deep instead of 2.12 m high x 0.44 m wide x 0.585 m deep).

This global dimensional change of the TBM has been imposed by ITER specifications related to the new dimensions of the ITER-FEAT equatorial port in which the TBMs shall be located [3]. This evolution represents however only ~ 5 % decrease in volume of the whole segment box and may not have a significant impact on the demonstrator specifications. However, due to a slight increase of the box sectors width (from 123 mm to 148 mm), it has appeared necessary to reinforce the Fisrt Wall (FW) corners and the side walls in order to withstand the accidental pressurization of the segment box at 15.5 MPa. Thermo-mechanical calculations [1] have shown that a side wall thickness of 26 mm (instead of 21 mm) would lead to acceptable temperature and stress level during normal and accidental situations. The thickness of the FW itself and of the radial/toroidal stiffeners remain unchanged at, respectively, 21 mm and 8 mm.

Double Wall Tubes

C-shape Double Wall Tubes (DWTs) have been preferred instead of the previous U-shape tubes foreseen for testing in ITER-FDR [2]. The C-shape concept allows indeed significant reduction of steel inventory at the top of the TBM (the water header are reported on the external side of the backplate).

This evolution will imply some significant modification of the manufacturing sequence. In the former concept, the TBM segment box with all internal stiffeners was prepared priory to the insertion of the U-shape DWTs from the bottom. In the updated concept for ITER-FEAT, C-shape DWTs can only be inserted from the back of the segment box. Thus, toroidal stiffeners cannot be welded before DWT positioning. TBM demonstrators will need to show that such manufacturing sequence is compatible with welding state-of-art: welding of a toroidal stiffener after DWT positioning must avoid any damaging of the DWT located behind. This constraint shall be assessed more precisely with the help of Industry.

An optimisation of the Breeder Zone (BZ) cooling conditions under ITER-FEAT operating conditions [1] has also permitted to reduce the total number of C-shape DWTs to 35 instead of 48 in the preliminary C-shape concept version [4]. The precision of the DWT location in the breeder zone will need to be defined precisely with the help of thermal calculations. The use of a DWT spacer grid, not shown in figures, is foreseen.

KEY ELEMENTS FOR A TBM DEMONSTRATOR

The qualification of the WCLL Blanket fabrication technologies has to go through the following stages:

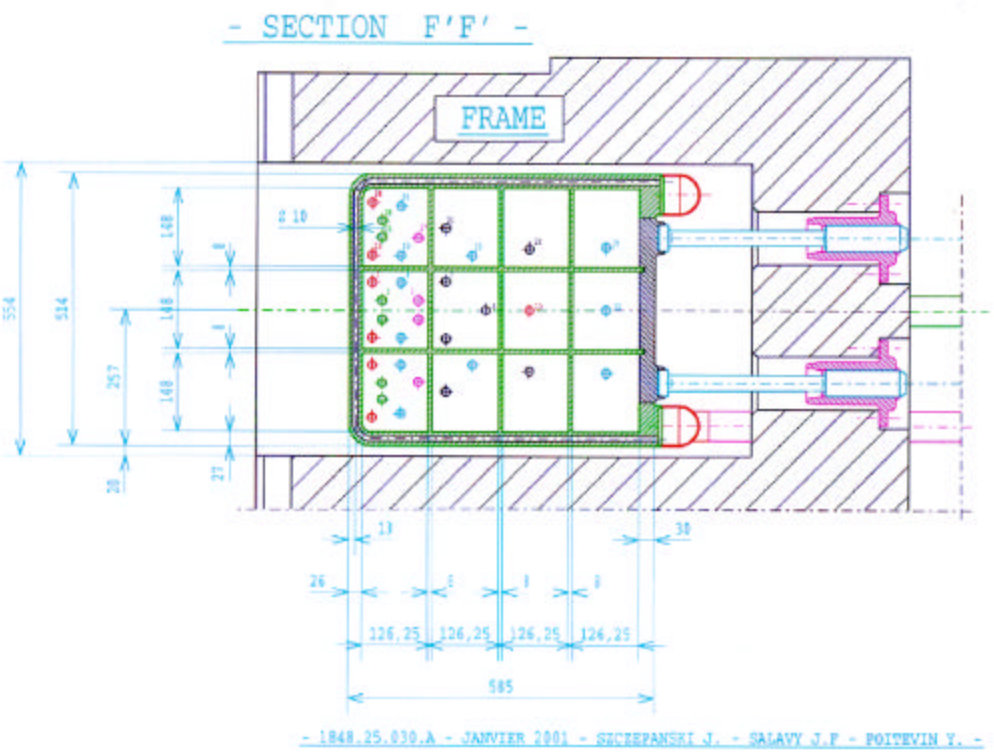

Figure 1 : Equatorial section of the WCLL TBM for ITER-FEAT

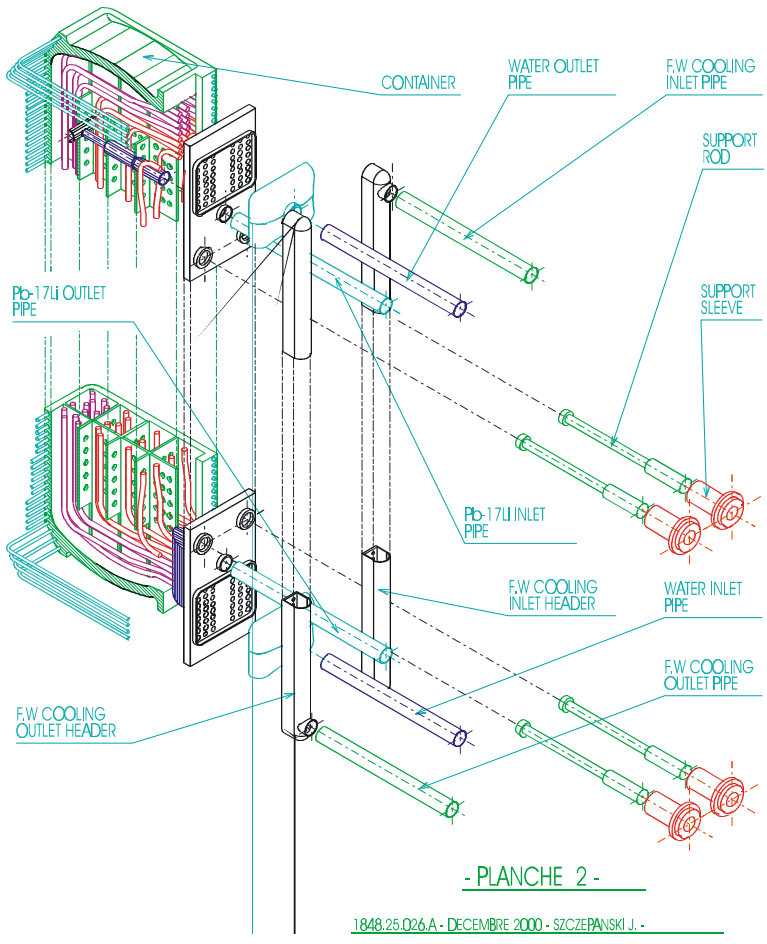

Figure 2 : WCLL TBM for ITER-FEAT

Fabrication and testing of small-scale mock-ups

R&D on critical issues of the WCLL blanket fabrication like double-wall tubes and first wall is already ongoing within EU for several years and shall be achieved through the fabrication and testing of dedicated small-scale mock-ups limited to specific part or technologies of the TBM: first wall, DWT, etc. Small-scale mock-ups are intended to demonstrate the feasibility of manufacturing all relevant subcomponents and provide qualification of their behaviour under relevant testing conditions.

Fabrication of a TBM medium-scale mock-up or demonstrator

After qualification of basic technologies, it is required to demonstrate the ability to integrate all manufacturing technologies within a medium-scale mock-up – called demonstrator. The main goal of the demonstrator is to demonstrate the ability to assembly subcomponents in a reproducible procedure which could be easily extrapolated to the TBM reference design.

The main objectives and features of the TBM demonstrator are then:

- To include all relevant technologies used for the final TBM prototype manufacturing.

- To be produced according to the reference TBM fabrication sequence: same order of operations, same technologies.

- The demonstrator is not required to be at scale with respect to the TBM. However, the following key dimensions shall be conserved: relevant thickness for plate welding, pitch between cooling tubes in segment box, pitch between tubes welding on back plate, accessibility for welding operations (ex: dimensions between stiffeners), curvature radii for double wall tubes and segment box.

- The demonstrator shall not include, in principle, any instrumentation for testing. One exception could however be the first wall that could be tested under cyclic heat load.

- Non destructive and destructive examinations will also bring a valuable information on the reliability of the used technologies (quality of the joints obtained by HIPing, welding and dimensional changes).

Table 1 reports the main components to be included in the WCLL TBM demonstrator with some indication on their features.

Fabrication of a TBM large-scale mock-up

After demonstration of the fabrication feasibility (demonstrator), a large-scale mock-up dedicated to relevant WCLL conditions shall be produced.

This large-scale prototype shall be fully instrumented and include a Pb-17Li heating system for reproducing the heat deposition for testing in suitable facilities (H/D permeation tests).

Table 1 : Main components to be included in a WCLL TBM demonstrator

Steel box	Eurofer Typical external dimensions: few tens of cm (typically W 400 x L 400 x H 800 mm)
Segment Box cooling channels	∅ 10 mm; 0.1 mm Cu coating; pitch 26 mm bent cooling tubes (Fist wall & Side walls)
Stiffeners	Thick. ~8 mm Rectangular sectors (minimum of 4 sectors); typical dimensions: ~100-150 mm
Internal coatings	Al-based coating Hot Dipping or Chemical Vapor Deposition
Top/bottom covers	Thick. min. ~10-20 mm
DWT	Eurofer ∅ 11/13.5-14/16.5 mm; 100 µm Cu-interlayer C-shape; curvature radius 50 mm 1 (minimum) DWT per sector Welded on back plate (double weld scheme) Pitch on BP: ~25 mm
Spacer grid	Eurofer Leaf thick. 0.5 mm
Back Plate	Thick. ~ min. 10-20 mm

CONCLUSION

The latest WCLL TBM design evolutions required by the ITER-FEAT specifications and which may have an impact on the TBM manufacturing sequence and, thus, on the definition of a TBM demonstrator have been analysed. A slight evolution of the external TBM dimensions shall not bring additional constraints to the previously envisaged R&D.

However key dimensions of internal components (pitch between tubes, distance between stiffeners, curvature radius, etc.) that should be taken into account for a demonstrator (medium-scale mock-up) have been reported. The respect of those specifications is mandatory, even at medium-scale, because they constitute dimensional constraints on the envisaged blanket manufacturing techniques that shall be used at a later stage for the TBM manufacturing.

REFERENCES

[1] Y. Poitevin et al., « Status of the design and testing programme of the WCLL Test Blanket Module for ITER-FEAT », CEA internal report SERMA/LCA/ RT/01-3019/A, December 2001.

[2] M. Fütterer et al., « Design Description Document (DDD) for the European Water-cooed Pb-17Li Test Blanket Module », CEA internal report SERMA/LCA/2125, 1997.

[3] Report from the Test Blanket Working Group (TBWG) for the Period of Extension of the EDA, May 2001.

[4] M. Fütterer et al., "Design modifications of the WCLL Test Blabket Module for ITER: reduction of header space", CEA internal report SERMA/LCA/TR/00-2761/A, February 2000.

REPORTS

Y. Poitevin et al., "Definition of specifications for a demonstrator of the WCLL Test Blanket Module for ITER-FEAT", CEA report SERMA/LCA/RT/01-2916, Sept. 2001.

TASK LEADER

Yves POITEVIN

DEN/DM2S/SERMA
CEA Saclay
91191 Gif-sur-Yvette Cedex

Tél. : 33 1 69 08 31 86
Fax : 33 1 69 08 99 35

E-mail : ypoitevin@cea.fr

TTBA-2.2

Task Title : BLANKET MANUFACTURING TECHNIQUES Solid HIP demonstrator for fabrication and coating, fabrication of double wall tubes

INTRODUCTION

This subtask is devoted to the fabrication of a WCLL mock up representative of a segment box, including first wall, double wall tubes and Tritium Permeation Barrier (TPB) coating. In 2000, a small first wall mock up was manufactured in order to check the behaviour of the copper coated first wall tubes. DWT were fabricated as well. Then, the solid HIP demonstrator was HIPed but the operation failed due to a defectuous weld. The failure was expertised.

2001 ACTIVITIES

SECOND ATTEMPT OF FABRICATION

An attempt was made to HIP again the demonstrator in early 2001. All welds bead were machined and the first wall plate was removed. The interface as well as the copper coated eurofer tubes were slightly oxidised. One tube was cracked.

The parts were heat treated under hydrogenated argon at 750°C to soften the materials. Then, the surfaces were brushed to remove the oxide layer, cleaned with a detergent, rinsed with water and alcohol and dried. The defective tube was filled with powder and closed with welded plugs to prevent its collapse during HIPing. Tubes were put back in place and the plate was TIG welded using only ER316L filler metal. Attention was paid to avoid excessive base metal dilution in order to maintain a low martensite content in the weld. The same HIP cycle was applied. Again, the operation was unsuccessful. Two leaks were detected at tube ends, due probably to the melting of the copper coating during welding.

MIXED SOLID/POWDER SOLUTION

In the meantime, the reference WCLL design moved from the U-shape DWT to the C-shape DWT design [1]. Also, recently available results showed that a HIP temperature above the copper melting point (1100°C) was needed to reach satisfactory Eurofer/Eurofer joint mechanical properties [2].

A general agreement between EFDA members was found that stated that :

(i) the fabrication of the U-shape DWT demonstrator was no more a priority,

(ii) sufficient indications existed that solid HIP had significant drawbacks with respect to the first wall fabrication (compliant layer damaging and insufficient joint properties),

(iii) a mixed powder/solid solution had to be investigated because it presents significant advantages over the solid HIP solution, including cost and powder material properties.

It was decided that the demonstrator had to be used in the frame of the development of a mixed solid/powder HIP solution [3].

DEMONSTRATOR COMPLETION

The weld beads of the demonstrator were machined out by milling. A layer about 2 mm thick was milled in order to remove the material affected by welding.

A new set of new eurofer tubes were bent and copper coated with an improved electrolytic process which permits to avoid the use of a nickel underlayer.

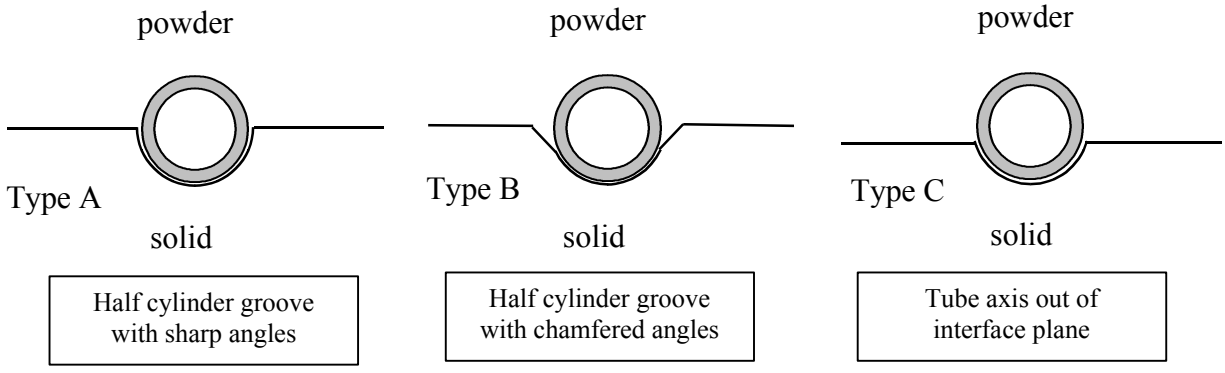

Figure 1 : Possible groove designs for the solid/powder HIP process applied to WCLL FW fabrication

The following samples were fabricated in order to prepare the demonstrator completion through the solid/powder HIP process :

- solid/powder joints HIPed at 1050°C to check joint mechanical properties;

- a small straight mock up, comprising tubes embedded at the solid/powder interface, has been manufactured in order to define a suitable groove design (figure 1). A suitable groove design shall allow to avoid damaging the compliant layer and shall insure a correct positioning of the tubes. As a sufficient clearance is necessary, the way in which the tube/groove gap is removed is of concern, too.

After HIP, all tubes showed a significant expansion on the powder side. The Eurofer powder particles have punched the copper layer as shown on figure 2. The copper layer was also damaged by the groove angles, specially when they are sharp (groove type A and C).

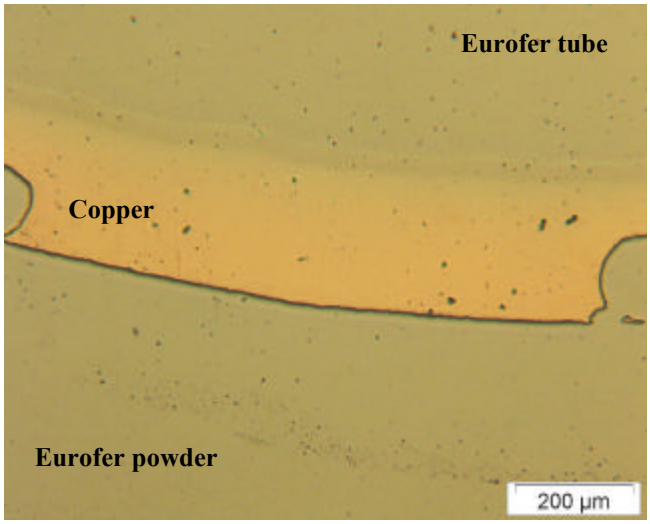

Figure 2 : Deformation of the copper layer during HIP

Type B grooves were chosen and machined on the WCLL mock-up representative of a segment box. Special tools were machined to position copper coated tubes. Other parts are added to form the canister for powder filling. A view of the demonstrator is given on figure 3. The WCLL demostrator will be HIPed with the following HIP cycle :

- 1050°C/140 MPa step during 2 hours.

CONCLUSIONS

The demonstrator could not be completed in 2001 due to technical difficulties and a change in the blanket design. However, samples and small mock ups have been manufactured with a mixed solid/powder HIP process in order to prepare the demonstrator completion. Emphasis has been put on the design of the grooves in which copper-coated tubes have to fit.

WCLL demonstrator is under fabrication. It will be hipped within the end of May 2002.

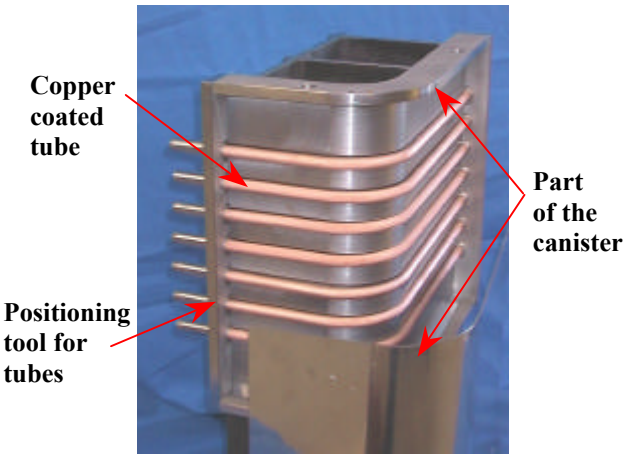

Figure 3 : View of the demonstrator

REFERENCES

[1] M Fütterer, Minutes of the 2000 monitoring and 2001 kick-off meeting, water cooled lithium lead blanket, CEA Saclay, 15-16 february 2001.

[2] E. Rigal "Solid HIP process and qualification : Eurofer/ Eurofer HIP joints, task TTMS4.5", NT DEM 111/00, 8/12/2000.

[3] 2001 monitoring meeting, water cooled lithium lead blanket, CEA Saclay, 2-3 july 2001.

REPORTS AND PUBLICATIONS

E Rigal, P Bucci, C Grandjacques, « Solid HIP demonstrator for fabrication and coating, fabrication of double wall tubes" CEA report, to be issued.

TASK LEADER

Emmanuel RIGAL

DRT/DTEN/SMP/LS2M
CEA Grenoble
17, rue des Martyrs
38054 Grenoble Cedex 9

Tél. : 33 4 38 78 97 22
Fax : 33 4 38 78 54 79

E-mail : emmanuel.rigal@cea.fr

Task Title : BLANKET MANUFACTURING TECHNIQUES Solid HIP demonstrator for fabrication and coating, fabrication of double wall tubes

INTRODUCTION

The double wall tubes (DWT) are among the most critical parts of the water cooled lithium lead blanket. This subtask is devoted to the fabrication of double wall tubes using the "solid" HIP process, as well as to a first assessment of their mechanical behaviour in terms of crack propagation.

2001 ACTIVITIES

IMPROVEMENT OF THE DWT DIMENSIONAL ACCURACY

Large U-bent DWT mock ups were manufactured in the frame of subtask TW0-TTBA22 using eurofer tubes. The fabrication sequence was bending + HIP + tempering. These mock ups were used for dimensional measurements. Two kinds of deformation were observed.

On one hand, the straight branches show a significant camber, which is thought to arise from the quenching stresses. This deformation exceeds the design specifications [1]. In order to solve this problem, it is proposed to change the fabrication sequence as follows : HIP + tempering + straightening + bending + stress relieving.

This new fabrication sequence is compatible with the new WCLL TBM design (C shape DWT), whereas it was not compatible with the old one (U-shape DWT).

On the other hand, the shape of the DWT section varies along the tube axis. This ovalisation phenomenon is due to uneven tube to tube gap removal during HIP. Despite there is no significant cross section reduction in straight parts, experiments have been made to improve the section shape.

Figure 1 shows the outer diameter of two straight double wall tubes after HIP. One DWT was expanded before HIP using a bore tool whereas the other one was not. It can be seen that, in the former case, the 0.2 mm tube-to-tube gap disappeared in an uneven way during HIP, which resulted in a diameter varying between 16.6 and 17 mm. In the case of the expanded DWT the outer diameter remains constant.

DOUBLE WALL TUBE BENDING

In the C-shape design, the DWT inner bending radius varies between 50 mm and 536.5 mm depending on the DWT considered. Bending experiments have been made to check whether the minimum bending radius was achievable and to compare the cross section reduction in bent zone to the design specification, i.e. < 15 % [1]. Bending was made with a basic process as a conservative approach, since numerous more sophisticated techniques can be used when the cross section reduction has to be minimised.

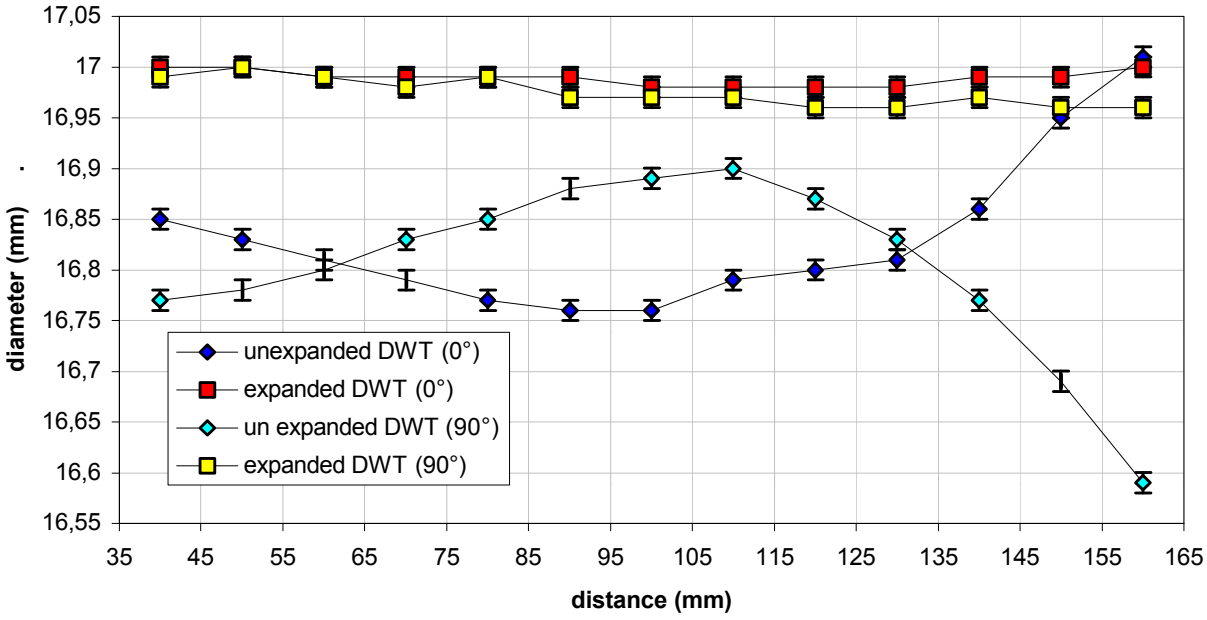

Figure 1 : Influence of an expansion treatment on the outer diameter variation of two DWT after HIP

In a first step, T91 single tubes of similar thickness as DWT were used. Figure 2 shows that the 15 % cross section reduction is exceeded for a radius smaller than ~43 mm with respect to the neutral axis.

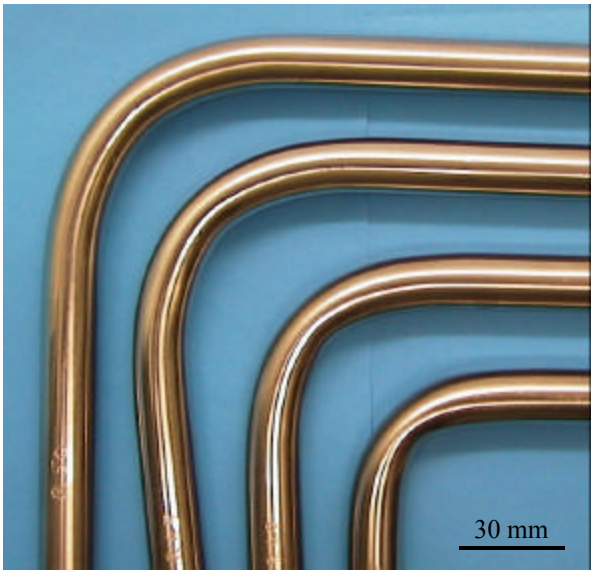

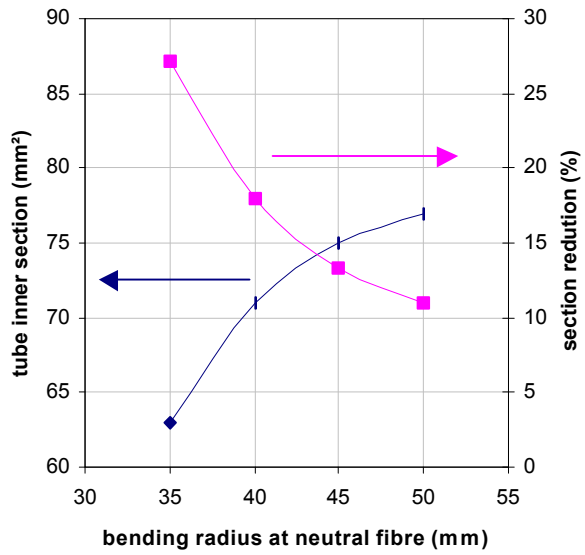

Figure 2 : Results of bending experiments with T91 single tubes

These good results were confirmed with DWT samples, since their cross section reduction for a 50 mm bent varies from 4 to 10 % (figure 3).

DOUBLE WALL TUBE CONICAL WIDENING

A proposed scheme for the DWT/backplate attachment is based on conical expansion and welding. The main advantage of this design is to provide a shape intrinsically resistant to DWT pull-out.

Experiments were made to check whether conical widening could damage the material. Figure 4 shows three DWT samples expanded following different parameters. The deformation on the inner side varies from 6 to 14 %. No crack could be detected after expansion.

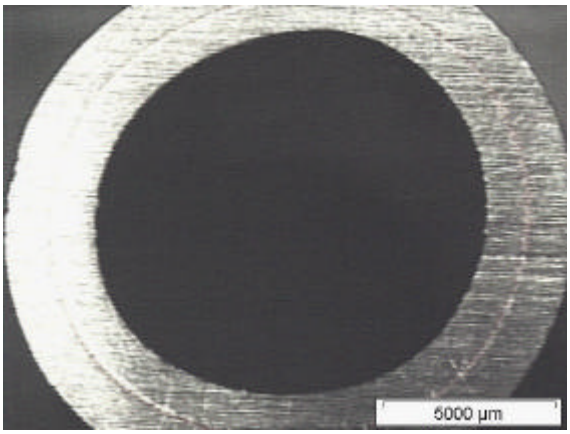

Figure 3 : Cross section of a DWT in bent zone (bending radius 50 mm with respect to the neutral fibre)

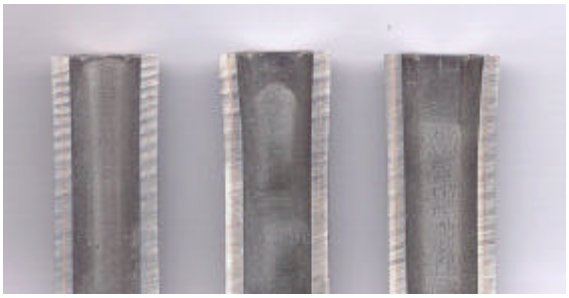

Figure 4 : DWT samples after conical expansion From left to right : cone height 15, 15 and 20 mm, cone angle 2, 3, 3°.

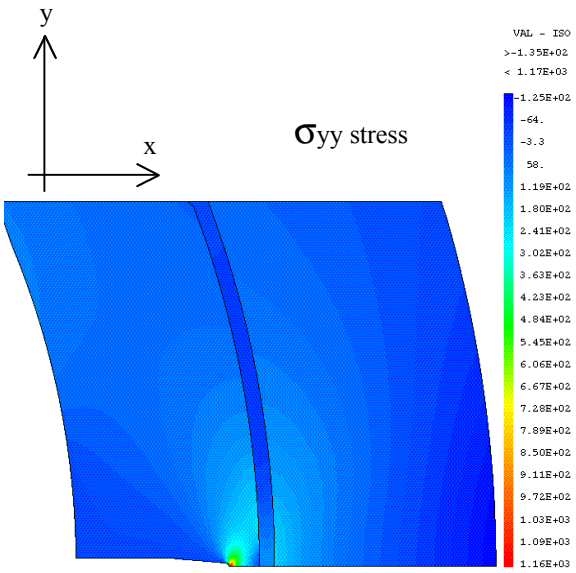

*Figure 5 : **S**yy stress in a DWT with an axial crack*

Figure 6 : 4 point bend test specimen (70 x 10 x 4 mm) tested under fatigue conditions at 20°C after 7.5 10^5 cycles between 750 and 1750 N
The crack deviates in the copper layer

CRACK PROPAGATION IN DOUBLE WALL TUBES

The stress repartition in DWTs under service conditions have been calculated by FEM using the Castem 2000 FE code. Uncracked and cracked DWT have been considered. Temperature and pressure data provided by the design team have been used for calculations [1].

In uncracked specimens, the Von Mises stress is about 130-140 MPa on the water side and 50 MPa on the LiPb side. There are two main contributions to the Von Mises stress : the axial stress and the hoop stress.

Each contribution is of tensile type on the water side and reaches 120-130 MPa. Both have negative values in the compliant layer, in which the Von Mises stress is about 15 MPa.

In cracked specimens, one of the two contributions largely dominates, namely the hoop stress for an axial crack (figure 5) and the axial stress for a circumferential crack.

As this situation is similar to bending, four point bending specimens were designed and manufactured for crack propagation testing (figure 6). First results show that, under fatigue testing, the crack tends to deviate in the copper compliant layer. Tests will be continued in the frame of subtask TW2-TTBA22.

CONCLUSIONS

The DWT fabrication process was adapted to the new WCLL TBM design and improved in order to increase the DWT dimensional accuracy. Forming experiments have demonstrated, from one hand, that the smallest design bending radius is achievable without exceeding the maximum cross section reduction and, from the other hand, that conical widening of DWT ends is feasible without DWT damage.

The stresses under service conditions in cracked and uncracked DWT have been calculated using FEM. It has been shown that four point bending specimens could be used to simulate crack propagation in DWTs. Specimens were manufactured and first results show that the crack deviates in the copper layer.

REFERENCES

[1] A. LI PUMA et al. WCLL Test Blanket Module Demonstrators: development program and specifications, CEA Report, CEA Saclay, SERMA/LCA/RT/01-3024

REPORTS AND PUBLICATIONS

E Rigal, P Le Gallo, C. Grandjacques, CEA report Note technique DTEN 03/2002, 4/01/02

TASK LEADER

Emmanuel RIGAL

DRT/DTEN/SMP/LS2M
CEA Grenoble
17, rue des Martyrs
38054 Grenoble Cedex 9

Tél. : 33 4 38 78 97 22
Fax : 33 4 38 78 54 79

E-mail : emmanuel.rigal@cea.fr

TW1-TTBA-002-D03

Task Title : BLANKET MANUFACTURING TECHNIQUES DIADEMO experimental program – Results of U bent DWT tests on Pb-Li

INTRODUCTION

Within the framework of the study on Water-Cooled Lithium-Lead (WCLL) tritigenous Blankets for fusion reactors, technological choices on cooling tubes must be validated. Within this context, tests on Double-Wall Tubes (DWT's) through which reactor power will be transferred must be carried out.

The state of the art of these tubes is of outmost importance. The behaviour of these tubes must be validated from both mechanical and thermal points of view. Before considering industrial manufacturing, samples have to be tested under fusion reactor nominal conditions.

The main objective of DIADEMO experimental program is to validate the choice of the double-walled tube used in the WCLL blanket.

After 2 tests on small size straight samples [1][2], the manufacturing of large size bent DWTs (~2.5 meters developed length) was carried out in order to be tested in the DIADEMO Pb-17Li test section.

2001 ACTIVITIES

In 2001, the experimental program performed on the U bent DWT on the "Pb-17Li test section" [6], is composed of two phases :

- Phase 1 : thermal fatigue cycling,
- Phase 2 : endurance tests.

The experimental device "DIADEMO" has been presented in details with the instrumentation of the U bent DWT in the reference [3][4][5].

CYCLING TESTS

More than 3000 thermal cycles have been done. In a first time, a chronological account of events is given. In a second time a typical thermograph of the U bent DWT and Pb-Li is presented.

Chronological account of events

After the conditioning of DIADEMO loop, and its Pb-Li test section, the thermal cycles began.

622 cycles have been realised until a leak on the water flow-meter probe was detected. The test was stopped, and this probe repaired.

After reconditioning, 1963 cycles have been realised before a level loss in the pressurizer was detected. This is due to a small leak on the circulation pump on the water loop. 165 cycles have been realized out of the nominal water pressurised conditions because of this problem.

Some dispositions have been taken in order to integrate the small leak on the circulation pump, and 461 more cycles have been made before the end of cycling tests.

AT THE END OF THE THERMAL CYCLING TESTS, 3046 CYCLES HAVE BEEN PERFORMED

Typical thermograph

Typical thermograph of U bent DWT are illustrated by graphs in figure 1.

The straight parts of the U bent DWT are correctly cycled ($\Delta T \approx 90°C$) (figure 1), but the U part do not see significantly thermal cycles.

During the Heating phase of thermal cycles, the signal given by the thermocouples is very disrupted.

It may be due to thermohydraulical phenomenon, induced by the proximity of electrical heaters and DWT (hot source near cold source) that may product some thermal fatigue on the external surface of DWT.

Thermal stratification was present in Pb-Li in the central part of the test section. Between DWT and electric heaters, a succession of "hot and cold points" occurs due to the natural convection flow.

ENDURANCE TESTS

After the cycling tests, the endurance tests have been launched. These tests have been divided in two parts, separated by the reparation of the circulation pump leak of the pressurized water loop, witch is become too big.

To maintain a mean temperature in Pb-Li of 500°C, the free level temperature had to reach 600°C. Moreover, the free level was not constant, and oscillated around a set point, determined by the gas circuit. So this situation induces severe conditions from thermal fatigue and corrosion in Pb-Li point of view.

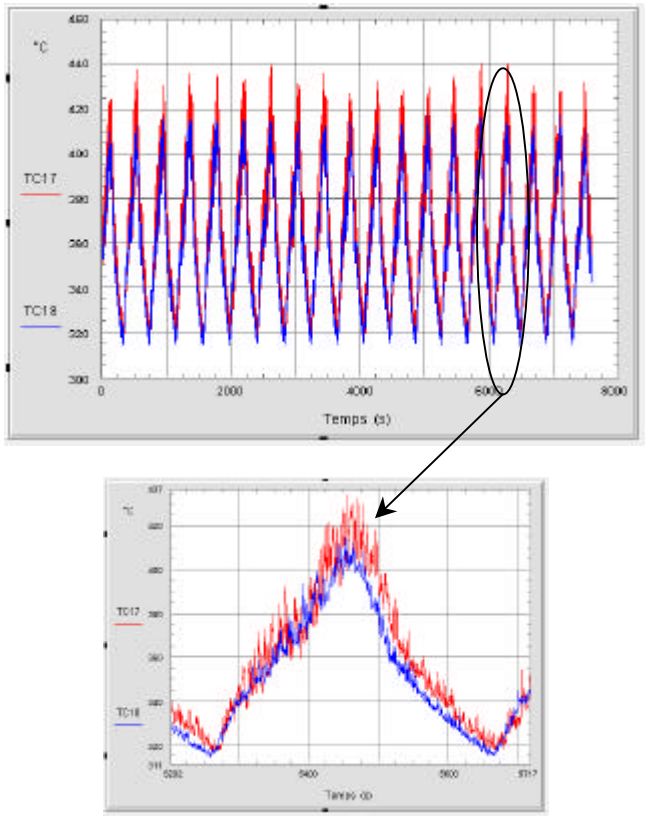

Figure 1 : Temperature given by 2 thermocouples diametrically opposed situated on straight part of the U bent DWT

After one day of endurance tests, we assumed that some thermocouples lost their insulation and indicated the temperature of the free level of Pb-Li. This phenomenon has been confirmed at the end of the test after dismantling the Pb-Li test section : thermocouple stainless steel sheath has been dissolved at the free level of Pb-Li (figure 2). The hot welding of thermocouples has been made by Pb-Li at the free level (figure 5).

After 3 or 4 days only a few number of thermocouples indicates the right temperature corresponding to the localisation of their initial hot welding. The other ones indicate an homogeneous temperature corresponding to the free level one.

After a little more than 5 days, a leak of water in Pb-Li has been detected (figure 3). The scenario of events is now described :

- The control command indicated a loss of Pb-Li level. This was due to the pressure groth in the head test section. Pb-Li has been drained by gravity in storage vessel.

- Pressure-reducing valve has been opened.

- A loss of water level in pressurizer has been detected. Isolation valves of test section have been shut down to stop the pressurised circuit water leak.

- Pressure has decreased in test section.

On DIADEMO device, this leak has been cautious. It could not be detected by viewing or earring. Only control command indicators have shown us its presence. More over, on the circuit, the relief lines, which are normally cold, have become very hot.

DWT HAS BEEN DAMAGED AFTER A LITTLE MORE THAN 5 DAYS OF ENDURANCE TESTS

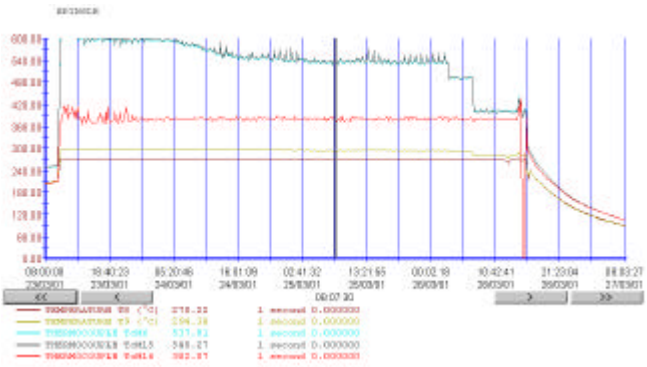

Figure 2 : Temperature on U bent DWT

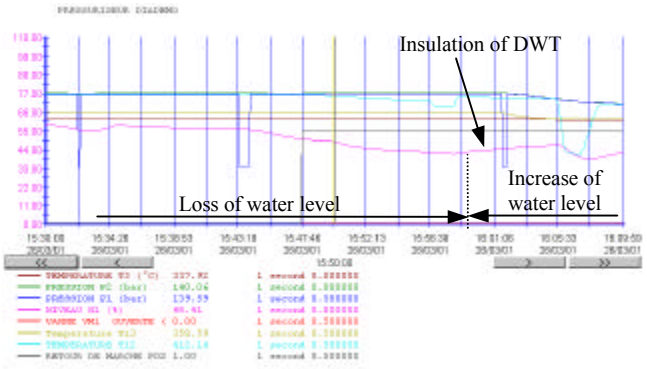

Figure 3 : Water pressurizer parameters : N1, loss of water level

DWT NON DESTRUCTIVE EXAMINATIONS.

After DWT removal, the leak has to be located.

The first observations of DWT surface, covered by a thin Pb-Li film (figure 4), did not indicate any presence of leak.

In a first time, an hydrostatic test has been made on DWT, until 300 bar of water : no leak. Then leakage helium test has been made without more success. The thin Pb-Li film probably plugged up any cracks.

So, a chemical cleaning of DWT surface has been realized with a nitrogen acid solution.

Inlet and outlet examinations have been carried out. The outlet DWT is very roughly and liquid penetrant examination did not show any cracks. The inlet borescope examination has shown a lot of corrosion pits and some erosion cracks only located in the elbow part.

Finally an another leakage helium test has been performed : no leak has been found.

Non destructive examinations did not allow to locate leak noted during experimental tests.

The U bent DWT has be sent to CEA/CEREM for destructive examination.

Figure 4 : U bent DWT after removal

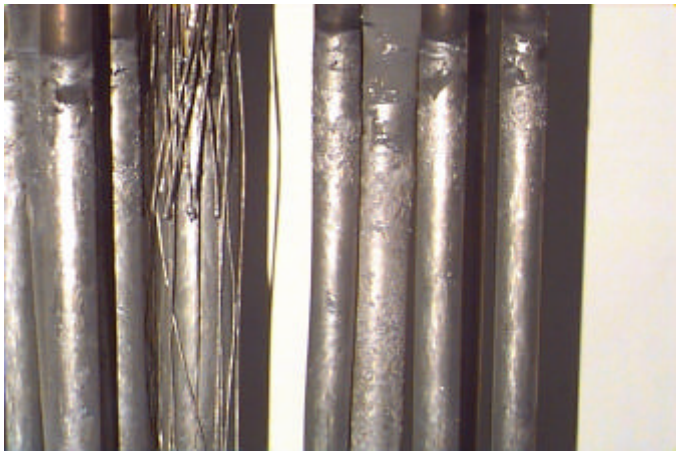

Figure 5 : Thermocouple stainless steel sheath dissolved by Pb-Li

CONCLUSIONS

The main objective of DIADEMO experimental program is to validate the choice of the double-walled tube for the future Fusion reactor. This task is performed in close collaboration with task TW1 – TTBA-002.4, driven by CEA/ CEREM, the responsible of the fabrication of the DWTs (choice of the DWT fabrication procedure, DWT manufacturing).

This report presents the results of the tests performed on the U bent DWT. The main events of the tests are :

- During thermal cycling tests, 3046 cycles have been performed.
- During endurance tests a leak of water in Pb-Li has been detected after a little more than 5 days.
- Non destructive examinations did not allow to locate leak noted during experimental tests.

REPORTS AND PUBLICATIONS

[1] Y. SEVERI et al « DIADEMO EXPERIMENTAL PROGRAM (WP A3-3), Test report on the Straight Double-Wall Tube Sample », NT DER/STPI/LCFI 99-018.

[2] L. CACHON et al « DIADEMO EXPERIMENTAL PROGRAM (WP A3-3), Test report on the second Straight Double-Wall Tube Sample », NT DER/STPI/LCFI 00-031.

[3] Y. SEVERI et al, “Installation DIADEMO, Dossier de sécurité”, NT DER/STML/LCFI 98-017.

[4] S. ALBALADEJO, « Spécification technique pour la réalisation d’une instrumentation permettant de tester un tube double paroi. », DER/STPI/LCFI 00-038.

[5] L. CACHON et al, « DIADEMO EXPERIMENTAL PROGRAM (TTBA-2.5)” -Technical report », NT DER/STPI/LCFI 00-056.

[6] L. CACHON et al, « DIADEMO EXPERIMENTAL PROGRAM ” –Results of U bent DWT tests on Pb-Li », NT DER/STR/LCET 01-065.

TASK LEADER

Lionel CACHON

DEN/DER/STR/LCET
CEA Cadarache
13108 St Paul Lez Durance Cedex

Tél. : 33 4 42 25 74 25
Fax : 33 4 42 25 66 38

E-mail : lionel.cachon@cea.fr

TW1-TTBA-002-D05

Task Title : BLANKET MANUFACTURING TECHNIQUES
Integrated mixed-powder HIP fabrication route for TBM with DWT

INTRODUCTION

Water Cooled Lithium Lead blanket modules (WCLL) have complex shapes and geometries with double curvature and embedded cooling channels. Conventional techniques such as forging, bending and welding result in very complex fabrication routes. Hot Isostatic Pressing (HIP) techniques appear to be one of the most suitable route for the manufacturing of such complex shape components.

The aim of this task is devoted to the fabrication route of the WCLL blanket modules. To investigate this new concept of fabrication, small mock-ups were produced to validate the manufacturing route.

Mechanical properties of solid/solid and solid/powder/solid junctions hipped at 1050°C have been carried out at room temperature. 2D and 3D computer modeling have been performed to check the efficiency of stiffeners in faulted conditions.

2001 ACTIVITIES

WCLL BLANKET MODULE

In this concept, the WCLL blanket module is entirely manufactured with Eurofer plates and powder. The first wall module is made of coolant channels embedded in a Eurofer structure. These tubes are copper coated, to avoid crack propagations. A drawing of this mock-up is presented in figure 1.

HIP CYCLE APPLIED

The influence of pressure and temperature on mechanical properties of HIP'ed Eurofer powder and Eurofer junctions has been checked in [1, 2, 3]. HIP cycle temperature was imposed by copper layer. All the mock-ups produced within the framework of this study have been HIPed in the CEA furnace with the following HIP cycle:

- 1050°C/140 MPa step during 2 hours.

Pressure was applied when the temperature reached 700°C. After HIP cycle, a heat treatment was applied to restore properties :

- austenitisation treatment : 1 h at 950°C + air cooling,
- tempering treatment : 1 h 750°C vessel cooling.

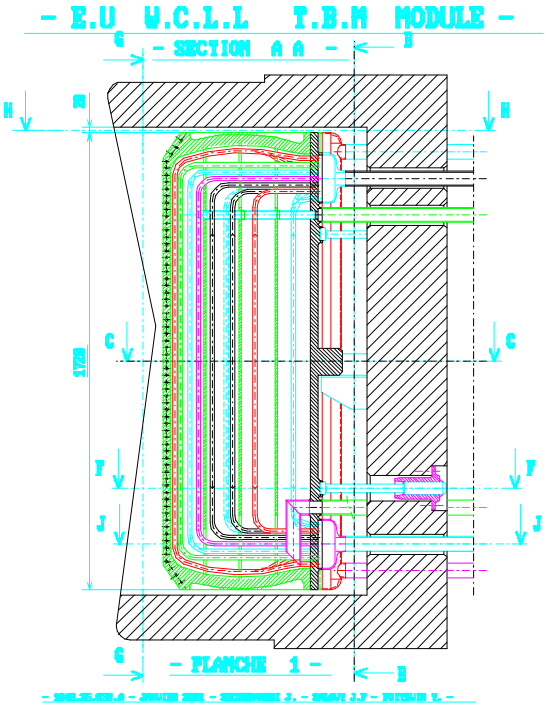

Figure 1 : Drawing of the WCLL blanket module

MECHANICAL PROPERTIES OF THE JOINTS

Two types of joints were studied : T91/T91 and T91/Eurofer powder/T91. Hardness, tensile and impact properties have been tested at room temperature. Results are displayed in table 1 and 2.

Table 1 : Results of hardness

	After HIP		After tempering	
	Eurofer powder	T91	Eurofer powder	T91
Hardness Hv.30	404	397	211	209

Table 2 : Results of impact tests

Junction	solid/powder	solid/powder/solid
Energy (J)	40/39/34/41	37.5/44/45.5/37.5

Tensile tests have been carried out with a strain rate of 4.10-4s-1. The cylindrical geometry of the specimens had a diameter of 4 mm and a gauge length of 20 mm. The joints were located in the medium part of the gauge length and oriented perpendicular to the loading axis. Results are displayed in table 3.

Table 3 : Results of tensile tests

Junction	Solid/powder		Solid/powder/solid	
Yield Stress 0.2% (MPa)	530	530	520	525
UTS (MPa)	650	652	642	643
Uniform Elongation (%)	6.5	7.0	6.6	7.2
Total Elongation (%)	24	24	22	19
Failure	T91	T91	T91	Junction

MOCK-UPS FOR VALIDATION

Small mock-ups, representative of the WCLL blanket module without cooling tubes, have been manufactured in 2001 [4]. Eurofer plates and powder were used. To avoid diffusion welding between the stainless steel canister and Eurofer plates, an anti-diffusion material was used. After stacking of the solid materials (figure 2), the canister was filled with powder and HIP'ed to achieve simultaneously diffusion welding and powder consolidation. The results obtained on this mock-up are encouraging but indicate that a tooling is needed in the inner part of the TBM to avoid deformation, as shown on figure 3.

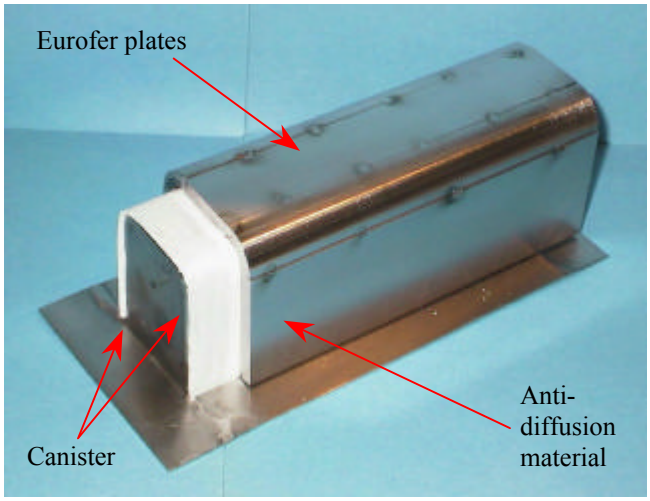

Figure 2 : Mock-up before hipping

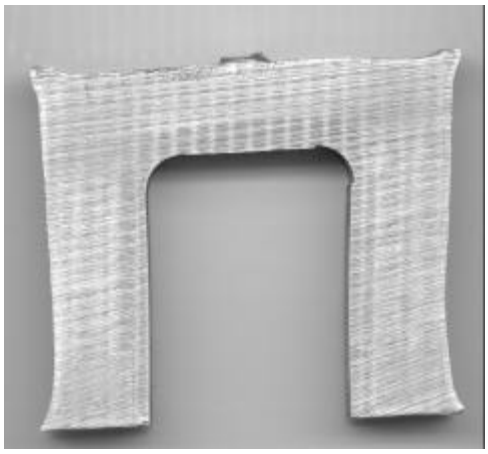

Figure 3 : Mock-up after hipping

To check that no damage occurred on the copper layer during the HIP cycle, a small mock-up was manufactured. On this mock-up different geometries of grooves where machined (figure 4). On figure 5 it can be seen that Eurofer powder particles deform the copper layer. However there is no preferential shear at the solid/powder interface, contrary to the solid HIP process.

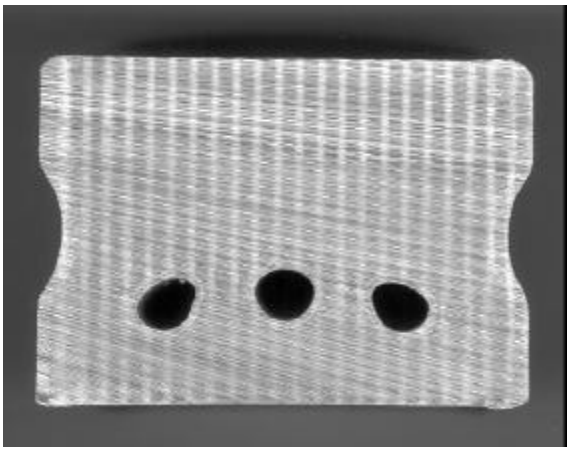

Figure 4 : Solid/powder mock up with embedded tubes

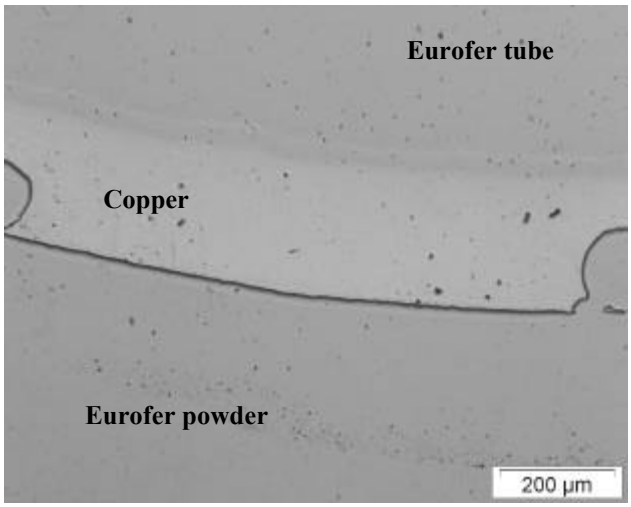

Figure 5 : Deformation of the copper layer by powder particles

TBM DESIGN OPTIMISATION

The objective of this work consisted in optimising the inside geometry of the WCLL blanket module in order to be able to increase its rigidity, to reduce its weight, but to also to increase its interior volume without changing its external dimensions. This last point would allow to introduce more LiPb into the module to increase its performance. 2D and 3D numerical simulations were carried out, with the software Catia®, to calculate stresses in the module but also to locate the most loaded zones.

Mechanical properties used for numerical simulation are synthesized in [5] and rules for the structural design of ITER are given in [6]. Results of thermo-hydraulic study [7] carried out with the finite elements software Castem 2000 [8] were used to know temperature distribution in the WCLL blanket module.

The hypothesis applied to the various calculations carried out during this work are as follows:

- The worst accident for the TBM is the hypothetical rupture of a Double Wall Tube (DWT). It is assumed that in this case the segment box will be pressurised to the cooling water pressure, 15.5 Mpa.
- No loads are applied on the external surfaces of the TBM.
- The module works at a constant temperature : 400°C.

To decrease stresses in the TBM, various ribs represented on figure 6 were used. Unfortunately this type of modification did not decrease significantly stresses in the TBM. Various simulations exhibit that stresses concentration are induced by the longitudinal stiffeners deformation. To contain these deformations in faulted condition, stiffeners must be embedded in the back plate of the TBM and stiffeners thickness must be increased to 10 mm instead of 8 mm. Von Mises stresses, calculated in 2D, are represented in figure 7. To obtain stresses lower than the limiting value, joining radius of 40 mm was used for the front wall.

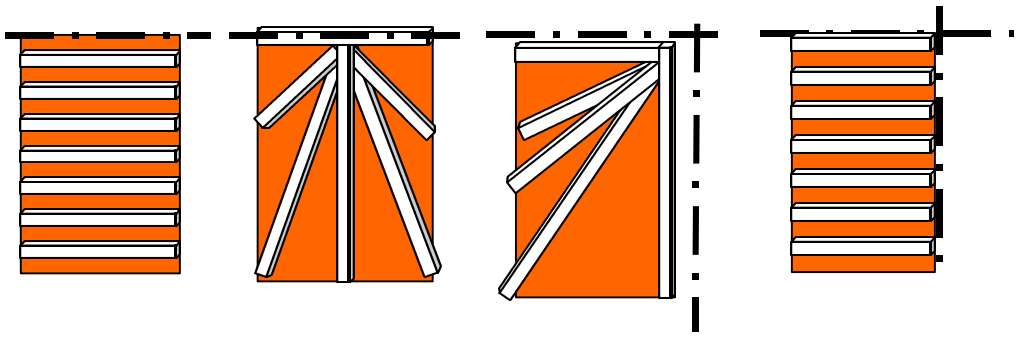

Figure 6 : Ribs used for segment box

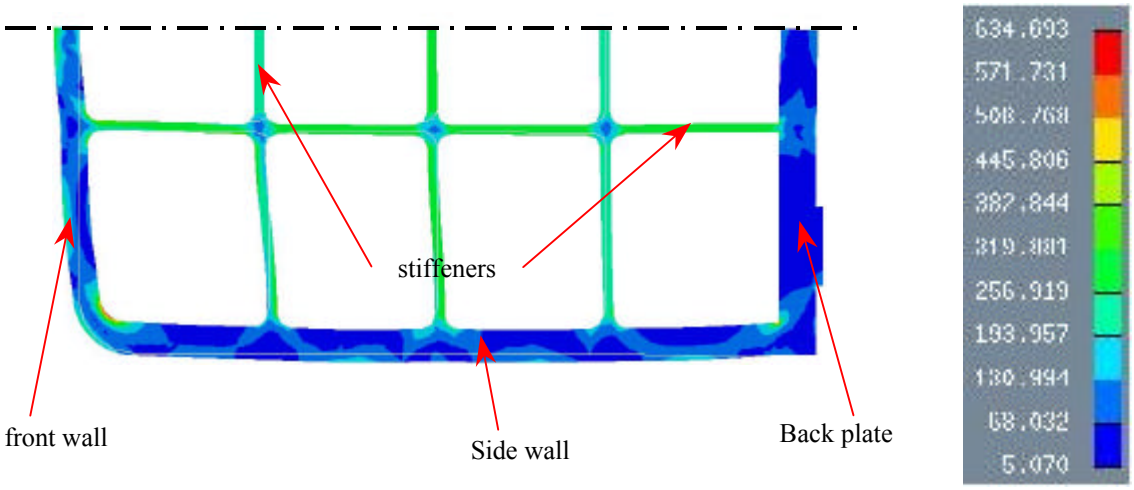

Figure 7 : Von Misès stresses calculated under faulted condition in 2D (MPa)

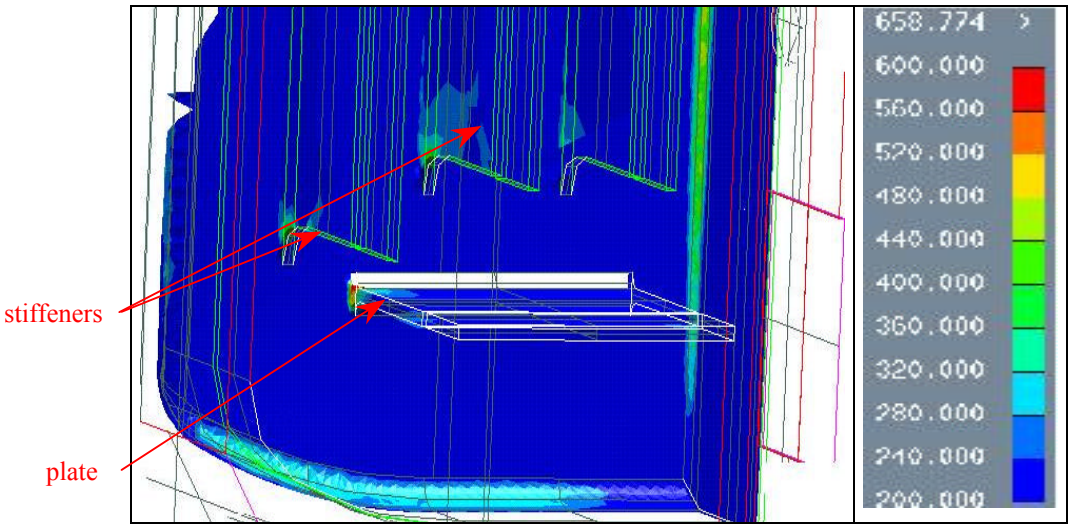

Figure 8 : 3D simulation with plate welded between side walls

3D calculations were carried out to validate the results of 2D simulations and also to calculate stresses which can be highlighted only by 3D simulation. The highest stresses are located at the bottom of the stiffeners, on the side wall and on the joining radii between the side wall and the front wall (figure 8).

To obtain stresses close to the dimensioning criterion, it was necessary to increase the number of stiffeners or to set a plate between the side walls. However if we want to adopt one of these solutions, it would be necessary to develop a specific tool to carry out welding.

CONCLUSION

The main conclusions of this study are the following :

- Hardness and the tensile properties are in accordance with the specification of Eurofer material. For all impact tests, fracture occurred at the interface Eurofer-T91. The impact value after tempering are about 82 J.cm^2 for the T91-powder Eurofer-T91 junction and about 77 J.cm^2 for the T91-Eurofer junction. These values are inferior to those of the bulk material (200 J.cm^2 for KCU). The analysis of the fracture surface reveals a ductile fracture mode.

- Small mock-ups were manufactured to validate the fabrication route. Copper layer damage has not been observed with solid/powder forming route.

- The numerical simulations carried out with the assistance of the Catia® software exhibit important stresses between side walls and stiffeners, side walls and front wall and side walls and plugs.

- Optimising the internal shape of the segment box using curved shapes, undulated forms or by increasing stiffeners thickness do not give the results expected on the stresses calculated on the TBM.

- It is not possible to increase stiffeners thickness and the joining radii without coming up against problems of manufacture and performance.

REFERENCES

[1] P. Bucci, J.M. Leibold, T. Portra : Blanket manufacturing techniques, Feasibility of powder HIP fabrication for TBM or TBM components. Note technique DEM 110-2000.

[2] J.M. Gentzbittel, I. Chu, : Mechanical properties of Eurofer HIP, Powder matérial. Task TTMS 2-4, Note technique DEM 28-2001.

[3] E. Rigal, F. Bruchon, : Qualification of fabrication processes solid HIP process ans qualification ; Eurofer/Eurofer HIP joints. Task TTMS 4-5, Note technique DEM 111-2000.

[5] Tavassoli . Material design limit data . A3.S18F IEA F82H STEEL. INTERIM SM 5.1 & SM 5.4 REPPORT ref.N.T.-DECM/Dir 2000-042.

[6] F. Touboul, ITER Interim Structural Design Criteria (IISDC), Final report, Par I Rapport DMT/95/243.

[7] A.Li Puma, M.A.Futterer, J.-F.Salavy : Impact of reactor parameters on the testing of the WCLL-TBM. Rapport DMT SERMA/LCA/RT/99-2713/A.

[8] CASTEM 2000. Verpeaux P., Millard A., Hoffman A., Ebersolt L. : a modem approach of computerized structural analysis 1988.

REPORTS AND PUBLICATIONS

[4] P. Bucci , L. Bedel, J. Calapez, C. Grangjacques, J.M. Leibold : “EFDA TW1-TTBA-2.5 Blanket manufacturing techniques integrated mixed-powder HIP fabrication route for TBM with DWT ”. Note Technique DEM n°30/2002.

TASK LEADER

Ph. BUCCI

DRT/DTEN/SMP/LS2M
CEA Grenoble
17, rue des Martyrs
38054 Grenoble Cedex 9

Tél. : 33 4 38 78 38 39
Fax : 33 4 38 78 54 79

E-mail : philippe.bucci@.cea.fr

TTBA-3.5

Task Title : COATING QUALIFICATION AND IRRADIATION TESTS Permeation out-of-pile testing

INTRODUCTION

In the water-cooled Pb-17Li blanket concept developed in Europe, the cooling is insured by pressurised water flowing in tubes immersed in Pb-17Li [1]. Due to its mechanical properties, behaviour under irradiation and compatibility with flowing Pb-17Li, the material constituting the tube could be a martensitic steel (Fe with 7 to 10 % Cr). For safety and economical reasons, the permeation through these tubes of the tritium produced in Pb-17Li has to be evaluated and minimised. One way considered to decrease tritium permeation is the use of coatings.

In order to measure the tritium which permeates through different materials from Pb-17Li towards water, a loop was designed [2,3] and built [4]. Moreover this device can be used to perform corrosion test in pressurised water.

Up to August 2001, this loop has been used to complete a corrosion test which had begun in 2000 for the TTMS3.3 programme [5]. After that, the work on permeation has been able to start.

2001 ACTIVITIES

THE MAIN FEATURES OF THE LOOP

The loop consists of an autoclave full of pressurised water at 17 MPa and 350°C respectively maximum pressure and temperature. The autoclave is linked to a water circuit allowing to insure a continuous water flow and to control the water chemistry. Some corrosion specimens can be placed in the autoclave.

In the autoclave, there is also a martensitic steel permeation membrane, which can be filled with gas or some Pb-17Li. It is connected to a gas circuit to insure a gas circulation inside and also to take gas samples to be analysed by a chromatograph.

This loop allows to perform on one hand corrosion tests in water and on the other hand hydrogen permeation measurements from gas or Pb-17Li towards water.

RESULTS

Due to some technical problems such as gas flow controller and hydrogen probe failures and loss of watertightness of the autoclave, experimental work has begun with some delays.

In order to assess all our procedures, a first test has been performed to evaluate the hydrogen permeation from the water to the gas. The operating conditions were:

In the water circuit :

- pure water with dissolved hydrogen at 0.2 bar partial pressure,
- autoclave temperature: 320°C,
- water flow rate: 10 L h^{-1},
- water pressure in the autoclave: 150 bars.

In the gas circuit :

- gas: pure helium,
- helium pressure: 2 bars,
- helium flow rate: 5 L h^{-1}.

The test was planed to last about 1000 hours but it was interrupted after 380 hours running due to a leak in the water circuit. Due to the significant volume of gas which is removed for gas sampling, and due to the early test stopping only two gas analyses were performed. It has been found (Figure 1):

- after 310 h running: about 5000 ppm H_2 in He from the gas circuit,
- after 380 h running: about 6700 ppm H_2 in He from the gas circuit.

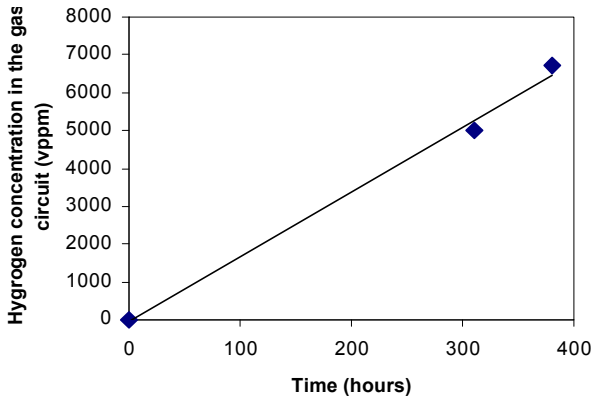

Figure 1 : Hydrogen permeation from the water to the gas

Long durations and more analyses would be necessary to determine a permeation rate but it can see that, in the tested conditions, significant hydrogen permeation from the water to the gas occurs.

After a general checking of the circuits, it turned out that the water leak is probably in the cooling system allowing to decrease the water temperature from 350°C to the room temperature. The repairing of this failure would need to cut a part of the loop, to fabricate a new cooler and to install the new on the loop. As at the beginning the leak was not too large, it has been decided to start a test to measure the hydrogen permeation from the gas to the water in the following conditions:

In the water circuit :

- pure water,
- autoclave temperature: 320°C,
- water flow rate: 10 L h^{-1},
- water pressure in the autoclave: 150 bars.

In the gas circuit :

- gas: helium with 4 % hydrogen,
- gas pressure: 2 bars,
- gas flow rate: 5 L h^{-1}.

The test started 500 h ago and probably due to the vibrations induced by the gas circulator, the leak has increased and water has to be added very often in the circuit. In these conditions, up to now, it has not been able to observe an increase of the partial pressure of the dissolved hydrogen in the water which is not surprising due to the frequent additions of water and no decrease of the pressure in the gas circuit.

CONCLUSION

After the corrosion test was completed, a first permeation test has been performed in order to estimate the hydrogen permeation from the water to the gas in the permeation membrane. It turns out that in the tested conditions, significant permeation has been observed but more investigations are necessary to quantify it. A test to investigate the hydrogen permeation from the gas to the water is carrying out but due to a large water leak prevent us from measuring a possible increase of the partial pressure of hydrogen dissolved in the water. After 500 hours running, no decrease of the gas pressure has been observed.

REFERENCES

[1] L.GIANCARLI et al., Development of the EU Water Cooled Pb-17Li blanket, Proc. ISFNT-4, Tokyo, Japan, April 6-11, 1997

[2] A.TERLAIN, T.DUFRENOY, Tritium permeation barrier testing devices, CEA report, RT SCECF 448 (December 1997)

[3] T. DUFRENOY, A.TERLAIN, Hydrogen permeation measurements with an aluminised martensitic steel, CEA Report, RT-SCECF 487 (December 1998)

[4] T. DUFRENOY, A. TERLAIN, Tritium permeation from Pb-17Li towards water and corrosion loop, CEA Report, RT SCECF 513 (December 1999)

[5] O. RAQUET, C. DUFOUR, L. SEJOURNE, Material compatibility in fusion environment, WP SM 3.3: aqueous corrosion of low activation steels, Final report, CEA Report, RT 540 rev.1, (November 2000)

REPORT

T. DUFRENOY, V. LORENTZ, O. RAQUET, A. TERLAIN - Tritium permeation from Pb-17Li towards water, to be issued.

TASK LEADER

Anne TERLAIN

DEN/DPC/SCCME/LECNA
CEA Saclay
91191 Gif-sur-Yvette Cedex

Tél. : 33 1 69 08 16 18
Fax : 33 1 69 08 15 86

E-mail : anne.terlain@cea.fr

TW1-TTBA-004-D03

Task Title : PROCESSES AND COMPONENTS Blanket neutronic instrumentation

INTRODUCTION

The neutronic instrumentation of the Test Blanket Modules (TBM) appears to be a key point of the TBMs Test Program in ITER, since it will contribute to validate the performances of the blanket in term of tritium production (a good evaluation of the neutron flux is fundamental for estimating the tritium production and thus making a relevant tritium balance in the TBM).

A neutronic instrumentation has to be assessed, taking into account specific constraints of Breeding Blankets (operating conditions, magnetic field, geometry,…).

In this objective, the tasks covered in 2001 the following activities:

- Preliminary assessment of the feasibility of a neutronic instrumentation in the TBM.
- Beginning of an experimental program in TORE SUPRA with a CFUE24 fission chamber.

2001 ACTIVITIES

PRELIMINARY ASSESSMENT OF BLANKET NEUTRONIC INSTRUMENTATION [1]

In order to measure the neutron flux and spectrum in the blankets, it has been checked that :

- on line (fission chambers) or off line (activation techniques) neutronic instrumentations are possible,
- qualified fission chambers can be suited to these specific measurements,
- others fission chambers (the development is in progress), i.e. ∅ 1.5 mm or double deposits fission chambers, could also be interesting solutions.

However, additional information will be necessary to achieve the dimensioning of the detectors (number, location, geometry, …) :

- 3D calculations of the neutron and gamma fields in the blanket (flux level and spectrum),
- characteristics of operation of ITER,
- normal operation check of the fission chambers in an intense magnetic field (5 teslas).

FIRST EXPERIMENTAL TESTS IN TORE SUPRA

Preliminary experimental tests with a CFUE24 fission chamber (manufactured by Photonis) were carried out in TORE SUPRA facility in 2001, in order to qualify its operation in an intense magnetic field.

It is the first time that such a detector was used in a field higher than 1 Tesla.

The main characteristics of the CFUE24 are as follows :

- external diameter : 7 mm,
- fissile material : enriched uranium with 93 % ^{235}U,
- mass of uranium : 16 mg,
- filling gas : argon with N_2 (4 %) ; P = 900 kPa.

The CFUE24 operated in an average magnetic field from 1.6 up to 2.3 T, with a longitudinal gradient up to 8 T/m.

The direction of the field was perpendicular to the axis of the chamber.

The temporal evolution of the counting rate is given on the figure 1: the signal of the CFUE24 located in the magnetic field of 2.3 T follows correctly the counting rate of a CFUL01 fission chamber located outside the facility where the magnetic field is weak (< 0.1 T).

A statistical study between the total number of counts given by the two fission chambers is presented on the figure 2.

These curves were obtained with different conditions of plasmas and with a lot of instantaneous counting rates and show a nearly perfect linearity between the two detectors.

CONCLUSION

As a preliminary conclusion, the tests carried out in TORE SUPRA in 2001 show that a fission chamber provide a normal counting rate in a magnetic field up to 2.3 T.

However, it will be of course interesting to continue the study up to 5 T.

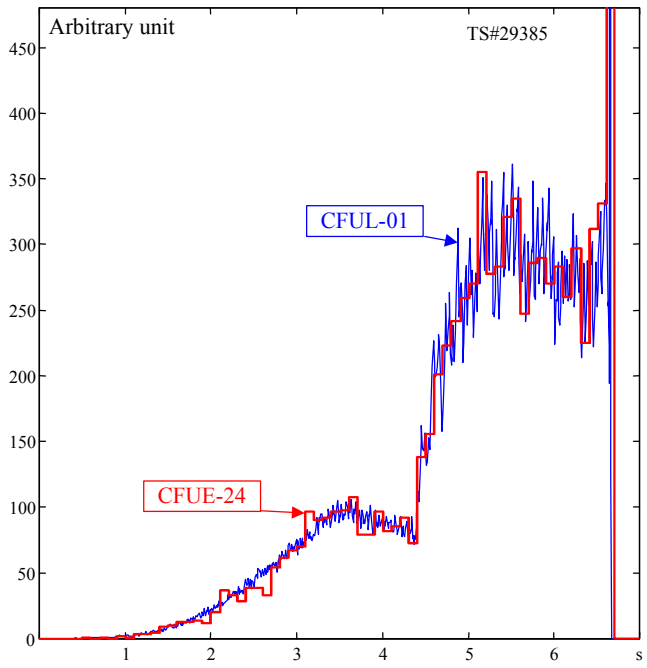

Figure 1 : Temporal evolution of the counting rates of 2 fission chambers : CFUE24 (B = 2.3 T) and CFUL01 (B < 0.1 T)

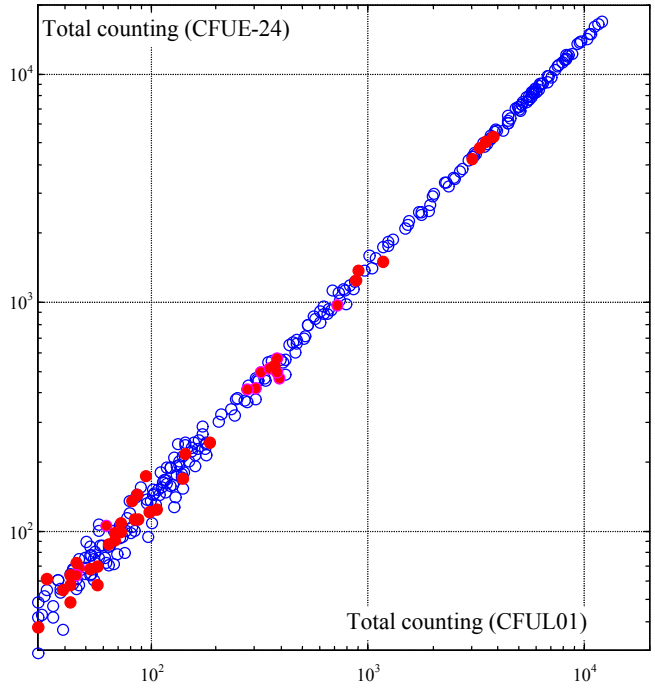

Figure 2 : Comparison of total counting (hollow symbol : B = 2.3 T ; full symbol : B = 1.6 T)

REPORT

[1] J.P. TRAPP, Ch. BLANDIN - "ITER FEAT : couverture tritigène. Considérations sur une instrumentation interne" - NT SCCD 2001-060.

TASK LEADER

Christophe BLANDIN

DEN/DED/SCCD
CEA Cadarache
13108 St Paul Lez Durance Cedex

Tél. : 33 4 42 25 48 04
Fax : 33 4 42 25 27 80

E-mail : christophe.blandin@cea.fr

TW1-TTBA-005-D02

Task Title : SAFETY AND LICENSING : Pb-17Li / WATER INTERACTIONS

INTRODUCTION

The general objective of this action is to validate the code modelling in order to be able to perform safety analyses for licensing.

In that frame, safety studies are specifically devoted to the transient behaviour of a liquid metal breeder blanket module under accidental conditions.

The accident scenario considers the complete failure of a water tube (coolant) into the liquid Lithium/lead (Li/Pb) blanket. Such a scenario was previously investigated and analysed through the experimental BLAST tests and, more recently, through the new and more detailed experimental LIFUS programme performed at Brasimone.

During the first part of the accident scenario, the violent thermal interaction between “hot” Li/Pb and injected “cold” water leads to a pressure transient due to a rapid water vaporization. This scenario was analysed using the Simmer-III code (multi-phase and multi-component thermal-hydraulics in a 2D/Rz geometry).

In the first study, core physical models and code options were widely investigated upon numerical simulation of the BLAST experiments in order to select and justify the most appropriate code parameters to correctly reproduce the involved phenomena.

It was then demonstrated the code ability to evaluate the resulting pressure transient, depending on initial conditions of the water injection (temperature and pressure), of the liquid hot Li/Pb pool (temperature) and on the liquid metal pool environment (containment structures, de-pressurization pipes, tube bundle obstacles,…).

In the second study, the selected code parameters were applied to the LIFUS 5 test numerical analysis that allowed to simulate the relevant phenomena shown in this experiment, which are mainly linked to the water jet fragmentation due to the U-tube bundle obstacles, affecting level and chronology of the pressure transient and to the rapid vapour bubble radial propagation through all reaction tank compartments leading to a similar pressure evolution.

Nevertheless, some deficiencies, particularly on a too rapid calculated pressurization compared to the experimental measurement, were noticed to be due to the important 3D effects inherent to the experimental device (water injection in one reaction tank compartment, U-tube bundle obstacles, de-pressurization pipes associated to each reaction tank compartment) not correctly simulated using a 2D/Rz geometrical approach.

2001 ACTIVITIES

Based on a previous Simmer-III analysis which showed that non-symmetrical effects on a jet evolution, as turbulence, cannot be simulated in a 2D/Rz geometrical approach but can be better reproduced using a 2D plane modelling, it was decided to conduct a similar approach on LIFUS 5.

So that, a new numerical simulation of a LIFUS 5, based on tests number 3 and 4, is developed considering a 2D plane (Cartesian coordinates) geometrical description in the Simmer-III.

Due to the complexity of the experimental device, the main difficulties associated to this modelling are firstly, to determine the best representative plane and secondly, to take into account the third dimension of the problem (conventionally set to unit in the code) for a correct dimensioning of the different elements and characteristics of the experimental set-up, particularly for the expansion tubes and their junctions to tanks (reaction tank compartments, expansion tank). This needs to determine a dimension factor which assumes the proportionality between the experimental volume of the interaction tank compartment (25 l) and its modelling using the Cartesian coordinates. This choice implies that the vapour bubble mainly expands into the reaction tank compartment (containing the water injector and the U-tube bundle) before a general pressurization is reached. This factor allows to correctly represent the injector and U-tube bundle positions in the reaction tank compartment, the four non-tight reaction tank compartments (sectors) and their associated expansion tubes (hydraulic diameter and cross section, friction surface), the free volume in the expansion tank.

Initial conditions of water injection are boundary conditions at injector similarly to previous studies. Flow pressure drop coefficients are considered at injector outlet, at U-tube bundle, at porous fin dividing the reaction tank, at junctions between reaction tank, expansion tubes and expansion tank.

The whole transient calculation of the LIFUS 5 test n°4 is performed up to 1000ms and shows pressure evolutions in the reaction and expansion tanks within a good agreement compared to the experimental recorded ones ; in particular, the calculated expansion tank pressurization is almost similarly delayed after the reaction tank pressurization ; using Cartesian coordinates allows to reproduce the noted important 3D effects, leading to a non-symmetrical radial expansion of the vapour bubble, mainly developing in the reaction tank compartment (containing the water injector and the U-tube bundle) before reaching the expansion tank pressurization ; that, a posteriori, validates the dimensioning factor assumption.

The calculated pressure level is underestimated due to the formulation taken into account in the code (and generally in such multi-phase, multi-component thermal-hydraulics codes) to evaluate a liquid component partial pressure which is obtained on the saturation curve (as a function of the liquid temperature). In the LIFUS 5 experiment n°4 for example, the injected liquid water at 325°C is quasi-instantaneously and quasi-totally vaporized in the "hot" Li/Pb pool (at 330°C) ; the temperature of the very small volume fraction of remaining liquid water is then quickly reduced to 287°C corresponding to a 70 bar partial pressure ; heat transfers between liquid water and liquid metal are then suppressed in order to avoid a too severe time step reduction ; so that, injected liquid water temperature and pressure remain quasi constant till expansion tank pressurization is not beginning.

To correctly evaluate partial pressures (taking into account vapour characteristics : temperature, mass, volume) needs a code development which is underway.

CONCLUSIONS

The LIFUS 5 analysis with Simmer-III using a Cartesian 2D modelling allows to correctly reproduce the important 3D effects on the vapour bubble expansion in the Li/Pb pool which was not possible using the previous 2D/Rz modelling. This allows also to avoid using the 3D code version, much more time consuming.

This LIFUS 5 analysis with Simmer-III will be completed in 2002, taking into account a code model correction for the partial pressure evaluation, now underway, and the representation of the water tank allowing the injected water sub-saturation conditions to be considered. This will achieve the Simmer-III (2D version) code validation devoted to the modelling of the Lithium/Lead water interaction.

REFERENCES

A technical report DER/SERI/LFEA will be available at mid 2002.

TASK LEADER

Jackie LOUVET

DEN/DER/SERI/LCSI
CEA Cadarache
13108 St Paul Lez Durance Cedex

Tél. : 33 4 42 25 27 57
Fax : 33 4 42 25 71 87

E-mail : jlouvet@cea.fr

TW1-TTBA-005-D03

Task Title : SAFETY AND LICENSING TBM and TBM system safety

INTRODUCTION

The International Thermonuclear Experimental Reactor in its reviewed version, ITER-FEAT (Fusion Energy Advanced Tokamak), is currently foreseen to be the only intermediate step towards a fusion power reactor [1, 2].

Apart from plasma studies and component testing, the ITER-FEAT shall be used as a test bed for test modules (TBM, Test Blanket Module) of different tritium breeding blankets for which various conceptual design are under developments in view of a fusion power plant. The Water Cooled Lithium Lead (WCLL) [3] is one of the breeding blanket concepts chosen to be tested in ITER. The testing of breeding blanket modules should not interfere with the ITER operation, decrease ITER reliability and compromise safety of operation or contradict to ITER operational plans [4].

This report summarizes the work carried out in the frame of the task 2001 TW1-TTBA-005-D03. The object of this activity was to perform safety evaluations to make sure that both the WCLL TBM and its ancillary systems comply with the updated ITER safety design limits (i.e. H_2 production, which limits the Pb-17Li inventory in the TBM and in the Pb-17Li loop) and operating conditions (neutron wall load, surface heat flux).

2001 ACTIVITIES

An exhaustive analysis of enveloping events with high potential risk was previously carried out for the WCLL TBM in the previous ITER Final Design Report (1998) and is reported in [5]. Safety analyses and considerations were reviewed in order to adapt them to the ITER-FEAT specifications and operating conditions [6].

Moreover, on the basis of the R&D results, which allowed to better understand the influence of the various parameters in the Pb-17Li/water interaction phenomenon, some preliminary considerations came out (e. g. on the components dimensioning, on the leak detectors) useful for the design of both the TBM and Pb-17Li ancillary circuit.

TBM SAFETY ANALYSES

Several LOCA (loss of coolant accident) events summarized in table 1, were investigated, the most relevant of which are reported thereafter.

Table 1 : Investigated safety relevant events

CASE	A	B	C = A + B	D (a)	D (b)	D (c)	D (d)
event	in-vessel LOCA	in-TBM LOCA	in-vessel and in-TBM LOCA	ex-vessel LOCA			
plasma burn	no at 0 s	yes until Be 1100°C	no at 0 s	yes until 3.5 s	yes until Be at 1100°C	yes until 13 s	yes until 13 s
surface heat flux MW/m^2	0.25 then no at 0 s	0.25 until Be 1100°C	0.25 then no at 0 s	0.25 until 3.5 s	0.25 until Be at 1100°C	0.25 until 13 s	0.25 until 13 s then 4.2 for 1 s
disruption	none	none	none	none	none	none	yes
nuclear heating	no at 0 s	yes until Be 1100°C C	no at 0 s	yes until 3.5 s	yes until Be at 1100°C	yes until 13 s	yes until 13 s
decay heat	yes at 0 s	yes after Be 1100°C	yes at 0 s	yes after 3.5 s	yes after Be at 1100°C	yes after 13 s	yes after 13 s
cooling of SB	no at 0 s	no	no	no	no	no	no
cooling of BZ	no at 0 s	no	no	no	no	no	no
convection on FW	no	no	no	no	no	no	no
radiation from FW	yes	yes	yes	yes	yes	yes/no	yes

Case B : In TBM LOCA

A LOCA in the TBM causes the interaction of the cooling water with the Pb-17Li. The maximum envelop value for reaction enthalpy and hydrogen production were evaluated considering an hypothetical complete reaction of all Pb-17Li inventory present in the TBM and Pb-17Li loop with water. The H_2 produced is higher than fixed limit, so a design modification was envisaged to reduce the Pb-17Li inventory. However, this solution has not been considered in the present TBM design since significant experimental and analytical R&D is underway in the EU to collect more realistic data on Pb-17Li interaction, in particular the release of reaction enthalpy and H_2 release. This experimental and modeling program should demonstrate and quantify soon the limited effect of this reaction.

As far as the thermo-mechanical behavior of the TBM is concerned, it was assumed that in case of a in-TBM LOCA the TBM segment box will be also submitted to the injected water pressure (15.5 MPa). In accord with IISDC criteria, in faulted conditions, total primary stresses must be lower than the minimum between 0.7 Sy and 2.4 Sm at corresponding temperature. It was demonstrated that only limited design evolution (increasing of the steel box corner radius) was necessary to guarantee the box integrity with regard to IISDC criteria [7]. The maximum Von Mises stress is 407 MPa and the minimum margin to IISDC criteria is 10 MPa. Results from thermo-mechanical calculations are summarized in table 2 and Von Mises stress distribution in steel is shown in figure 1.

Table 2 : Thermo-mechanical behaviour of the steel segment box in case of 15.5 MPa pressurization

Max. von Mises stress level [MPa]	407
Min. margin to IISDC criteria [MPa]	10

Case D: Ex Vessel LOCA

No safety credit is given for the fact that two independent cooling systems are available. Here, two large ex-vessel breaks in the cooling circuits are assumed so that no active cooling is available at all. Concerning the behavior of the TBM itself during these accidents, four distinguished sub-cases are considered As far as thermal behavior is concerned, ex-vessel LOCA without active plasma shutdown and ex-vessel LOCA with active plasma shut-down after delayed accident detection with disruption are the most stringent accidents because of plasma burning even after event.

In the case of **ex-vessel LOCA without active plasma shutdown** it assumed that the accident remains undetected and the plasma continues to burn with the surface heat flux of 0.25 MWm^{-2} until the Be reaches a temperature of 1100 °C. At this temperature, the Be armor starts to sublimate into the plasma and extinguish it so that the nuclear heating and the surface heat flux drop to zero. No disruption is assumed and decay heat remains the only heat source. Radiation from the FW is considered as the only heat sink.

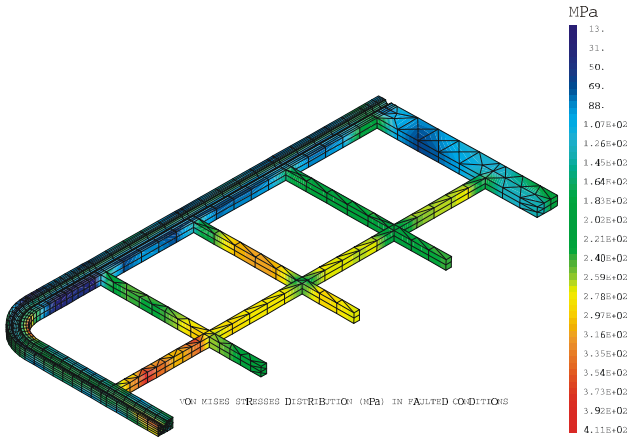

Figure 1 : Von Mises total stresses distribution in faulted conditions

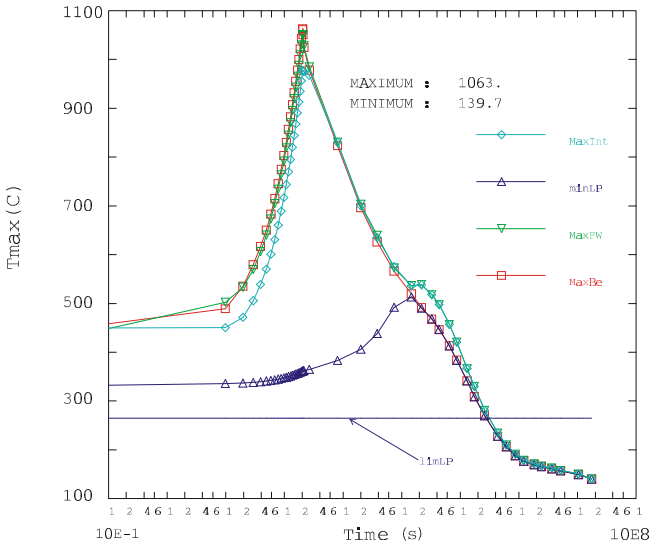

Figure 2 : Temperature evolution in the TBM: no active plasma shutdown until T_{Be} = 1100°C, no disruption, radiation from the FW

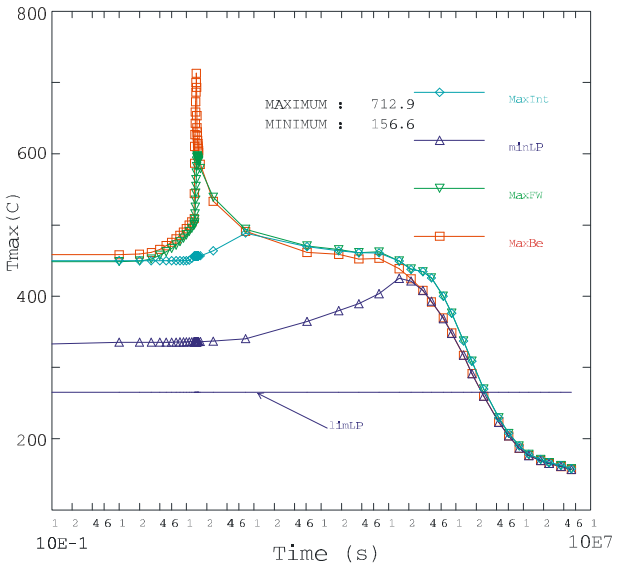

Figure 3 : Temperature evolution in the TBM: active plasma shutdown after delayed accident detection, disruption, radiation from the FW

The temperature of the inboard blanket is assumed to be identical to the coolant inlet temperature there, i.e. 100 °C, the emissivity of the Be is taken as å= 0.3. The resulting temperature evolution is plotted in figure 2. The Be armor reaches a temperature of 1100°C after slightly more than 200 s.

The Pb-17Li starts to solidify after 3.5 days (minimum temperature reaches 235° C), then the TBM temperature would remain constant at 235°C due to the release of latent heat of fusion (115 MJ).

Another relevant case is **ex-vessel LOCA with active plasma shut-down after delayed accident detection and with disruption**. In this case it is assumed that the accident can be detected only after 10 s (instead of 0.5 s, e. g. due to failure of detection) and the plasma can be shut-down in another 3 s after the event (total delay between accident and plasma shut-down 13 s).

The plasma shut-down is assumed to be followed by a disruption. The peak surface heat flux of 0.25 MWm^{-2} and nominal nuclear heating continue until 13 s. Then the nuclear heating drops to decay heat while the disruption discharges a surface heat flux of 4.2 MWm^{-2} for 1 s on the TBM FW. Afterwards, radiation from the FW is assumed to be the only heat sink.

In this conservative case, the Be temperature reaches a very short peak of 720 °C just after the disruption. The decay heat can then be evacuated by radiation only, as shown in figure 3.

Pb-17Li ANCILLARY CIRCUIT

Recent R&D activities allowed to better understanding the influence of the various parameters in the Pb-17Li/water interaction phenomenon. Some preliminary considerations came out (e. g. on the components dimensioning) useful for the Pb-17Li loop design.

Purge Pipe diameter

BLAST experiences showed that diameter of the expansion tube strongly influences pressure peak reached in the reaction vessel during the first phase of the reaction [8]. In BLAST 7 and 9 tests, where diameter of the expansion tube was decreased from 50 to 8 mm, this peak overcame the pressure of injected water, the value of which has been used for the dimensioning of the TBM segment box. While modeling of the Pb-17Li/water interaction in the real TBM geometry is not still available, preliminary considerations can be drawn comparing hydraulic diameters of the TBM with those of the LIFUS facility, where the pressure reached in the reaction vessel never overcame the pressure of the injected water.

In LIFUS facility, hydraulic diameter of the reaction sector is 7 cm, and the expansion tube one is 1 cm. Hydraulic diameter of a TBM elementary cell varies between 7 cm (for the channels nearest the FW) and 12 cm (for the rear channels), and the diameter of Pb-17Li purge line is fixed to 1.7 cm, which should guarantee against the overpressure.

Expansion vessel

Looking at pressure evolution in the test n 3 of LIFUS-5 facility, it can be seen that pressure decreases in the expansion vessel coincide with the pressurization of expansion vessel, which takes place when gaseous products reach free surface.

Furthermore, a second pressurization in reaction vessel starts when expansion vessel free volume was pressurized. Expansion vessel plays, thus, a very important role in the evolution of various parameters.

In the TBM detritiation system, drain tank, which would accomplish also this function, is placed about two meters behind the TBM. Eventually, the line relying the two components leaves TBM from the bottom and it is not straight.

A modification of the Pb-17Li ancillary circuit is, thus, envisaged with the addition of an expansion vessel having a volume of 0.036 m^3, corresponding to 10% of Pb-17Li volume in the TBM.

It is placed behind the TBM as close as possible from the TBM and as high as possible, compatibly with the other connecting pipes.

Two possible arrangements are actually in study, shown in figures 4 and 5. In the first option the TBM is directly connected with the expansion vessel, which is partially filled with the liquid metal. Varying the filling level the compressibility of the entire system can be varied, and then the pressure evolution.

In particular, increasing the free volume leads to lower value of first pressure peak and slows the reaction kinetics. On the other hand, as shown by LIFUS 4 experience, increasing the free volume involves reducing pressure in the reaction vessel, which could increase the quantity of injected water and then released energy.

In this frame, a compromise could be the option 2, which aims to maximize the free volume of the expansion vessel, keeping it separate from the drain tank. The expansion vessel is connected to the TBM through a rupture disk dimensioned for a pressure slightly higher than the nominal one.

Only in case of accident, liquid metal will enter the expansion vessel. However, the rupture disk is in direct contact with the liquid metal, what constitutes a serious drawback because of the corrosion.

In both cases, expansion vessel is connected with the drain tank through a rupture disk dimensioned for 15 MPa.

In accord to the strategy actually proposed to manage a Pb-17Li water accident, once the leak is detected and compatibly with vaults closing times, the TBM, together with the expansion vessel is sealed off in order to confine hydrogen and other reaction products and reduce the quantity of injected water.

Therefore, either it is displaced in the hot cell without previous Pb-17Li draining (only TBM and expansion vessel will be, thus, affected by the accident) or Pb-17Li is discharged in drain/storage tank before the TBM moves to the hot cell.

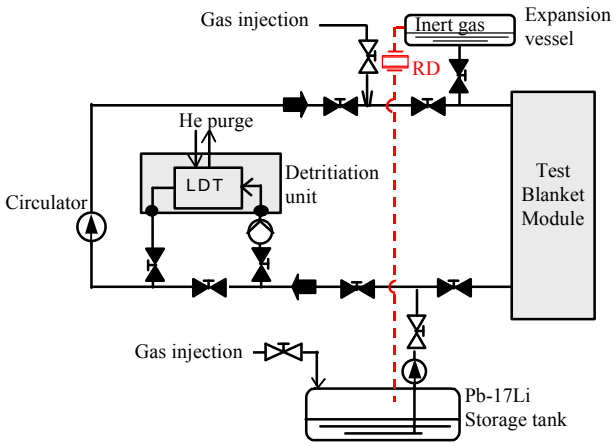

Figure 4 : Flow diagram of the Pb-17Li ancillary circuit, option 1

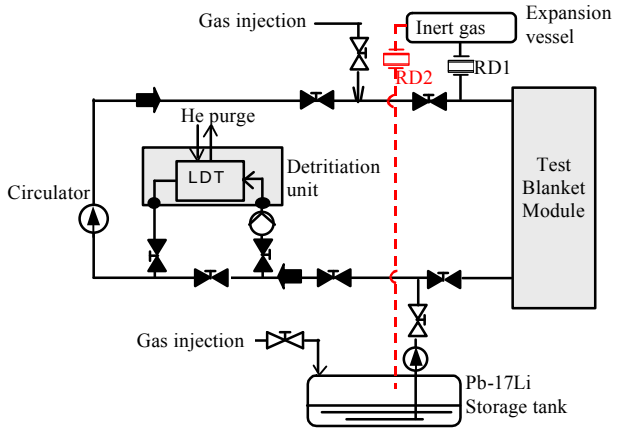

Figure 5 : Flow diagram of the Pb-17Li ancillary circuit, option 2

The choice between the two strategies depends on the allowed limit weight of the transporter task, but also on the evolution of various parameters (pressure in the TBM and in the expansion vessel, temperature, etc.) after the accident. The modeling of the water/Pb-17Li interaction in a TBM like geometry appears, thus, of fundamental relevance. This modeling should be coupled with those of the **BZ water circuit**, in order to evaluate the quantity of water injected in the Pb-17Li. Actual accident management strategy foresees the pumps stop and the seal off of the BZ water circuit after the tube break. Due to depressurization at the tube break, water present in other tubes and in collectors is sucked in towards tube ends. At the same time, blow down of the circuit is contrasted by increasing pressure on the Pb-17Li side. Eventually, the complexity of the tubes geometry and in particular bends could generate steam plugs and then stop the flow. Finally, the eventuality of stopping pumps failure should be taken into account. The study of the transitory following a tube break in the BZ circuit needs more detailed analyses with suitable thermal-hydraulic codes.

CONCLUSIONS

This report summarizes the work carried out in the frame of the task 2001 TW1-TTBA-005-D03, the object of which was to perform safety evaluations to make sure that both the WCLL TBM and its ancillary systems comply with the updated ITER-FEAT specifications and operating conditions.

Several transient scenarios following a LOCA have been assessed, showing that for examined cases, consequences are of manageable gravity. Calculations showed that the only radiation from the FW could guarantee the evacuation of the residual heat. Pb-17Li inventory present in the TBM and Pb-17Li loop is higher than the limit value.

However, this limit was fixed supposing, in a conservative manner, that all liquid metal will react with water in case of accident, while experimental and modeling program is underway in the EU, which should demonstrate and quantify soon the limited effect of this reaction (in particular in terms of the reaction enthalpy and H_2 releases).

On the other hand, a design modification was envisaged to reduce this inventory, if that will be mandatory.

From the thermo-mechanical point of view, only little modifications are needed to the design in order to guarantee the box integrity in case of pressurization.

Finally on the basis of the experimental results, some modifications have been brought about. An expansion vessel will be placed as close as possible from the TBM in order to better control the pressure and temperature evolution inside the TBM in case of water leak in the liquid metal.

REFERENCES

[1] R. Aymar, ITER achievements by July 1998 and future prospects, Fus. Eng. Des. 46 (1999) 115-127.

[2] R. Aymar, The ITER Reduced Cost Design, Fus. Eng. Des. 49-50 (1999) 13-25.

[3] L. Giancarli et al., Development of the EU water-cooled Pb-17Li blanket, Fus. Eng. Des. 639 (1998) 39-40.

[4] EFDA, ITER Final Design Report, Design Requirements and Guidelines Level 1(DRG1), July 2001.

[5] M. Fütterer, L. Giancarli & WCLL Team, Design Description Document (DDD) for the European water-cooled Pb-17Li Test Blanket Module (version included in the ITER final design report), CEA report DMT 97/549, December 1997.

[6] EFDA, ITER Final Design Report, Plant Design Specification, July 2001.

[7] F. Toubol, IISDC (ITER Interim Structural Design Criteria) Final Report (Contract NRT 93-315): Part I, Rapport DMT/95/243, 10/05/95.

[8] P. Sardain, G. Benamati, I. Ricapito, G. Marbach, Modelling of the Pb-17Li/Water interaction within a blanket module, Fus. Eng. Des., 51-52, (1999) 611-616

REPORTS AND PUBLICATIONS

[1] A. Li Puma, Y. Poitevin, Safety of the WCLL blanket module system: impact of the ITER specifications and integration of the R&D, CEA Report, SERMA/LCA/RT/01-3023

TASK LEADER

Antonella LI PUMA

DEN/DM2S/SERMA/LCA
CEA Saclay
91191 Gif-sur-Yvette Cedex

Tél. : 33 1 69 08 79 76
Fax : 33 1 69 08 99 35

E-mail : alipuma@cea.fr

Task Title : MHD EFFECTS
Test and modelling of natural MHD convection

INTRODUCTION

The international project of a thermonuclear fusion reactor generates a lot of technological problems. In the blankets around the plasma is a liquid metal (Pb-Li) that is submitted to the high heat flux due to fusion and to the strong horizontal magnetic field necessary to confine the plasma.

The blanket has the double role to transfer the heat to a network of water coolant U-tubes, and to regenerate, by neutronic reaction, the fuel of the fusion (Tritium). Contrary to the heat, this last one must not penetrate in the water, but must be carried outside by a low flow rate, where it can be extracted from the Pb-Li.

The mechanics and the transport phenomena in the blankets have motivated the present study about buoyancy driven magneto hydrodynamic convection in vertical enclosures.

The basic phenomena are investigated with a simplified geometry: the liquid metal is in a vertical enclosure with a square cross section, heated at one vertical wall, and cooled at the opposite wall.

The magnetic fields of main interest are horizontal, either parallel, either perpendicular to adiabatic walls (and so to the mean heat flux). The study has been done considering all walls as electrically insulating, which gives the most interesting phenomena, and also corresponds to the case where U-tubes have permeation barriers. This report gives the main results obtained during the third and last year of this study.

Without coming back on what has been done in the two past years, I want to remind that this study has three approaches, analytical, experimental and numerical. All of them have been necessary to understand the basic phenomena, and to improve our numerical tool.

2001 ACTIVITIES

New tools have been built under Matlab to help visualisation of numerical results:

- 2D: plot of scalar (3D plot or isolines for temperature, electric potential) and of lines of conservatives vectors (velocity),

- 3D: 3D plot of scalar by planes of isovalues; particle tracing.

THE PERPENDICULAR CONFIGURATION

The thermal jets regime (or stratified flow)

The temperature in the stratified core has a linear variation with the vertical coordinate, and a cubic variation which is confined in the end regions, as it is shown by the numerical simulation:

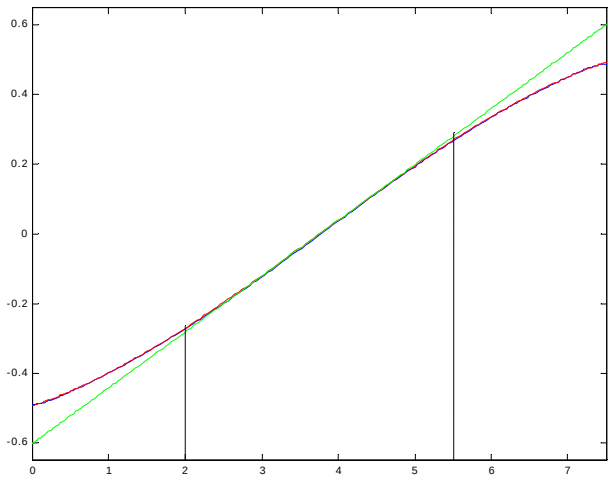

Figure 1 : Temperature along the vertical plane x=0 (blue) Green : Linear approximation; Red: cubic approximation

The value of the slope α depends on the end regions. One way to remedy to the incomplete characteristic of the model is to take the value of the slope given by numerical simulation. The figure below shows this value in function of the parameter Ra/Ha.

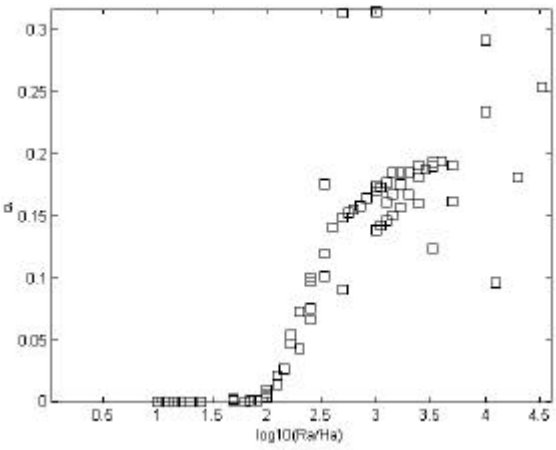

Figure 2 : Central temperature gradient in function of the parameter Ra/Ha

The simulations shows that stratified flow occurs for Ra/Ha>300, and that the order of magnitude of α is H^{-1} (H=7.5 is the aspect ratio of the cavity).

A pure analytical model can be build taking $\alpha=H^{-1}$, and it gives the scaling laws for the thickness of the jet, for Nusselt number, etc...

But a better comparison should be done with the value of the slope of α given by a numerical simulation.

The following graph compare the thickness obtained both by the numerical simulation (in black) and the analytical modelling (in red).

It shows that even if a factor 2 exist between both thickness, their order of magnitude and their evolution with z agree.

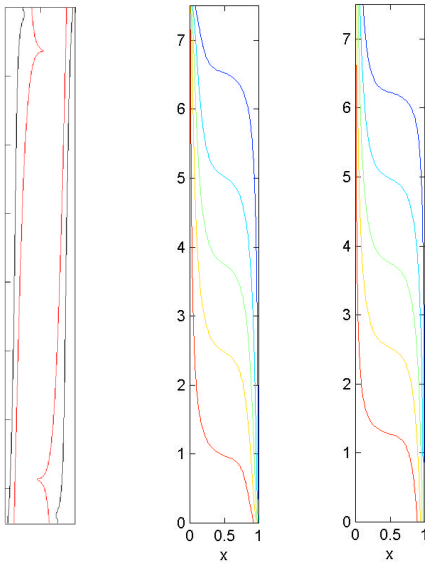

Figure 3 : Comparison of the analytical and numerical modelling of thermal jets. Left: thickness of the jet. Black : numerical, red: analytical. Centre: isotherms obtained by numerical simulation. Right: isotherms obtained by the analytical modelling

The flow rate is confined in the jet, so that the length L is not significant, and the viscous sub layer is not $Ha^{-1/2}$, but $Ha^{-1/2}.\delta_{th}$. We can remind that the simulation of the stratified flow has been confirmed by the experiment, as shown in figure 4.

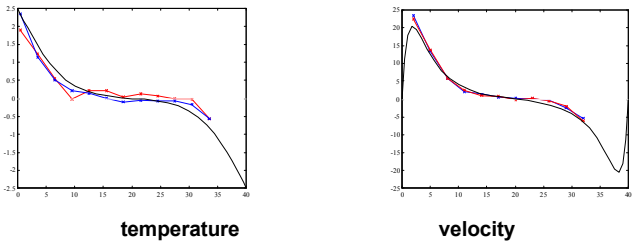

Figure 4 : Profiles of temperature and velocity at mid-high of the cavity. Black: numerical / red & blue: experimental

The pluri-cellular regime

The numerical simulation shows that a transition from mono to pluri-cellular regimes occurs for given Ra/Ha^2. At low Ra and Ha, this transition lead to a stable and well-structured flow, whereas for high values of these parameters, it leads to a very less structured flow, subject to oscillations, and near from chaos. In the first case, each vortex has the structure described in the precedent paragraph of a stratified core flow and thermal jets (figure 5).

This transition needs a strong re-organization, and should happen with hysteresis (figure 6). The following graph shows the result of a numerical simulation with decreasing and increasing Hartmann number ($Ra=10^5$ constant). The abscissa axis gives, in a logarithmic scale, the Hartmann number, and the ordinate axis gives the mean velocity.

The transition from the mono-cellular to the 3-cellular regime (Ha decreasing, solid curve) occurs when the slope change from Ha^{-1} to Ha^{-2}, ie for Ha*~300. Since the code use the modelling of Hartmann layers, it cannot well simulate flows for Ha<50. The second curve (Ha increasing, dashed curve) shows that the 3-cellular regime remains a longer time, but become instable. The reverse transition (3 to 1 cell) occurs at Ha**~630. At higher Raleigh numbers, other transitions can be observed, as “3 to 5 cells”, with 2 contra-rotative vortex, and also a “5 to 7 cells” transition, with 3 contra-rotative vortex.

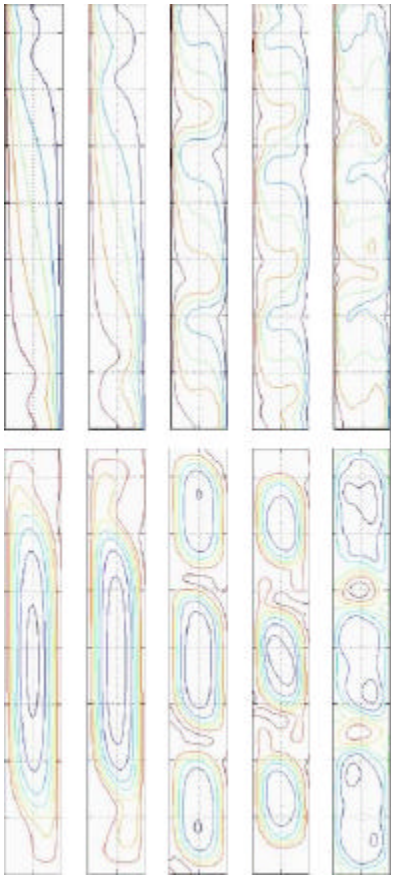

Figure 5 : Numerical simulation for increasing parameter Ra/Ha : (Ra, Ha)=(10^5,300); (10^5,250); (10^5,200); (10^5,100); (10^6,100). Above : isotherms; Below: streamlines

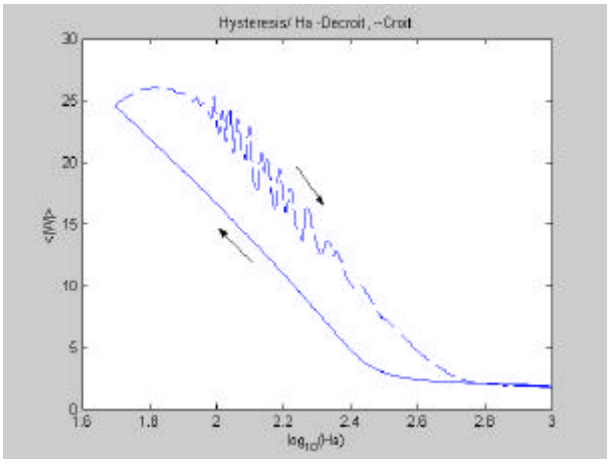

Figure 6 : Hysteresis cycle for the mono/pluri cellular transition. Absolute average of vertical component W of velocity in function of Hartman number (logarithmic scale)

Simulation of bidimensional turbulence

Bidimensional turbulence is much more determinist than classic three-dimensional turbulence. This is why the numerical code, developed for laminar flows can easily be used to simulate steady turbulent bidimensional flows. However, transient regimes (necessary to begin a simulation) are computed with a violation of conservation laws, in order to reduce the computation time. The following graph shows the result for $Ra=10^7$, Ha=400. Let us make some observations: the vortices stir the fluid so that the temperature is locally uniform, and the main variations are located in thermal boundary layers (they are no longer jets). The heat flux is carried by the external part of vorticies. The vorticies are always moving, merging each other, and dividing themselves.

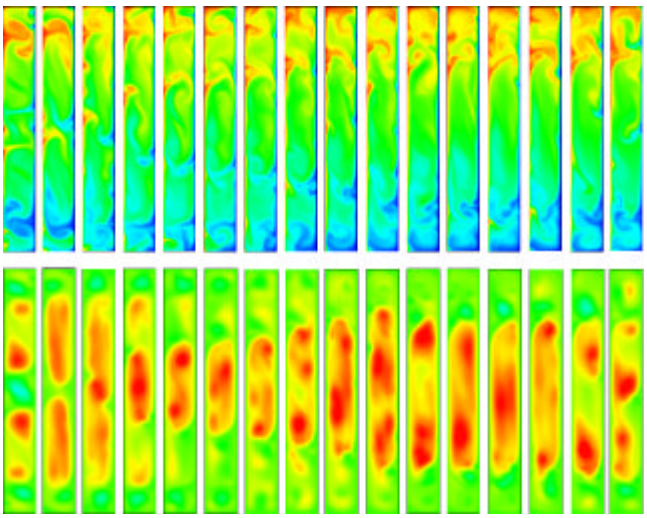

Figure 7 : Simulation of turbulent flow for $Ra=10^7$, Ha=400

The bifurcation diagram

The numerical simulation allows to draw a bifurcation diagram (fig 8) where the main regimes are situated.

Depending on increasing parameter Ra/Ha, there are successively: a conductive regime (mono-cellular); a stratified regime (mono-cellular); some pluri-cellular regime (laminar or turbulent, depending on the Raleigh number); and a chaotic regime.

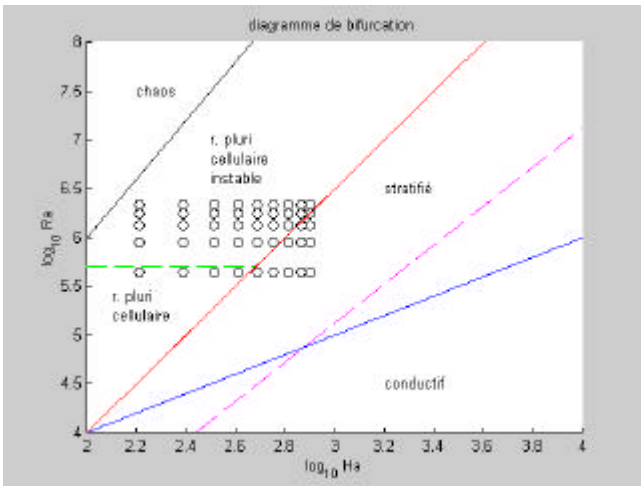

Figure 8 : Bifurcation diagram in $log_{10}(Ra,Ha)$ plane. Solid lines: frontiers between regimes; dotted line: theoretical frontier between stratified and pluri-cellular regime; circles: experimental points

THE PARALLEL CONFIGURATION

One of the most important challenges was to understand the instabilities and the turbulence in jet side layers. Let us remind that in laminar regimes, side layers of thickness $Ha^{-1/2}$ carry out almost all the flow rate. The sign of buoyancy, and so of velocity change along the layer (in the direction of the magnetic field). Those characteristics are shown in figure 9. The Reynolds number of the laminar layer is $Re \sim Gr.Ha^{-3/2}$.

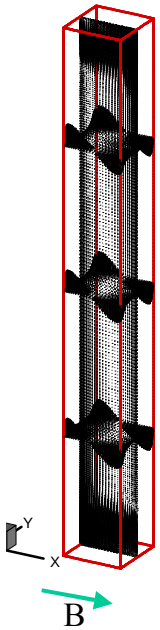

Figure 9 : Velocity vectors in the parallel configuration, laminar flow

Some previous studies for jet side layers, but in forced flows (so that the velocity has the same direction in the whole side layer) suggest that critical Reynolds number to reach instabilities in such jets should be about 2000. Some experimental work have shown that due to the parabolic shape of the velocity in the layer, a vortex is carried away with a higher velocity in the centre of the jet than in the border. The consequent distortion of the vortex causes its extinction, until the laminar profile is regenerated and leads to another vortex. Jets side layers are therefore at the origin of a periodic phenomenon, with low frequency turbulence. In the buoyancy driven convection studied here, the diffusion of vorticity is hindered by two factors. First both parts of the layer generate opposite vorticities, and second, the mean laminar flow carry both parts in opposite direction. This is why we suggest that the symmetry of each side layer is broken with the lengthening of one jet, at the disadvantage of the other. As in forced flows, the time life of a vortex is its distortion time, given by the mean flow. To reach instabilities and turbulence in this configuration, we must simulate a high flow rate in a thin layer, which means that both Hartmann and Raleigh numbers must be high. The difficulties are first that computation times are long with high Ra, and needs a lot of meshes for thin side layers. As the computation as already 3D, the mesh grid cannot be refined. We decided to make a computation with 32 (magnetic field direction) x 64 (direction normal to the side walls) x 240 (vertical direction), with Ha=300, so that there are 8 points through the jet. A first series of simulations have been done, allowing larger violations of conservation laws, in order to compute faster transient regimes. The first instability has been observed for $Ra=2.10^8$, and correspond to the very high critical Reynolds number $Re^*\sim2.10^6$. The figure 10 represents the temperature variations in the middle of the side layer. The distortion time (the red segment), calculated with the in homogeneities of the laminar jets, is compared to the typical period of oscillations. The agreement confirms our scenario of the birth and death of vorticies.

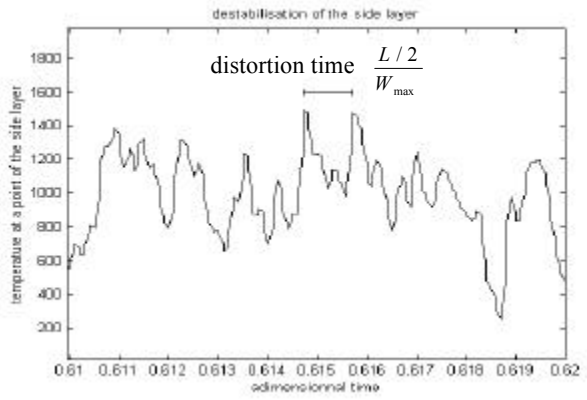

Figure 10 : Temperature signal in a turbulent jet side layer. $Ra=2.10^8$, Ha=300

A more precise simulation has been done for $Ra=3.10^8$, with an optimisation of the tolerances on conservation laws. 1 month was needed to perform the computation. It shows that turbulence do not appear immediately. The transient regime leads to a laminar flow with local instabilities, which needs some time before becoming turbulent.

This shows that two regimes exists for the same conditions, the laminar regime being metastable. This phenomenon is also interpretable in terms of sub-critical bifurcation between laminar and turbulent flow.

CONCLUSIONS

At the end of this study, the main characteristics of the flows have been cleared. In both perpendicular and parallel configurations, we have a more accurate view of the different regimes, the place they take in the (Ra, Ha) plane, the magnitude of some quantities of interest depending on these two parameters, and the kind of transitions which happen between different regimes. An analytical modelling of Hartmann layers has already allowed to avoid a difficult meshing in a such thin layer, to save CPU time and memory, and to give an exact result. Now our analytical modelling of thermal jets and of their viscous sub-layers, shows that these sub-layers are also too thin to be correctly meshed. It is therefore possible to give simple boundary conditions that should be applied to the jet, on the side of the wall. Some variations of our numerical tool have already been realized to improve computations. This kind of experimentation allows to develop and to test some methods to extend the possibilities of the numerical code. Therefore, our knowledge allows to lay the foundations for a more powerful numerical tool, adapted to more complex geometries.

REPORTS AND PUBLICATIONS

[1] G. AUTHIER et al, “NATURAL CONVECTION UNDER INTENSE MAGNETIC FIELD IN VERTICAL ENCLOSURES”, NT DER/STR/LCET 01-083,

[2] G. AUTHIER “Convection naturelle sous champs magnétique en cavité verticale élancée. Application aux couvertures des réacteurs de fusion. », Thèse de l’Institut National Polytechnique de Grenoble soutenue de 28 Mars 2002.

TASK LEADER

Lionel CACHON

DEN/DER/STR/LCET
CEA Cadarache
13108 St Paul Lez Durance Cedex

Tél. : 33 4 42 25 74 25
Fax : 33 4 42 25 66 38

E-mail : lionel.cachon@cea.fr

TW1-TTBB-002-D02

Task Title : BLANKET MANUFACTURING TECHNIQUES Mock-up of first wall manufactured with alternative reduced cost fabrication technique

INTRODUCTION

The Helium Cooled Pebble Bed (HCPB) blanket concept is one of the two european breeding blanket concepts.

This task is devoted to a preliminary assessment of the HCPB first wall feasibility (i) using HIP diffusion welding and (ii) starting from simple raw components like rectangular tubes and thin plates. The material is Eurofer.

2001 ACTIVITIES

DESCRIPTION OF THE PROCESS

The HCPB FW is shown on figure 1 together with cooling/stiffening plates. Two different processes have been up to now considered for the fabrication of the FW, both relying on the Hot Isostatic Pressing technique [1], [2] with bending of the whole structure as a last step.

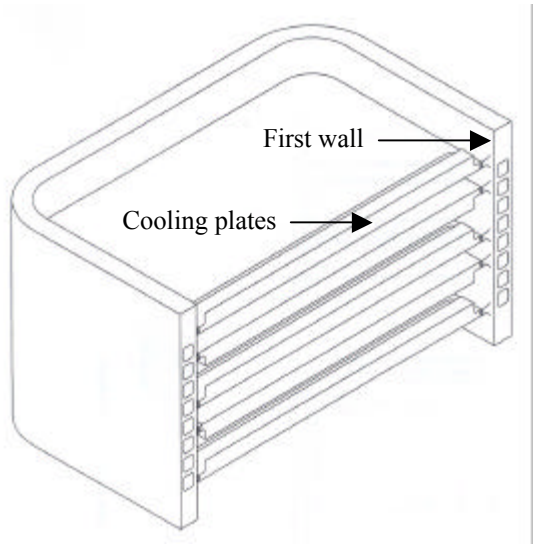

Figure 1 : Simplified 3D view of the HCPB blanket

In this work, a first preliminary study of an alternative process has been made. It consists in manufacturing the FW from simple components, namely rectangular tubes and thin plates.

The main difference with previous processes is that tubes and plates are individually bent before HIP, controlled and eventually rejected. Then, the structure is HIPed and heat-treated.

The main advantages of this alternative method are the following :

- only small components have to be bent, there is no need for highly powerful presses and the failure of a tube during bending does not have large consequences from the cost point of view;
- the design of the structure allows avoiding risks of channel deformation during HIP because the tubes are kept open;
- there is no need to add high extra thickness to the components to account for machining after HIP.

SMALL STRAIGHT MOCK-UP MANUFACTURING

First, Eurofer rectangular tubes were manufactured by machining and electron beam welding. Figure 2 shows the EB weld (made by one pass transparency welding). The overall dimensions after EBW were close to the expected ones, with the exception of some excess material at the weld exit (figure 2, right hand side). The tubes tightness was controlled by helium leak testing. No leak could be detected. As far as the weld microstructure is concerned, some delta ferrite grains have been observed in the melted zone (or close to it) but no cracks nor pores.

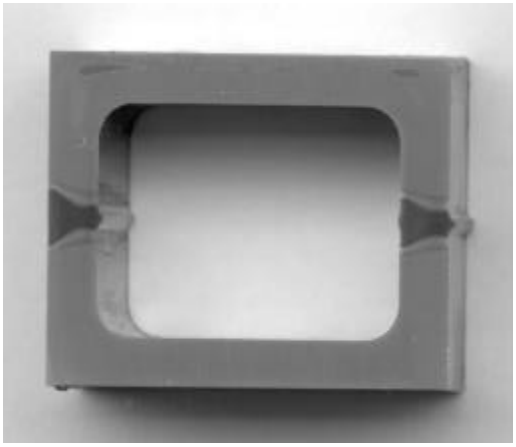

Figure 2 : Cross section of an EB welded rectangular channel (real size 20x24mm)

A small HCPB FW mock-up was manufactured as follows : the excess material on the channels right side was machined by dry milling, the channels and two plates were degreased using solvents, dried and seal welded as shown on figure 3. The mock-up was HIPed at 1100°C, 100MPa for 2h, heat treated at 950°C for 2h, gas quenched and tempered at 750°C for 2h.

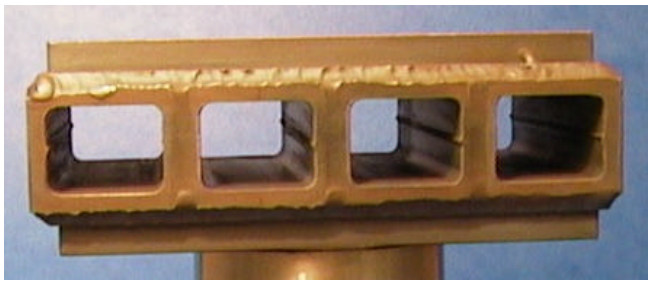

Figure 3 : Small straight HCPB FW mock-up (four channels 100mm long)

SMALL MOCK-UP CHARACTERISATION

As expected, no significant deformation was observed after HIP. The corners of the tubes were not perfectly sharp, resulting in a gap at the tube/plate/tube triple line. Figure 4 shows that the gap was filled by plate deformation : the joint has a V shape at the triple line. It can be also seen from figure 4 that the joint presents numerous inclusions, due to a slight oxidation of the tube surfaces during EB welding. In the weld region, where the excess material was removed by dry milling after EBW, the interface does not present any inclusions (figure 5).

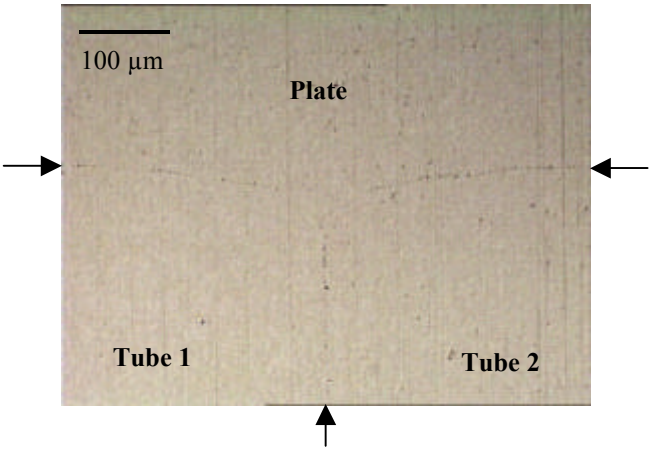

Figure 4 : Small straight HCPB FW mock-up, tube/plate/tube joint (marked by arrows)

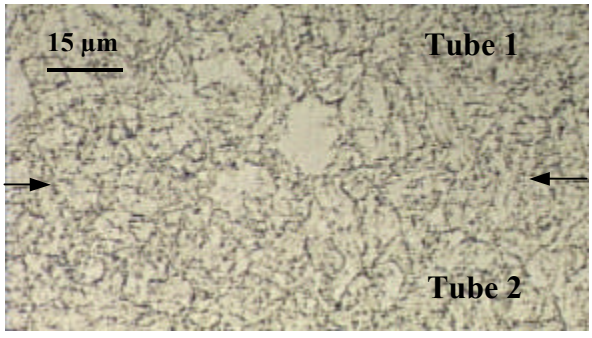

Figure 5 : Tube/tube joint microstructure in the EB weld zone.

Reduced size V notch specimens have been machined from the mock-up and broken at 20°C. As expected from the joint microstructure, the mean absorbed energy is low : 2.5J (mean value over 5 specimens) compared to 9.5~J for the base material. The rupture occurs mainly at the joint with little plastic deformation (figure 6).

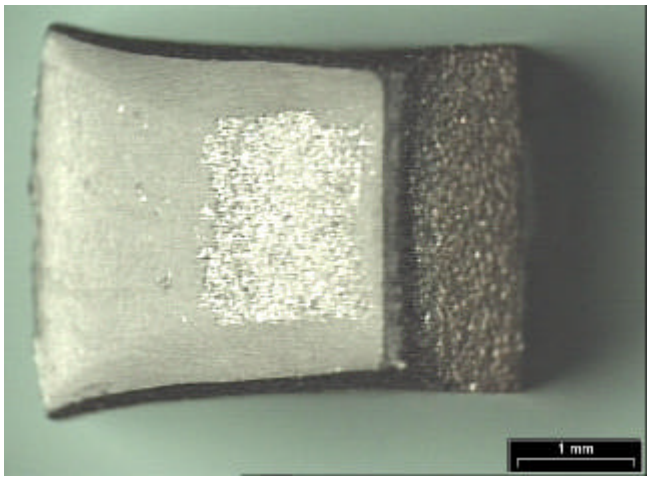

Figure 6 : Joint surface of rupture at 20°C (reduced size impact toughness specimen).

BENDING OF CHANNELS

On the basis of the experience gained with the small straight mock-up, the fabrication of channels by EB welding was abandoned. A set of Eurofer channels, 400mm long, was manufactured by deep drilling and electro-discharge machining. Before machining, the material was soft annealed in vacuum in order to decrease its hardness down to the minimum achievable. This facilitates bending because it decreases the yield strength of the material, increases its ductility and reduces springback.

The channels will be bent at 90° and used for the fabrication of a curved mock-up by the end of march 2002.

CONCLUSIONS

Short first wall channels have been manufactured by machining and electron beam welding. The dimensions of the channels were satisfactory. A small straight mock-up was fabricated by HIP diffusion welding using such Eurofer channels and two plates. As expected, no significant deformation was observed after HIP. Due to a slight oxidation during EB welding, the diffusion-welded joints did not exhibit sufficiently high mechanical properties. To avoid this problem, long channels have been manufactured with another process in view of the fabrication of a curved mock-up. Work is in progress.

REFERENCES

[1] S Gordeev, T Lechler, K Schleisiek, HJ Fiek “Revised design and manufacturing of the EU HCPB Test Blanket Module (TBM) for ITER, Subtask B2.1.1”, report IRS Nr 23/98 – PKF Nr 126, december 1998.

[2] E Rigal, Ch Grandjacques, F Bruchon “Second bent HCPB first wall mock-up manufactured by improved HIP forming techniques, subtask TW0-TTBB2.3”, report NT DTEN no. 61/2001, 27 june 2001.

REPORTS AND PUBLICATIONS

E Rigal, C Grandjacques, F Bruchon “HCPB First wall mock-up manufactured with an alternative reduced cost fabrication technique”, CEA Report, to be issued.

TASK LEADER

Emmanuel RIGAL

DRT/DTEN/SMP/LS2M
CEA Grenoble
17, rue des Martyrs
38054 Grenoble Cedex 9

Tél. : 33 4 38 78 97 22
Fax : 33 4 38 78 54 79

E-mail : emmanuel.rigal@cea.fr

Task Title : BLANKET MANUFACTURING TECHNIQUES
First wall manufacturing by HIP forming technique

INTRODUCTION

The Helium Cooled Pebble Bed (HCPB) blanket concept is one of the two european breeding blanket concepts. This task is devoted to the feasibility assessment of the HCPB first wall using the HIP forming method. In late 2000, a mock-up was manufactured using grooved plates and tubes inserted in-between them. The material was Eurofer. The characterisation of the mock-up is described hereafter.

2001 ACTIVITIES

BENDING AND DIMENSIONAL ACCURACY

The mock-up was heat treated to restore a fine grain size (austenitisation at 950°C, 2 h) and to soften the material in view of bending (tempering at 750°C, 2 h). The mock-up was bent by Forschungsgesellschaft Umformtechnik using an hydraulic press. In order to limit the deformation of the channels, they were filled with a low melting point alloy (Bi-Sn eutectic alloy).

Due to the limited press capacity, it was not possible to add carbon steel plates as usually done to minimise the deformation. Bending location was at about $^2/_3$ of the total length. A 50 mm radius stamp was used, which corresponds to a ~75 mm bending radius at mid-plane of the mock-up. The mid plane (neutral plane) is the plate-to-plate bond.

The mock-up was controlled after bending. The bending angle was 89°15' (the specification was 90°± 1) and the radius 47.6 mm. A view of the mock-up during dimensional measurement is given in figure 1.

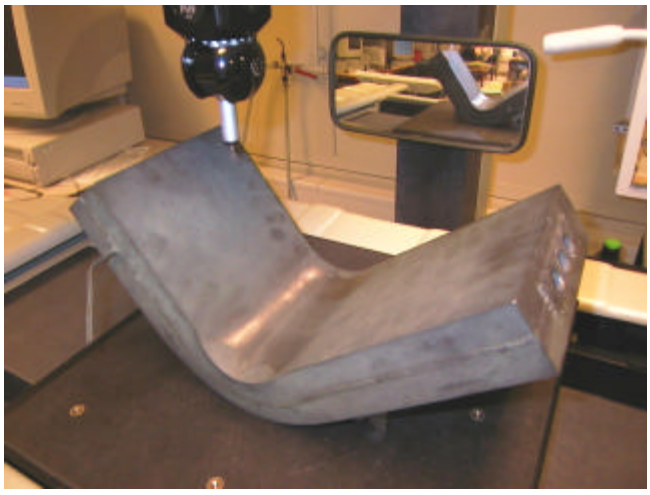

Figure 1 : HCPB FW mock-up after bending

The mock-up was heated to 150°C to empty the channels and stress relieved at 720°C for 1 h. During this treatment, the bend angle increased to 90°53'. A view of the mock-up after machining is shown in figure 2.

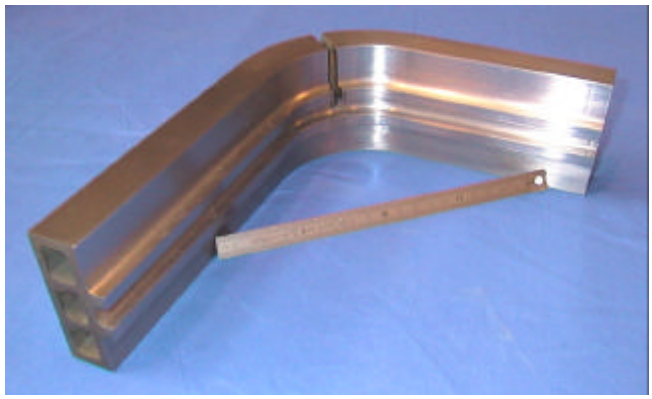

Figure 2 : HCPB FW mock-up after machining

In the straight region (figure 3), the maximum plate thickness reduction is about 0.7 mm. Due to tube expansion, the size of the channels exceeds the design value. Thicker tubes would be necessary to counterbalance the tube wall thinning. The width and the height oversize are roughly proportional for the side channels (+2 to 2.5 %), but for the middle channel, only the width is too large (table 1). In the bent region (figure 4), the channels are no more located at the mid-thickness of the plate. The radius at the centre of the channel axis is however very close to the aimed value : 74.9 mm and 74.7 for channels B and C respectively. The channels are more severely flattened than in the straight zones.

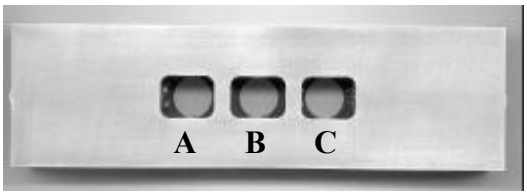

Figure 3 : Channels in straight region

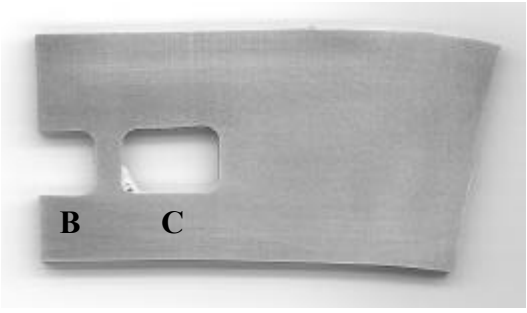

Figure 4 : Channels in bent region

Table 1 : Channel and rib dimensions (design values : channels 14x18mm, rib 6mm)

Zone	Channel A	Rib A-B	Channel B	Rib B-C	Channel C
Straight	14.3 x 18.5	5.2	14.0 x 18.8	5.2	14.3 x 18.6
Bent	-	-	12.2	5.3	12.3 x 18.9

Table 2 : Joint tensile properties (tested at 4 10^{-4} s^{-1})

Specimen	σy 0.2%	σr	Total elongation	Uniform elongation	Reduction of area	rupture
1	523 MPa	642 MPa	15.3 %	5.3 %	77 %	Away from the joint
2	533 MPa	642 MPa	18.1 %	7.4 %	74 %	Away from the joint

Table 3 : Joint and base material impact properties. (*) notch machined away from the joint

Specimen	Individual values (J)	Mean value (J)
Joint	7.4 / 7.4 / 7.5 / 6.8 / 7 / 7.4 / 7.6 / 7.1 / 7.3 / 7.8	7.3
Base material*	11 / 11.2 / 11 / 11.4 / 11	11.1

JOINT MECHANICAL PROPERTIES

The mean hardness of the material is Hv10 = 206 (5 indents). The stress relieving heat treatment did not significantly decreased the hardness achieved after tempering. Tensile and 27 x 4 x 3 mm KLST impact specimens were cut from the mock-up. Specimens were cut from the central zone side and broken at 20°C. The results are given in table 2 and table 3.

The joint tensile properties are fully satisfactory as they fulfil the Eurofer specifications.

The joint impact toughness is rather high, about 7.5 J. Rupture occurs at the joint. Despite a 50 J lever was used, the specimens did not broke completely, so the real toughness is underestimated.

CONCLUSIONS

A second HCPB first wall bent mock-up was fabricated with the HIP forming process. The manufacturing conditions were properly chosen and the tube expansion during HIP did not lead to failure, contrary to the first bent mock-up which failure was due to an inappropriate soft annealing treatment applied to the tubes.

The channel dimensions in the straight part of the mock-up are slightly larger than the specified values for the HCPB first wall. An improvement should be possible by better adjusting the tubes dimensions. In the curved region, the channels are significantly flattened due the bending process.

The joint cleanliness is satisfactory except in the region close to the TIG weld, which is not representative of the rib-to-rib joints.

Away from this zone, room temperature tensile properties fulfil the Eurofer specifications. The room temperature joint toughness, as measured with KLST specimens, reaches satisfactory values about 7.5 J. Nevertheless a further improvement is possible since the joint toughness reaches only 65 % that of the base material.

REPORTS AND PUBLICATIONS

E Rigal, C Grandjacques, F Bruchon “Second bent HCPB first wall mock-up manufactured by improved HIP forming technique”, CEA Report Note technique DTEN no. 61/2001, 27 june 2001.

TASK LEADER

Emmanuel RIGAL

DRT/DTEN/SMP/LS2M
CEA Grenoble
17, rue des Martyrs
38054 Grenoble Cedex 9

Tél. : 33 4 38 78 97 22
Fax : 33 4 38 78 54 79

E-mail : emmanuel.rigal@cea.fr

TW1-TTBB-005-D03

Task Title : DEVELOPMENT OF CERAMIC BREEDER PEBBLE BEDS Characterization of Li_2TiO_3 pebble beds

INTRODUCTION

The characterization of Li_2TiO_3 pebbles, in support of both their fabrication technology and the investigation of the performance of Li_2TiO_3 pebbles and pebble beds, plays a major role in the development of Li_2TiO_3 pebbles for the HCPB blanket.

It includes the determination of the geometrical, microstructural, crystal phase, purity, and mechanical strength characteristics of :

- the intermediate products in the sequence of the steps of the fabrication process,
- pebbles sampled from each produced batch,
- the pebbles once they have been subjected to the various out-of-pile tests of pebbles and pebble beds, and to the HCPB mock-up tests.

2001 ACTIVITIES

Focus in 2001 was placed on the determination of :

CHARACTERISTICS OF THE Li_2TiO_3 PEBBLES OF THE 6 kg BATCH PRODUCED IN 2000 AT CERAMIQUES TECHNIQUES ET INDUSTRIELLES

It is recalled that the goal of this 6 kg batch was dual :

- produce a sufficient amount of Li_2TiO_3 pebbles to control the fabrication process parameters,
- produce an amount of Li_2TiO_3 pebbles necessary and sufficient to supply the campaign of the functional tests of Li_2TiO_3 pebble beds foreseen in 2001.

Thus, a batch of 6 kg of Li_2TiO_3 pebbles, reference "CTI 13B0 Ti 1090 CTI" comprising 6 sub-batches has been produced in 2000.

This batch of Li_2TiO_3 pebbles was sintered at 1100°C instead of 1050°C (1999 reference sintering temperature) in order to increase the stability of the pebble bed at high temperature.

In fact, the large increase in creep strain observed during the uniaxial compression tests at high temperature, performed in 2000 at FZK on bed of Li_2TiO_3 pebbles sintered at 1050°C, is assumed to be due to the material small grain size resulting from the low sintering temperature [1].

Relevant characteristics, i.e., pebble bed density, pebble open/closed porosity, grain size, specific surface area, and average crush load of the sub-batches are listed in table 1.

One can observe that the uniformity of the sub-batches is relatively satisfactory showing that temperature conditions throughout the industrial furnace are quite uniform.

The impurities analysed by Spark Source Mass Spectrometry are listed in figure 1.

The significant decrease of Cr, Fe, and Ni content observed in the 2000 batch demonstrates the successful effect of the measures taken at all steps of the process to limit the contamination of Li_2TiO_3 by those elements.

Table 1 : Characteristics of the 6 kg-batch of Li_2TiO_3 pebbles sintered at 1100°C (Reference of pebbles: CTI 13B0 Ti 1090 CTI)

Reference of batch	Pebble size (mm)	Porosity (%)		Bed density (g/cm^3)	Grain size (µm)	Specific surface area (m^2/g)	Average crush load (N)
		Open	Closed				
Sub-batch 1	0.8 – 1.2	-	4.3	1.73	1.5 - 4	0.25	34
Sub-batch 2	0.8 – 1.2	-	4.3	1.73	1.5 – 4	0.21	32
Sub-batch 3	0.8 – 1.2	10.0	4.5	1.75	1 – 4	0.22	33
Sub-batch 4	0.8 – 1.2	-	4.7	1.75	1.5 – 4	0.22	37
Sub-batch 5	0.8 – 1.2	-	4.9	1.75	1 – 4.5	0.21	38
Sub-batch 6	0.8 – 1.2	7.5	5.1	1.79	1.5 – 4	0.19	41

Major impurities	CTI pebbles 2000
Al	5 ppm
Ca	20 ppm
Cr	1.5 ppm
Fe	7 ppm
K	8 ppm
Ni	3 ppm
S	1 ppm
Si	30 ppm
Na	30 ppm
C	50 ppm
Other elements	< 10 ppm

Figure 1 : Impurity analysis using Spark Source Mass spectrometry of Li_2TiO_3 pebbles

EXAMINATION OF Li_2TiO_3 PEBBLES AFTER THE FUNCTIONAL TESTS OF PEBBLE BEDS

In order to evaluate the performance of the Li_2TiO_3 pebbles and, as a consequence, to improve it if needed, relevant functional tests of pebble beds both out-of-pile and in-pile are carried out in collaboration with FZK, ENEA, and NRG.

Characterization of the Li_2TiO_3 pebbles after the out-of-pile tests is carried out at CEA in order to identify any changes and, thereby, help interpretation of test results.

Principal out-of-pile tests of pebble beds carried out in 2001 and post-test examination results :

Annealing test at 970°C in air at CEA during three months

This test was made within the framework of the pebbles optimisation. It aimed at comparing the behaviour of the Li_2TiO_3 pebbles as a function of their sintering temperature, in other words, as a function of their microstructure. The above temperature and time conditions were representative of DEMO end-of-life conditions at the higher temperature of the breeder in the HCPB blanket. Comparison annealing tests at CEA were performed in 2000 on Li_2TiO_3 pebbles sintered at 950°C and 1050°C. Results showed that pebbles sintered at 1050°C are more stable on annealing than those sintered at 950°C.

In 2001, annealing test was performed on pebbles sintered at 1100°C. Characteristics of the specimens (weight loss, open and closed porosity, crush load, and grain size) were checked on the initial pebbles and on pebbles annealed in air at 970°C during 1 month, 2 months, and 3 months, respectively. Contrary to the expectations, those results show that pebbles sintered at 1050°C are more stable on annealing than those sintered at 1100°C regarding lithium vaporization (weight loss).

The control of the temperature of the furnace shows that the actual temperature during the test is higher than 970°C. In view of these results, a new annealing test at 970°C with the pebbles sintered at 1100°C was decided and is in progress.

Uniaxial compression tests in He at FZK

Several samples of pebbles were delivered to perform the uniaxial compressive tests at FZK aiming at evaluating the thermal creep of the pebbles sintered at 1100°C, and of the smaller diameter pebbles fabricated in 2001. A compilation of the results of the tests performed is reported in [2]. The experiments were performed in an uniaxial test facility with a maximum temperature of 850°C and a pressure of 8 MPa. Thermal creep rates tend to decrease with increasing sintering temperature, increasing density and increasing grain size of Li_2TiO_3 pebbles. The smaller pebbles (0.7 to 1 mm) compared to regular pebbles (0.8 to 1.2 mm) showed very satisfactory results. This might be caused by the larger achievable packing factor which is desired for other reasons (breeding ratio, heat transfer).

Characteristics of 0.8-1.2 mm Li_2TiO_3 pebbles sintered at 1100°C, before and after the tests are identical (grain size, crush load, porosity). Figure 2 shows a cross section of the Li_2TiO_3 pebble bed agglomerated after the test at 800°C and 1.2 MPa. One can see that pebbles are in close contact but are not "merged" together as are the Li_2TiO_3 pebbles sintered at 950°C under similar test conditions.

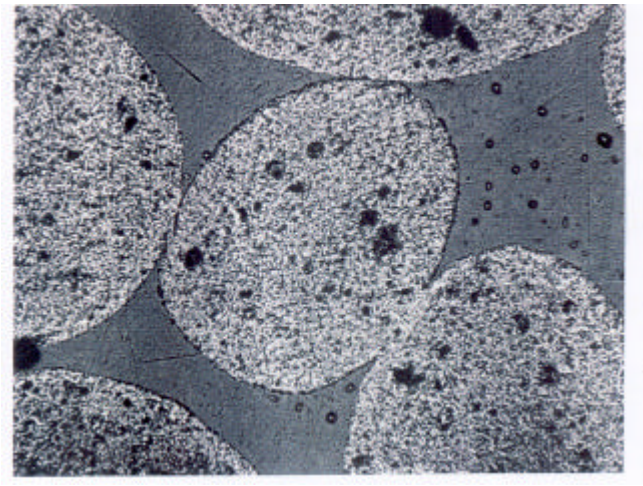

Figure 2 : Li_2TiO_3 pebble bed after uniaxial compression test at 800°C

CONCLUSION

The extensive work of characterization of the Li_2TiO_3 pebbles allowed to optimise the parameters of the extrusion-spheronization-sintering process so as to obtain Li_2TiO_3 pebbles. That best satisfy at best the requirements of the HCPB blanket. In addition, comparing the characteristics of the Li_2TiO_3 pebbles before and after the out-of-pile tests of pebble beds, performed so as to evaluate the performance of the Li_2TiO_3 pebbles option, was very useful to help understanding any phenomena occurring during the tests.

REFERENCES

[1] N. Roux. Compilation of blanket relevant properties data for Li_2TiO_3 pebbles and pebble beds. Presented at CBBI-9, Toki (Japan), September 2000.

[2] J. Reimann, J.D. Lulewicz, N . Roux, G. Worner. Thermal creep of metatitanate pebble beds. Presented at CBBI-10, Karlsruhe (Germany), October 2001.

REPORT AND PUBLICATIONS 2001

J.D.Lulewicz. Interim report of the activity on the optimization of the fabrication process of Li_2TiO_3 pebbles. Internal report CEA/SE2M/LECMA 01-DT-011. June 2001.

J.D.Lulewicz. Annual report on sub-task TTBB-005-3 and sub-task TTBB-005-4. Internal report CEA/SE2M/LECMA 01-DT-025. November 2001.

J. Reimann, J.D. Lulewicz, N . Roux, G. Worner. Thermal creep of metatitanate pebble beds. Presented at CBBI-10, Karlsruhe (Germany), October 2001.

J.D. Lulewicz, N. Roux. The fabrication of Li_2TiO_3 pebbles by extrusion-spheronisation-sintering, a suitable process for tailoring pebbles properties. Presented at ICFRM-10, Baden-Baden (Germany), October 2001.

J.D. Lulewicz, N. Roux, F. Pourchet, J.P. Joulin. Status of fabrication of Li_2TiO_3 pebbles by extrusion-spheronisation-sintering process. Presented at CBBI-10, Karlsruhe (Germany), October 2001.

TASK LEADER

Jean-Daniel LULEWICZ

DRT/LIST/DECS/SE2M/LECMA
CEA Saclay
91191 Gif-sur-Yvette Cedex

Tél. : 33 1 69 08 48 24
Fax : 33 1 69 08 57 54

E-mail : jean-daniel.lulewicz@cea.fr

TW1-TTBB-005-D04

Task Title : DEVELOPMENT OF CERAMIC BREEDER PEBBLE BEDS Validation of Li_2TiO_3 fabrication with pre-industrial means of the lab fabrication steps – Mastering/optimisation

INTRODUCTION

Li_2TiO_3 pebbles are developed at CEA as candidate ceramic breeder option for the Helium-Cooled-Pebble-Bed (HCPB) blanket investigated in Europe. The extrusion-spheronization-sintering process was selected in order to produce Li_2TiO_3 pebbles fullfiling the HCPB blanket requirements, and was developed with the collaboration of the industrial firm Céramiques Techniques et Industrielles.

In 2001 the work was continued, focusing on mastering and optimising the parameters of the fabrication process as of 2000. The good behaviour of the Li_2TiO_3 pebbles observed in the functional tests of Li_2TiO_3 pebble beds performed to-date substantiates the optimisation initiative [1]. For example the results of the first extruded Li_2TiO_3 pebbles irradiated in EXOTIC 8 up to 6.5% burnup are excellent. The pebbles are intact (no fragmentation, no cracks) after 650 Full Power Days and a total neutron fluence of about 3.10^{25} n/m^2 [2].

The activity during 2001 is reported hereafter. It includes essentially four parts:

- Investigation of the lower limit of pebble diameter using the extrusion process.
- Evaluation of production yield and preliminary study of enhancement.
- Investigation of the feasibility of lithium recycling with ENEA.
- Production of a 6 kg-batch of Li_2TiO_3 pebbles with the improved 2001 process.

2001 ACTIVITIES

INVESTIGATION OF THE LOWER LIMIT OF PEBBLE DIAMETER USING THE EXTRUSION PROCESS

The current sintered Li_2TiO_3 pebbles have diameters in the range 0.8 mm to 1.2 mm. Investigation was made to determine the lower limit of Li_2TiO_3 pebble diameter achievable with the extrusion process with a view to find out any benefit for the design of the Helium-Cooled-Pebble-Bed blanket. Indeed, smaller pebbles can be advantageous to better fill the ceramic breeder space and to increase pebble bed density and thermal conductivity.

The fabrication process parameters were once more adjusted in order to obtain Li_2TiO_3 pebbles with a smaller diameter.

First, a nozzle of 0.8 mm instead of 1 mm was used during the extrusion step and a spheronization plate was re-designed for the spheronization of the smaller granules.

The same extrusion machine and cutting system as for the preparation of the current pebbles were used for these trials.

A batch of smaller Li_2TiO_3 pebbles was produced. The pebbles of this batch were sintered at 1100°C and 1140°C. The shape, the size and the microstructure of the smaller Li_2TiO_3 pebbles was observed using scanning electron microscopy.

As shown in Figure 1, the shape is close to spherical, and the pebble size distribution is 0.7 to 1 mm. A comparison of the characteristics of the 0.8-1.2 mm Li_2TiO_3 pebbles with the characteristics of the 0.7 mm-1 mm pebbles is displayed in Table 1 showing that open and closed porosity values decrease slightly for smaller pebbles and pebble bed density increases significantly. Grain sizes are very similar for both diameter pebbles sintered at 1100°C.

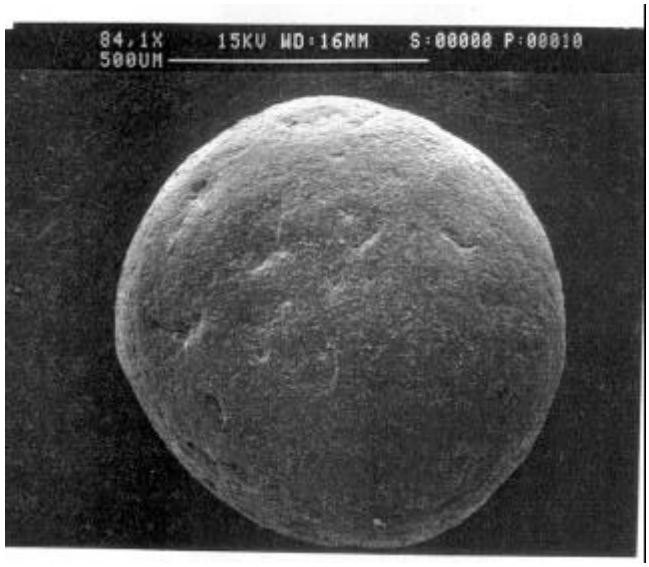

Figure 1 : Shape of smaller Li_2TiO_3 pebbles

The feasibility to produce small Li_2TiO_3 pebbles in the range 0.7 mm to 1 mm with the extrusion process was shown in this study. Although there is no experimental evidence that perfect sphericity of the pebbles constituting the pebble bed is a must, an attempt will be made to obtain an even better sphericity. In addition, further adaptations can be made to decrease pebble diameter down to 0.5 mm.

Table 1 : Characteristics of Li_2TiO_3 pebbles sintered at 1100°C and 1140°C

Reference	Pebble size (mm)	Porosity (%)		Bed density (g/cm^3)	Grain size (µm)	Average crush load (N)	Remark
		Open	Closed				
CTI 641 Ti 1100 CEA	0.8 - 1.2	6.0	5.2	1.81	1.5 - 5	40	current pebbles
CTI 641 Ti 1140 CEA	0.8 - 1.2	5.0	5.2	1.86	2 - 7	38	current pebbles
CTI 951 Ti 1100 CEA	0.7 – 1.0	4.0	4.8	1.89	1 – 4	32	smaller pebbles
CTI 951 Ti 1140 CEA	0.7 – 1.0	2.0	4.6	1.93	over sintered	28	smaller pebbles
CTI 1271 Ti 1100 CEA	0.8 – 1.2	4.2	5.5	1.85	1.5 – 5	40	with recyclable powder
CTI 1271 Ti 1140 CEA	0.8 – 1.2	-	5.4	1.87	2 – 7	39	with recyclable powder

EVALUATION OF PRODUCTION YIELD AND PRELIMINARY STUDY OF ENHANCEMENT

For economical purpose (high cost of ^6Li material to be used in the future), it is required to minimise lithium losses throughout the fabrication process of Li_2TiO_3 pebbles. A preliminary (no attention paid to save the materials) value of 50% was calculated for the fabrication yield of 6 kg of Li_2TiO_3 pebbles "CTI 13B0 Ti 1090 CTI" produced in 2000. Losses of lithium materials during the process originate from elimination of the too long granules after the cutting step, and from elimination by sieving of the green pebbles which do not meet the size specification.

The objective is to recover the lithium materials separated during the process (granules, green pebbles) and to recycle them after transformation into a Li_2TiO_3 powder having the same characteristics as the initial one.

To this end, granules and green pebbles are subjected to calcination, in order to remove binder and plasticizer, and to sieving as shown in Figure 2.

A recyclable powder is obtained and can be used directly at the first step of the process, i.e., the preparation of the paste for extrusion.

Comparison in table 2 of the characteristics of the initial powder and of the recyclable powder shows a very good agreement regarding apparent density, specific surface area and mean particle size. Crystal phases are identical. A batch of Li_2TiO_3 pebbles was produced with this recyclable powder. The pebbles of this batch were sintered at 1100°C and 1140°C. A comparison of the characteristics of the current Li_2TiO_3 pebbles with the characteristics of the pebbles obtained with the recyclable powder is displayed in table 1. It shows a very good agreement regarding open and closed porosity, grain size, pebble bed density and crush load.

Table 2 : Comparison of the characteristics of the initial powder and of the recyclable powder

	Initial powder	Recyclable powder
X-ray diffraction	$Li_2TiO_3 + Li_4Ti_5O_{12}$	$Li_2TiO_3 + Li_4Ti_5O_{12}$
Specific surface area	4.0 m^2/g	4.2 m^2/g
Mean particle size	.6 µm	0.58 µm
Apparent density	0.38 kg/l	0.37 kg/l

INVESTIGATION WITH ENEA OF THE FEASIBILITY OF LITHIUM RECYCLING

With the same economical purpose as above, a wet chemistry process is developed at ENEA [3] for extracting lithium from Li_2TiO_3 in the form of Li_2CO_3 powder. This process will be used for the recovery of ^6Li from a lithium titanate breeder burned up to its end of life in the European HCPB blanket. The process was optimised with respect to the chemical attack of titanate and the precipitation of carbonate from aqueous solutions to get a Li_2CO_3 powder, with the suitable chemical and morphological characteristics, for re-exploitation in the extrusion process of fabrication of Li_2TiO_3 pebbles.

In order to simulate a real reprocessing of Li_2TiO_3 breeder, the procedures first set up with Li_2TiO_3 powder have been confirmed by using sintered Li_2TiO_3 pebbles delivered by CEA. A batch of Li_2CO_3 powder has been produced by ENEA. A “fresh” Li_2TiO_3 powder was produced at CEA from the Li_2CO_3 powder prepared at ENEA. A comparison of the characteristics of the current Li_2TiO_3 powder and of the Li_2TiO_3 powder obtained with recycled lithium shows that they are similar. “Fresh” Li_2TiO_3 pebbles will be fabricated by CTI.

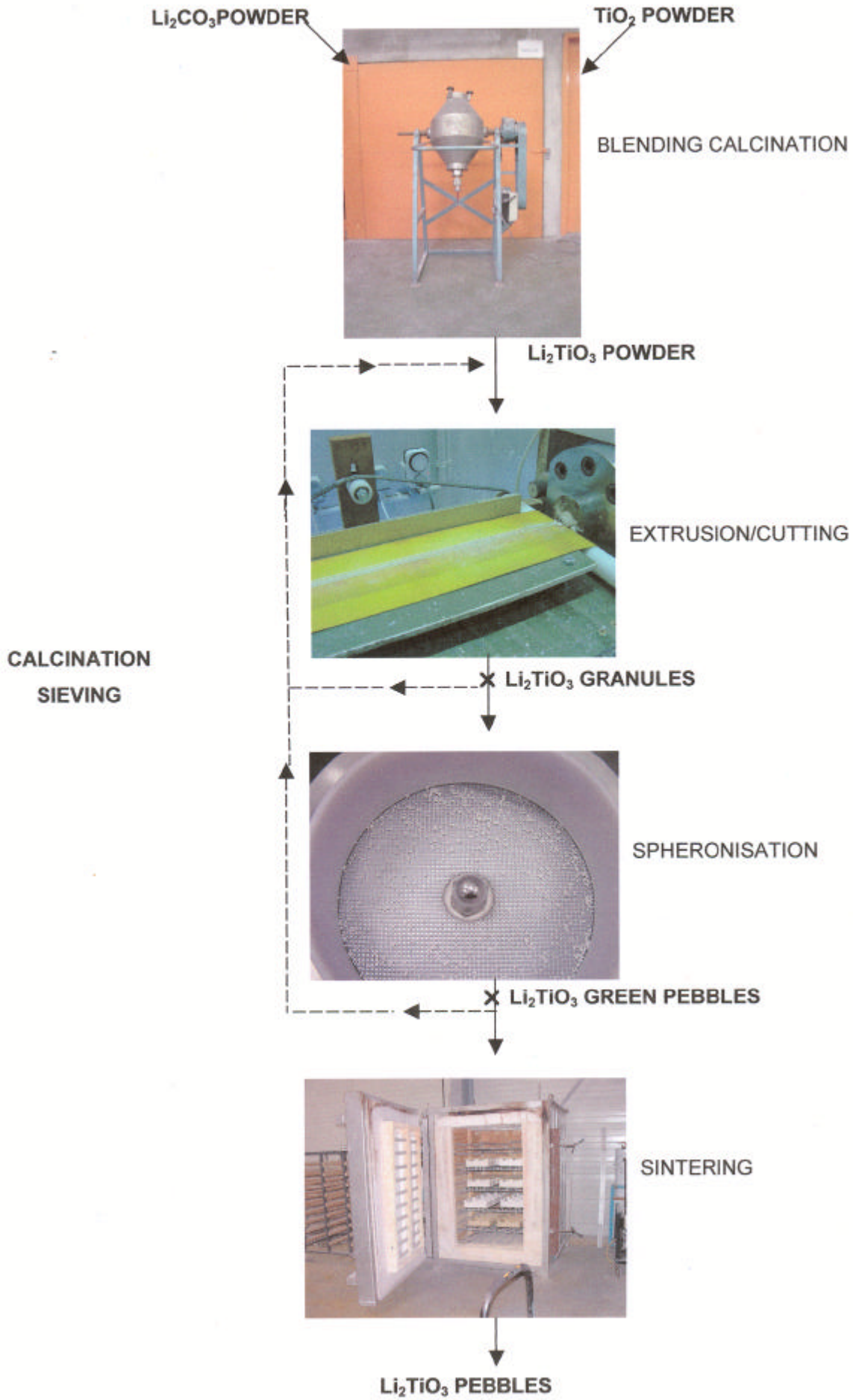

Figure 2 : Flow sheet of the process with recyclable powder

FABRICATION OF A 6 kg BATCH OF Li_2TiO_3 PEBBLES

In order to master the fabrication process parameters as improved in 2001, as well as to dispose of the amount of Li_2TiO_3 pebbles necessary to supply the campaign of functional tests of Li_2TiO_3 pebble beds and HCPB mock-up tests foreseen in 2002, a 6 kg-batch of Li_2TiO_3 pebbles was produced at the end of 2001.

CONCLUSION

The activity at CEA regarding mastering and optimisation of the fabrication parameters of the extrusion-spheronization-sintering process for the production of Li_2TiO_3 pebbles was achieved in accordance with the foreseen time schedule. Specimens for the functional tests of pebble beds, and for irradiation experiments (i.e., in-pile tests of HCPB pebble bed assemblies in the HFR reactor starting in 2002) were delivered in due time to the European partners. Advances were continued in the fabrication of Li_2TiO_3 pebbles at the semi-industrial scale.

The good behaviour of the Li_2TiO_3 pebbles observed in the different functional tests of pebble beds shows the great interest of lithium titanate for the HCPB blanket of a fusion reactor.

REFERENCES

[1] N. Roux. Compilation of blanket relevant properties data of Li_2TiO_3 pebbles and pebble beds. Presented at CBBI-9, Toki (Japan), September 2000.

[2] J.G. Van der Laan et al., Performance of ceramic breeder pebbles to DEMO representative lithium burnups. Presented at ICFRM-10, Baden-Baden (Germany) October 2001.

[3] C. Alvani et al. Li_2TiO_3 pebbles reprocessing, recovery of ^6Li as Li_2CO_3. Presented at CBBI-10, Karlsruhe (Germany), October 2001.

REPORT AND PUBLICATIONS 2001

J.D.Lulewicz. Interim report of the activity on the optimisation of the fabrication process of Li_2TiO_3 pebbles. Internal report CEA/SE2M/LECMA 01-DT-011. June 2001.

J.D.Lulewicz. Annual report on sub-task TTBB-005-3 and sub-task TTBB-005-4. Internal report CEA/SE2M/LECMA 01-DT-025. November 2001.

J. Reimann, J.D. Lulewicz, N . Roux, G. Worner. Thermal creep of metatitanate pebble beds. Presented at CBBI-10, Karlsruhe (Germany), October 2001.

J.D. Lulewicz, N. Roux. The fabrication of Li_2TiO_3 pebbles by extrusion-spheronisation-sintering, a suitable process for tailoring pebbles properties. Presented at ICFRM-10, Baden-Baden (Germany), October 2001.

J.D. Lulewicz, N. Roux, F. Pourchet, J.P. Joulin. Status of fabrication of Li_2TiO_3 pebbles by extrusion-spheronisation-sintering process. Presented at CBBI-10, Karlsruhe (Germany), October 2001.

TASK LEADER

Jean-Daniel LULEWICZ

DRT/LIST/DECS/SE2M/LECMA
CEA Saclay
91191 Gif-sur-Yvette Cedex

Tél. : 33 1 69 08 48 24
Fax : 33 1 69 08 57 54

E-mail : jean-daniel.lulewicz@cea.fr

UT-TBM/BB-IMBLA

Task Title : IMPROVED BREEDING BLANKET

INTRODUCTION

Studies have been performed in the past years and are still ongoing to yield improved specifications of what could be an attractive fusion power reactor (FPR). In this frame, the main objectives of this task are, for 2001 and 2002:

- to develop improved version of existing breeding blanket designs in view of their use in a FPR,
- to assess the potential performances of new advanced breeding blanket designs,
- to make progresses on high heat-flux components (HHFC) design and analyses.

2001 ACTIVITIES

2001 activities have been devoted essentially to the assessment of the breeding blankets, which are key components of a D-T fusion power plant. In fact, they have a large impact on the overall plant design, its performance and availability and on the cost of electricity.

Two different blanket concepts have been selected, the Water Cooled Lithium Lead (WCLL) and the SiC_f/SiC Pb-17Li (TAURO).

WCLL BLANKET

The WCLL blanket is one of the two European candidate concepts to be used in a DEMOnstration reactor [1]. It is based on technology expected to be available in the medium term with moderate R&D requirements. It employs steel as structural material, the liquid alloy Pb-17Li as breeder and multiplier material, and pressurized water as coolant. Water-cooled components offer advantages for fusion reactors, in particular due to the high capacity for heat extraction and because they can rely on widely applied technology in nuclear and fossil fired power plants.

The WCLL blanket, as designed for the DEMO reactor, consists of 48 outboard and 32 inboard segments. The segments are constituted by a poloidal steel box, which is reinforced by a grid of stiffener plates. The steel box comprises the first wall of the blanket and is separately cooled by pressurized (15.5 MPa) water. The box constitutes a container for slowly circulating Pb-17Li. The power deposited in the liquid metal pool is extracted by bundles of Double Walled U-Tubes (DWTs). The headers for the breeder zone (BZ) are located in the top of the module.

Structural integrity and lifetime of the WCLL blanket

The structural integrity of this blanket concept under a realistic operating scenario was firstly evaluated. Because of uncertain data on a FPR operating conditions, the DEMO scenario and specifications were assumed, that is a surface heat flux of 0.5 MWm^{-2} and a power density distribution corresponding to a neutron wall loading of 1.2 MWm^{-2}. Thermal and thermo-mechanical steady state calculations were carried out on a model representative of an outboard segment for nominal power, over power (+20 %) and underpower (-20 %) [2]. The mechanical properties of the Z10 CDVNb9.1 were used for the analyses due to leak of data on EUROFER.

Thermo-mechanical results

Obtained thermal results are summarised in table 1. Even in the case of overpower, temperatures are everywhere lower than corresponding limits (550°C for the steel and 480°C for the interface between Pb-17Li and steel).

Table 1 : Outboard segment temperatures (°C) at various operating conditions

	Overpower		Nominal		Underpower	
	T_{max}	T_{min}	T_{max}	T_{min}	T_{max}	T_{min}
Front wall	490	313	460	313	430	313
Pb-17Li	482	297	453	296	423	295
BZ tubes	336	293	329	292	327	292
Pb-Li/steel	443	315	420	315	398	314

The thermal fields so obtained were used to determine thermal and total stresses on the structure. The hydrostatic pressure of the Pb-17Li on the box walls (1.5 MPa) and the water pressure inside the FW tube (15.5 MPa) constitute mechanical loads. Maximum equivalent stresses (Von Mises and Tresca) are reported in table 2.

Table 2 : Von Mises and Tresca equivalent stresses in the outboard segment at various operating conditions

	Overpower		Nominal		Underpower	
	V M	Tresca	V M	Tresca	V M	Tresca
Total	468	534	395	453	323	372
Mechanical	64	67	64	67	64	67

Maximum stresses are located in the FW tube.

More solicited sections are the ones corresponding to the stiffeners locations and the ones between two stiffeners.

Thus, it is on these sections that were chosen the supporting line segments to verify the design criteria.

Results postprocessing

Obtained results were checked following the RCC-MR [3], [4] the IISDC [5], [6] design criteria. A procedure proposed by Karditsas [7] was also used to take into account irradiation effects (swelling and creep). As far as damage due to monotonic type loading is concerned, requirements on primary loads are largely fulfilled. For unirradiated material, the creep usage fraction will not exceed 1 for holding time greater than 10^6 hours (>100 years), while the lifetime of the blanket is not supposed to exceed 10 years.

With regard to damage due to cyclic loading, a loading histogram was studied consisting of N cycles from power off to nominal power state with n overpower events and n underpower events [7].

Obtained stresses met everywhere criteria against progressive deformation. As far as the fatigue-creep damage is concerned, the blanket lifetime obtained using the fatigue creep interaction diagram, depends on duration between two power off periods (T_N) and on method used to calculate equivalent stress.

If the equivalent stress is calculated following Von Mises, lifetime ranges between 7 years (for $T_N = 1$ day) and 20 years (for $T_N = 1$ year). If equivalent stress is calculated following Tresca, these values decrease to 3.5 years and 10 years respectively. Finally, with regard to swelling, it will be negligible during a period lasting 5.4 years.

Karditsas proposed a procedure to estimate the lifetime of the first wall taking into account thermal and irradiation creep plus fatigue [7].

A similar procedure has been applied for the WCLL blanket. Lifetime, so calculated ranges from 3 (for $T_N = 1$ day) to 4 years (for $T_N = 1$ year), if the equivalent stress is calculated following Von Mises, and from 2 to 3.5 years if equivalent stress is calculated following Tresca. These results are preliminary because of leak of data on irradiated materials. They could be modified due to R&D results on EUROFER properties under irradiation.

Evaluation of limits and potential of alternative WCLL blanket configurations

Further design improvements have been envisaged for the WCLL blanket concept to adapt and better exploit it in a FPR. Common requirement to foreseen modifications is the displacement of BZ coolant collectors from the top to the rear of the module.

This solution is not compatible with the U-configuration actually foreseen for the breeder zone (BZ) cooling tubes. In this report, alternative configurations of the BZ cooling system have been assessed, horizontally oriented serpentine tubes or poloidally oriented C-tubes, and their advantages and drawbacks have been pointed out.

Horizontal tubes

In this configuration, horizontal instead of poloidal tubes cool the breeder zone, much in the same way as it is done for the segment box.

The cooling pipes are inserted between horizontal steel plates acting as stiffeners. The stiffeners must be properly spaced and perforated to provide a meander-shaped pathway for the Pb-17Li flow. BZ water manifolds are located in the rear of the segment. As for the segment box, they are constituted by vertical half cylinders welded to the back plate.

Figures 1 and 2 show the generic outboard segment with water collectors, liquid metal pathway and feeding pipe and cooling tubes.

The serpentines are taken in place by grids. The arrangement of the BZ tubes is optimized with regard to thermo mechanical behaviour. Three tubes are needed in the region between two stiffeners with two different configurations.

C Tubes

An interesting alternative could be to use poloidally oriented C-shaped tubes as currently adopted for the present WCLL ITER-FEAT Test Blanket Module, TBM [8]. This modification allows to move the coolant headers to the rear and to gain space for tritium breeding, without major modifications to the segment box.

Differently from U-Tube configuration, where the tubes coming down in the front part of the module must come up in the rear part, in the C-Tubes configuration, tubes are independent. This allows reducing their number in the rear channels, where the deposited power is lower.

Thermal and thermo-mechanical analyses and results

Thermal and thermo mechanical analyses have been carried out on both concepts assuming a surface heat flux of 0.5 MWm^{-2} and the power density corresponding to a neutron wall load of 1.2 MWm^{-2}.

Maximum temperature in the FW steel is 534°C for the horizontal tubes concept and 460°C in C tubes configuration, so increasing margin to assumed limit (550°C) and allowing higher surface heat flux on the FW. This difference is due to different FW profiles.

In the C tubes configuration, as well as in the reference WCLL geometry, the FW surface follows tubes profile, assuming a corrugated profile, while a straight FW is needed in the horizontal tubes configuration. In fact, analyses carried out in faulted conditions (in which the box is assumed to be pressurized 15.5 MPa) showed that in the horizontal tubes configuration Von Mises stress are unacceptable in the section between two cooling tubes, where the resistant section is minimum, so a straight profile has to be adopted for the FW.

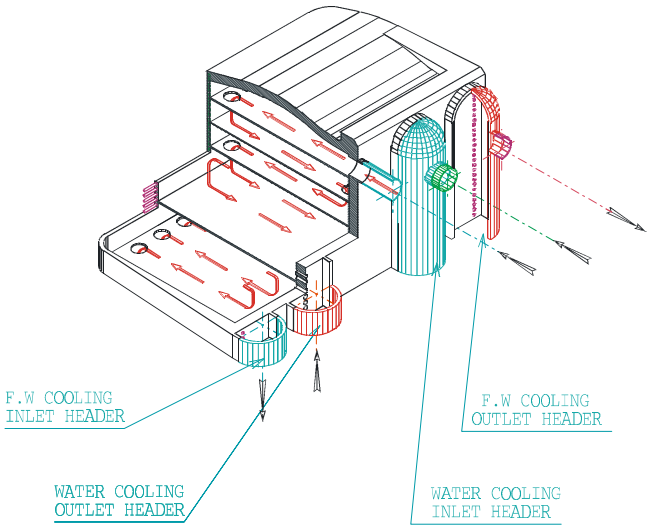

Figure 1 : 3D view of a horizontally cooled OS: Pb-17Li pathway and feeding pipes

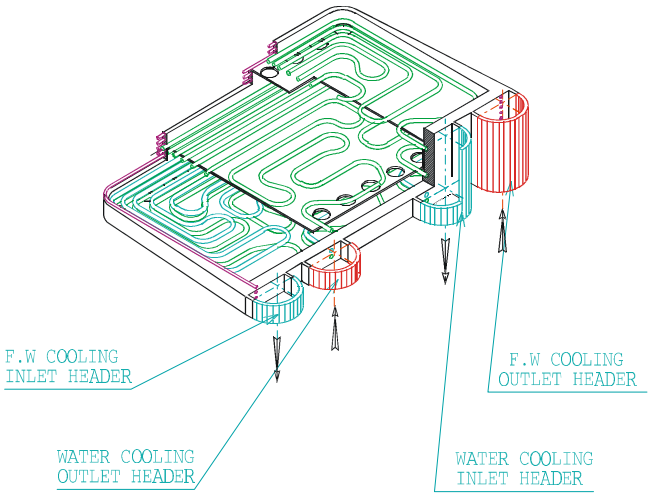

Figure 2 : 3D view of a horizontally cooled OS: cooling tubes and corresponding collectors

Advantages and drawbacks of the two alternative concepts compared to reference U tubes concept

When compared to the reference U-tubes concept, the two alternative concepts present some various advantages and shortcomings, discussed thereafter. For both alternative concepts, even in different measure, principal advantages are the displacement of cooling water manifold in the rear of the module, the modular character and the adaptability to all blanket segments (inboard, outboard and topboard).

On the other hand, due to greater number of welds and bends, compared to the U-tube concept, segmentation of the blanket into smaller modules, implicates reliability decrease for both alternative concepts, in lower measure for the C-tubes than for horizontal tubes. Furthermore, some steel is required to account for the additional segment covers, which could be detrimental for the tritium breeding ratio (TBR). The effect of geometry variation on TBR requires a refined neutronic analysis.

With regard to horizontal tubes configuration, main issue concerns the complex manufacturing of double walled serpentines. The technique actually foreseen for the fabrication of the double walled U-tubes may not be applicable to serpentine tubes. In order to guarantee the double confinement between water and liquid metal, an alternative was proposed to double walled tubes [9], which, however, would considerably increase the steel amount with losses in terms of TBR. On the other hand, insofar high quality data for fusion are unavailable, the presence of a double wall is a mandatory project choice aiming at decreasing the probability of water/Pb-17Li interaction. Another main concern could be represented by thermal hydraulic, especially in faulted conditions. For example in case of less of coolant, because of horizontal flow, a phenomenon of coolant stratification could take place with aggravated risk of steam plug favored by tube bends. Particular design and analysis effort should be, thus, invested to master the thermal-hydraulic.

With regard to C-tubes concept, collectors would be rectangular boxes located at the top and at the bottom of the segment, between those of the SB, so requiring 3D bending of some BZ tubes. R&D activities are ongoing, in the frame of the TBM studies, and seem to prove the feasibility of such a type of bends on double walled tubes and with suitable tolerances. However, the number of DWTs in a reactor segment is much higher than in the TBM, which could require further effort in the collector design. Finally, the C-tubes concept requires only very little modification to the reference concept if compared to the one with horizontal cooling tubes.

TAURO BLANKET

The TAURO blanket offers the capability of heat extraction at high coolant temperatures and promises favorable conversion efficiencies. It is essentially formed by a SiC_f/SiC box with an indirectly cooled FW, which acts as a container for the Pb-17Li (figure 3). The Pb-17Li acts as coolant, breeder multiplier material, and tritium carrier. Each blanket segment is poloidally divided into several straight modules, attached on one common thick back-plate.

The number of modules cooled in series depends on the assumption on inlet and outlet Pb-17Li temperatures. The feeding pipes are located behind the module. The coolant enters the inlet collector through a single tube and is divided into 5 sub-flows, one for each sub-module. This flow scheme enables high operating Pb-17Li temperature without exceeding limit imposed by thermal and thermal-mechanical criteria.

In this study, the limits and potential of this blanket have been assessed, using the appropriate thermo mechanical behavior model and resistance criteria recently developed at CEA and implemented in the FEM code CASTEM2000. At the present time, the main difficulties are related to the scarce data available for the new composite and therefore the maximum allowable stresses and temperature to be used for the dimensional analyses.

The actual limits must be upgraded with new data, and could be evolved with the influence of neutron damage on the mechanical properties of the composite.

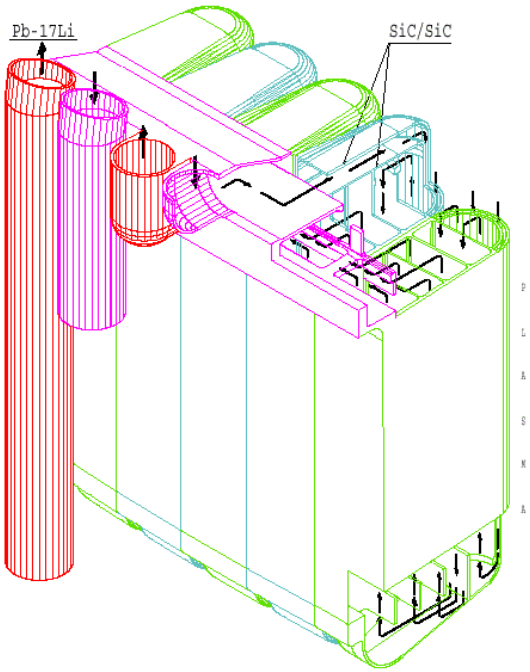

Figure 3 : TAURO outboard blanket module

Evaluation of the improved TAURO performances

Parametric thermo-mechanical analyses have been performed aiming to maximize the liquid metal outlet temperature and thus to achieve high thermal conversion efficiency, meeting temperature limits and thermo-mechanical criteria. The thickness and height of the module, the inlet velocity and temperature of the liquid metal, the surface heat flux and the neutron wall load have been assumed as parameters. Furthermore, various cooling arrangements (modules cooled in series or in parallel) have been assessed. The limiting factors appear to be both the maximum and minimum Sic_f/SiC allowed temperature (assumed equal to 1050°C and 500°C respectively).

As results of this optimization, a reference case has been identified with following parameters:

- 2x2 modules in series,
- Module height of 2 m,
- FW thickness of a 3 mm,
- First channel thickness of 8.5 mm,
- Inlet velocity around 2.25 m/s,
- Inlet Pb-17Li Temperature of 640°C.

Allowed limits in temperature are everywhere respected as well as mechanical criteria, as shown in table 3 which summarizes the results related to this case for a surface heat flux of 0.5 MWm^{-2}.

As far as thermo-mechanical results are concerned, obtained equivalent stresses are normalized to their maximum allowed value.

Table 3 : Thermal and thermo mechanical results for the reference case

T_{out} (°C)	$\ddot{A}T_{FW}$ (°C)	T_{max} (°C) SiC_f/SiC	T_{max} (°C) interface
957	115	995	915

Criterion for stresses in plane	$\frac{<s_{zz}>}{Z^+}$	$\frac{<s_{zz}>}{Z^-}$	$\frac{t_{zz}}{S}$
0.75	0.26	0.04	0.72

At present, a Brayton cycle using helium is foreseen for power conversion. In the reference case, obtained thermal efficiency is 55 % for a compression ratio of about 1.77. However, the precise determination of the global blanket system efficiency depends on the optimization of the blanket module, the pressure drop, the compression ratio, and the requirement of efficient Pb-17Li/helium heat exchangers and recuperator.

CONCLUSIONS

In this report, the limits and potential of two different blanket concepts have been assessed, the Water Cooled Lithium Lead (WCLL) and the SiC_f/SiC Pb-17Li (TAURO), in view of their use in a FPR. WCLL blanket is based on technology expected to be available in the medium term with moderate R&D requirements. The structural integrity of this blanket has been verified.

The lifetime, calculated taking into account fatigue and thermal creep, ranges from 3,5 to 20 years depending on the method used to calculate stress intensities (Von Mises' or Tresca's method) and on the duration between two power off periods. These results should be verified when more materials properties (loss of ductility due to irradiation, negligible creep curves) will be known. Two alternative configurations of the BZ cooling system have been assessed for further improve the blanket design and better adapt it to the recently refined reactor specifications.

If modularity is required, C-tubes configuration is the most promising because of it needs lower modifications compared to horizontal tube configuration. However, the impact of such a modification on the blanket performance should be fully evaluated in the near future. In particular, once reactor specification will be fixed, and a maintenance scheme defined, more detailed neutronic, thermo-mechanical and thermal-hydraulic analyses will be needed. The TAURO system can achieve high performances (in terms of plant efficiency) while maintaining attractive safety feature, reasonable maintenance and fabrication processes. In the reference design, which assumes a surface heat flux of 0.5 MW/m^2, Pb-17Li outlet temperature of 950°C the estimated efficiency is approximately 55 % for a compression ratio of about 1.77. However this concept requires more advanced R&D.

REFERENCES

[1] L. Giancarli et al., Development of the EU water-cooled Pb-17Li blanket, Fus. Eng. Des. 639 (1998) 39-40.

[2] G. Vella, L. Giancarli, E. Oliveri, G. Aiello, Neutronic and photonic analysis of the single box water-cooled lithium lead blanket for a DEMO reactor, Fus. Eng. Des. 41 (1998) 577-582.

[3] Règles de Conception et de Construction des Matériels mécaniques des îlots nucléaires Rapides (RCC-MR), French design and construction rules for fast breeder reactor power stations, ed May 1993, Tome I Volume B: Matériaux de niveau 1.

[4] B. Riou, Compendium of DCRC recommendations for EFR fifth edition up to october 1998, Appendix 1 RCCMR- properties group 18-S revised, European Fast Reactor associates, Novatome, File reference NVPM DC 98 410 RIO/CPA.

[5] F. Toubol, IISDC (ITER Interim Structural design Criteria) Final report (Contract NRT 93-315): Part I, Rapport DMT/95/243, 10/05/95.

[6] F. Toubol, IISDC (ITER Interim Structural design Criteria) Final report (Contract NRT 93-315): Part II, Rapport DMT/95/244, 10/05/95.

[7] P.J. Karditsas, Lifetime and thermal structural performance of various first wall concepts and implications of creep fatigue for design and licensing, Fus. Eng. Des. 39-40 (1988) 575-584.

[8] Y. Poitevin et al. First status of the conceptual design and testing sequence of the WCLL test blanket module for ITER-FEAT, CEA Report, SERMA/LCA/RT/01-2917/A, February 2001.

[9] E. Riegal, personal communication.

REPORTS AND PUBLICATIONS

C. Guerin et al., Water Cooled Pb-17Li DEMO Blanket. A thermo-mechanical study using CASTEM 2000. Structural integrity verification and lifetime determination, CEA Report, DM2S/SEMT/LM2S/ RT/02-009.

H. Golfier, at al, High performances for TAURO blanket system. CEA Report DM2S/SERMA/LCA/ RT/01-3021/A.

A. Li Puma et al., Potential and limits of WCLL alternative blanket concepts, CEA Report, DM2S/SERMA/LCA/RT/ 01-3026/A.

TASK LEADER

Antonella LI PUMA

DEN/DM2S/SERMA/LCA
CEA Saclay
91191 Gif-sur-Yvette Cedex

Tél. : 33 1 69 08 79 76
Fax : 33 1 69 08 99 35

E-mail : alipuma@cea.fr

UT-TBM/MAT-LM/MAG

Task Title : LIQUID METAL CORROSION UNDER MAGNETIC FIELD

INTRODUCTION

Corrosion of materials exposed to liquid metal depends on many parameters such as temperature, hydrodynamics, thermal gradient. In the high magnetic field confining the plasma, the flow of the liquid alloy is characterized by the presence of a core velocity in the central region and various boundary layers in the vicinity of the channel-walls which exhibit a strong velocity gradient.

When the mass transfer between a solid and a liquid is controlled by the velocity gradient at the wall, a modification of the corrosion process may thus be expected in the presence of the magnetic field.

It is important to study this phenomenon and quantify the effect of the field on the corrosion of steels in contact with the Pb-17Li alloy.

For this purpose, it has been proposed to perform corrosion tests in Pb-17Li under magnetic field in flows driven by a rotating disk inside a cavity.

Such a study is of interest because the hydrodynamics in this configuration can be well described by numerical simulation and thus the influence of the field on the mass transfer can be well characterized.

The work already performed has allowed to design the experimental device (a rotating disk inside a cylindrical crucible) and to characterise the liquid hydrodynamics [1], [2], [3]. Here, are presented the first experimental results.

2001 ACTIVITIES

In 2001, corrosion tests of an austenitic steel in liquid Pb-17Li were performed without and under a magnetic field with a flow generated in a cylindrical cavity by a rotating disk whose hydrodynamic was known. Moreover, some hydrodynamic complementary studies and device modifications were performed. This work has been carried out in collaboration with the LEGI laboratory at INPG, Grenoble.

EXPERIMENTAL

The experiment (Figure 1) is based on the fluid motion generated by a rotating disk. The Pb-17Li alloy is contained in a cylindrical crucible made of the austenitic steel, which has been aluminised to prevent it from corrosion.

The rotating disk, which is the specimen to study (austenitic steel), constitutes the upper part of the crucible.

The crucible is heated with an electrical furnace composed of two heating elements allowing to produce a stable temperature gradient between the top (480°C) and the bottom of the crucible (410°C).

The rotation of the disk was obtained by a motor. To avoid rotating the disk (specimen) and Pb-17Li oxidation, argon is continuously delivered at a small flow rate above the top of the crucible. The device can be placed inside the solenoid which allows to impose a longitudinal magnetic field, continuously adjustable between 0 and 0.5 Tesla.

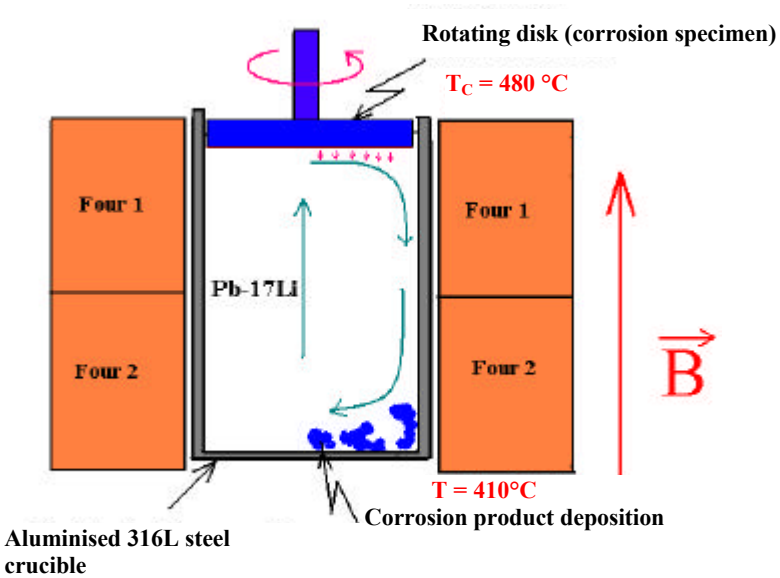

Figure 1 : Presentation of the device

The chemical composition of the austenitic steel disk is: 25.7 Cr, 20 Ni, 1.9 Mn, 0.4 Si, 0.3 Mo. In order to avoid the corrosion of the upper part of the rotating disk, this latter has also been aluminised. But the aluminised coating of the studied rotating disk face in contact with Pb-17Li was mechanically removed.

All the operations required to introduce the rotating disk and the liquid Pb-17Li in the crucible were carried out in a glove box with purified argon gas to prevent air contamination. In a first step, the rotating disk was placed at the bottom of the crucible and all was heated in a furnace at 350°C.

The Pb-17Li was melted in another furnace and the liquid was poured into the crucible.

The space between the crucible and the rotating disk (about 1 mm) is such that it allows the liquid Pb-17Li to flow through. At the end, due to its lower density, the rotating disk float on the liquid Pb-17Li at the top of the crucible. About 800 g of Pb-17Li were introduced into the crucible corresponding to about 600 mm Pb-17Li height.

After cooling, the crucible with rotating disk was introduced into the device in the container closed at its top by a cover supporting the motor. This equipment was sent to the LEGI laboratory and it was put in the furnace to perform the corrosion test without or under magnetic field.

The system was heated and then, the disk velocity and if necessary the magnetic field intensity were adjusted to reach the expected values of the dimensionless parameters R_e, H_a and N.

After test and cooling, the device was sent to CEA and the rotating disk was removed from Pb-17Li. The remaining Pb-17Li adhering to the specimen surface was then removed by immersing the specimen in an alcohol, acetic acid and hydrogen peroxide mixture. Then, the observations to characterise the corrosion were performed.

Results-Discussion

During experiment with Pb-17Li, it is not possible to measure the velocity of the alloy in the cavity. Therefore, a numerical simulation has been carried out to predict the flow configuration in this system.

Last year, ultrasonic velocity measurements were carried out in mercury flows for different Reynolds and Hartmann numbers in order to validate the numerical simulation of the velocity profiles [10].

Due to the bad electric contact between the stainless steel rotating disk and the mercury, the wall cavity was assumed to be insulating and thus the experimental results were compared with the theoretical ones obtained in a complete insulating cavity. In order to confirm definitely the velocity profiles in the case of insulating wall and to take into account the conductivity of the rotating disk, new experiments were performed without and under magnetic field with a conductive copper rotating disk and the same insulating Plexiglas cavity.

The tests show a good agreement between the experimental and numerical results for both the profile and the intensity of the velocity distribution.

The theoretical approach can be used to describe the velocity field in the liquid Pb-17Li alloy for, which experimental measurements cannot be performed, if we assume that electrical conductivity of the aluminised crucible was negligible (in fact it is 100 times less conducting than the corrosion rotating disk).

Figure 2a recall the profiles of three components of the dimensionless velocities $=(U_r,U,U_z)/\Omega R$ along z in the line $r/R = 0.5$ and Figure 2b the profile of the dimensionless azimuthally velocity gradient $\frac{\partial U}{\partial z}\Big/\Omega R$ just under the rotating disk ($z = 0$).

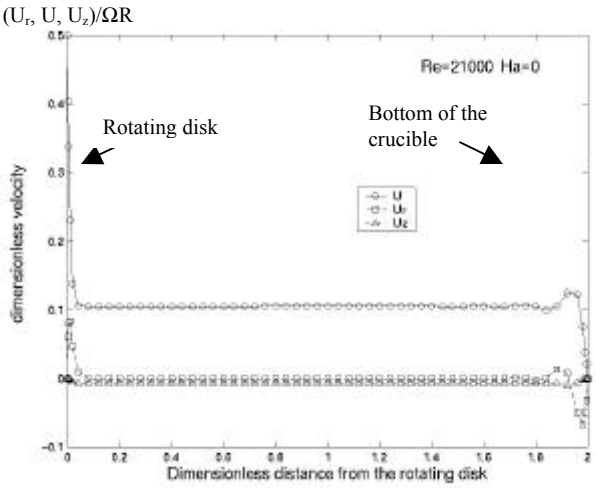

a) Profiles of three components of the dimensionless velocity (U_r, U, U_z) along z on the line $r/R = 0.5$

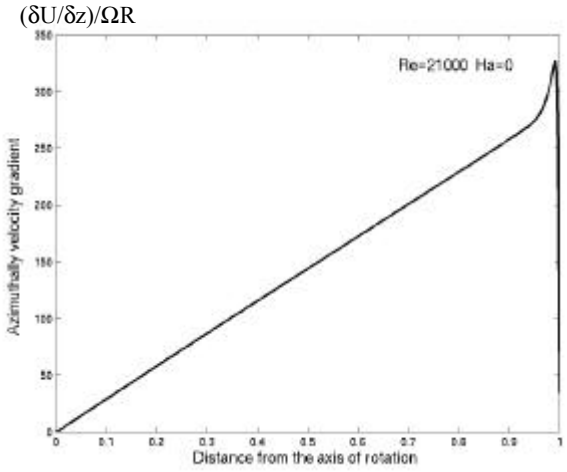

b) Dimensionless azimuthally velocity gradient $\frac{\partial U}{\partial z}\Big/\Omega R$ *along the dimensionless radial coordinate r/R just under the rotating disk ($W = 2.1$ rad.s^{-1}, $R_e = 21000$, $H_a = 0$)*

Figure 2

Figure 3 shows the variations of the corrosion layer thickness at the surface of the rotating disk along the dimensionless radial coordinate r/R after 350 h at 480 °C without magnetic field in liquid Pb-17Li.

It can be seen that between the disk centre and r/R = 0.2, the corrosion layer thickness is nearly constant. In the 0.2-0.8 r/R range, the corrosion layer thickness increases moderately. For r/R higher than 0.8, an accelerate increase of the corrosion layer thickness can be observed.

Cross section micrograph and X ray analyses of the disk show a superficial porous ferritic corrosion layer (Figure 4). These results are qualitatively similar to those obtained for 316L steel in contact with dynamic liquid alloy Pb-17Li at this temperature.

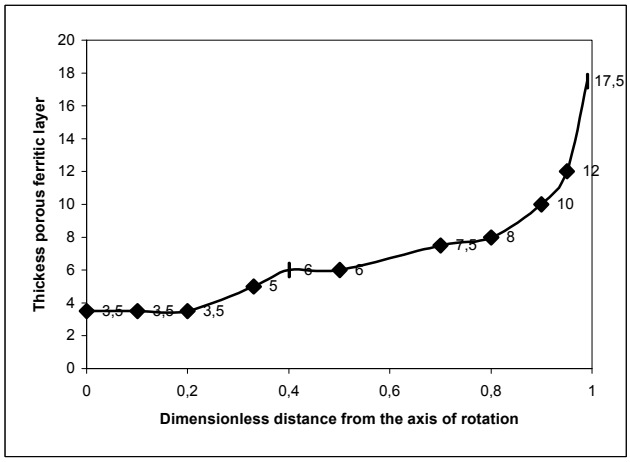

Figure 3 : Thickness of the porous ferritic corrosion layer of the austenitic steel rotating disk along the dimensionless radial coordinate r/R after 350 h at 480 °C without magnetic field in liquid Pb-17Li (W = 2.1 rad.s^{-1}, R_e = 21000, H_a = 0)

If we look at figure 2b, we can see that $\frac{\partial U}{\partial z} \Big/ \Omega R$ at z = 0 between r/R = 0.2 and r/R = 0.8 varies qualitatively in a similar way as the thickness of the corrosion layer.

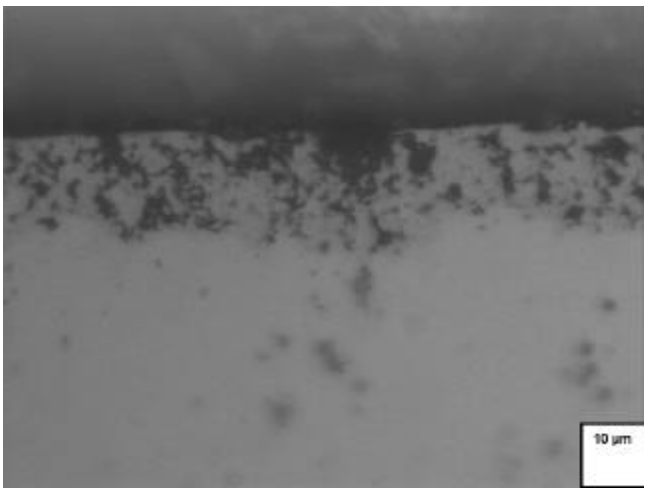

Figure 4 : Cross section micrographs of an austenitic steel rotating disk after 350 h at 480 °C without magnetic field in liquid Pb-17Li, (W = 2.1 rad.s^{-1}, R_e = 21000, H_a = 0)

These first results show that the liquid velocity may affect the corrosion layer thickness of the investigated steel. But more tests are necessary in order to determine the influence of all the velocity components on the thickness variations. Moreover, the ferritic layer thickness results on one hand from the growth by dissolution (mainly preferential Ni dissolution) of the layer and on the other hand from the dissolution of this Fe-Cr layer. It can be expected that the dissolution of the ferritic layer, directly in contact with the liquid can depend on the velocity of this latter (as it has been shown for the Fe-7/12 Cr martensitic steels). But it is not obvious to determine how the liquid velocity influences the growth rate of the ferritic layer because the steel is no longer in direct contact with the liquid but only via the Pb-17Li channel network inside the corrosion ferritic layer.

Moreover, the thermal gradient inside the crucible may influence the thickness of the ferritic layer due to the dissolved species solubility variations with the temperature.

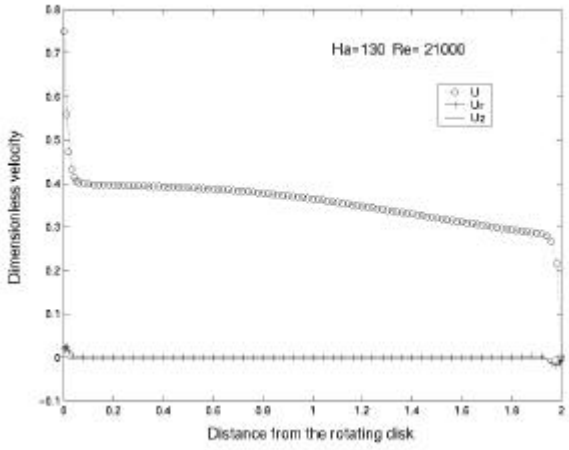

a) Profiles of three components of the dimensionless velocity (U_r, U, U_z) along z on the line r/R = 0.5

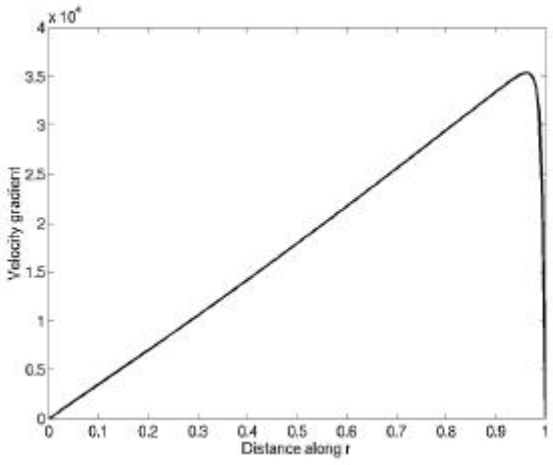

b) Dimensionless azimuthally velocity gradient $\frac{\partial U}{\partial z} \Big/ \Omega R$ *along the dimensionless radial coordinate r/R just under the rotating disk under a magnetic field (W = 2.1 rad.s^{-1}, R_e = 21000, H_a = 130)*

Figure 5

In our experimental conditions with a magnetic field, the electric properties have been taken into account through the conductance ratio k = 0.1. The figures 5a and 5b give respectively the profiles of three components of the dimensionless velocity $(U_r,U,U_z)/\Omega R$ along z on the line r/R = 0.5 and the profile of the dimensionless azimuthally velocity gradient $\frac{\partial U}{\partial z} \Big/ \Omega R$ just under the rotating disk (Z = 0) for our experimental conditions. In this case, the azimuthally velocity *(U)* and azimuthally velocity gradient $\frac{\partial U}{\partial z}$ are higher than without magnetic field but velocities U_r, U_z under magnetic field are lower than without magnetic field.

At the moment, the test carried out under magnetic field does not yield the influence of the magnetic field on the corrosion rate because the aluminised coating at the rotating disk surface studied in contact with Pb-17Li was not completely removed. Only 20 µm of the aluminised coating were removed. However, this test highlights that aluminised coating is not altered by Pb-17Li even if its external part very rich in Al, Cr and O is removed.

CONCLUSION

In order to perform corrosion tests in flowing Pb-17Li under a magnetic field, a specific device has been designed and built. The experiment is now totally operational.

A first test with an austenitic steel without a magnetic field has been performed and shown that the corrosion ferritic layer rate of the austenitic steel by Pb-17Li seems to depend on the hydrodynamics of the flow.

Under a magnetic field, the corrosion test performed with an austenitic steel rotating disk partially de-aluminised highlights that aluminised coating is not altered by Pb-17Li even if its external part very rich in Al, Cr and O is removed.

In 2002, it is planned to perform an experiment with 316L austenitic steel without and under a magnetic field. The same study with an Fe-9cr martensitic steel will also be carried out.

REFERENCES

[1] F. Barbier, A. Alemany and A. Kharicha - Corrosion in moving liquid Pb-17Li under magnetic field: Hydrodynamic modeling in rotating flows - CEA report, RT-SCECF 510 (December 1999).

[2] A. Kharicha, A. Alemany and F. Barbier - Influence of the magnetic field and the conductance ratio on the hydrodynamic of a fluid driven by a rotating disk in a cylindrical enclosure - Proceedings of the 4th International PAMIR Conference on Magnetohydrodynamic at Dawn of Third Millennium, Presqu'île de Giens, France, September 18-22, 2000, 1 (2000) 405-410.

[3] F. Barbier, A. Alemany and A. Kharicha - Hydrodynamics in liquid metal flow driven by a rotating disk under magnetic field: experiment and simulation - CEA report, RT-SCECF 545 (November 2000).

REPORT

Ph. Deloffre, A. Terlain, A. Alemany, A. Kharicha, Corrosion study of an austenitic steel in pb-17li under magnetic field and rotating flow, CEA report, RTSCCME 587 (December 2001)

TASK LEADER

Anne TERLAIN

DEN/DPC/SCCME/LECNA
CEA Saclay
91191 Gif-sur-Yvette Cedex

Tél. : 33 1 69 08 16 18
Fax : 33 1 69 08 15 86

E-mail : anne.terlain@cea.fr

UT-TBM/MAT-LM/Refrac

Task Title : COMPATIBILITY OF REFRACTORY MATERIALS WITH LIQUID ALLOYS

INTRODUCTION

High flux components in a fusion reactor will be submitted to high thermal flux and to high temperatures.

Liquid metals and in particular liquid eutectic Pb-17Li, due to their high conductivity are good candidates for removing such high heat flux.

However, it is well known that liquid metals can be very corrosive at high temperatures.

It is therefore necessary to assess the corrosion behaviour of high flux component materials in contact with liquid metals. As far as the constitutive materials of these components are concerned, tungsten alloys appear to be the best choice.

Concerning the interaction between tungsten material and liquid Pb-17Li, it is expected that dissolution can occur.

When the corrosion proceeds by dissolution, the solubility of the dissolved species has a large influence on the corrosion rate.

Concerning the solubility of W in Pb-17Li, only a few experiments were performed with W-crucibles and no reliable information on the solubility of tungsten in Pb-17Li exist and it is very important to determine.

In a previous study, it has been shown that no corrosion of tungsten occurs at 800°C for 1500 hours in static Pb-17Li [3].

However, in cooling systems, high thermal gradients are present and the liquid metal flows with a significant velocity (a few m s^{-1}). In these conditions, the corrosion could be larger than the observed one in static liquid and isothermal conditions.

Therefore, the work performed in 2001 to characterise the compatibility of tungsten with liquid Pb-17Li consisted in two main parts:

- First to determine the solubility of tungsten in order to delimit the temperature range in which significant dissolution can occur and a large influence of liquid velocity is expected: In a first step we have designed and tested some device to perform such measurements.

- Second, a first attempt has been made by performing a test in a closed container to evaluate if a thermal gradient and a Pb-17Li liquid flow at very low velocity can increase the corrosion of tungsten.

2001 ACTIVITIES

SOLUBILITY MEASUREMENTS IN Pb-17Li LIQUID

Experimental set up for the solubility determinations

The device for the determination of the metallic species solubility in Pb-17Li consists of (figure 1):

- a small crucible made of TZM: its size has been chosen not too large to recover all the Pb-17Li after the experiment in order to analyse it and to avoid any thermal gradient which can induces mass transfer and not too small to put in contact with Pb-17Li a sample with a sufficient surface area to favour the dissolution process. The crucible is closed by a TZM cover on which is fixed a rod used as a sample holder. The cover is welded to the crucible under vacuum by electron beam technique,

- a container made of alloy 601 in which is the crucible. The container is closed by welding (by electron beam technique) a cover made of the same material. The aim of this container avoids the excessive oxidation by air of the TZM crucible during the experiment,

- a furnace at the bottom of which is placed the container.

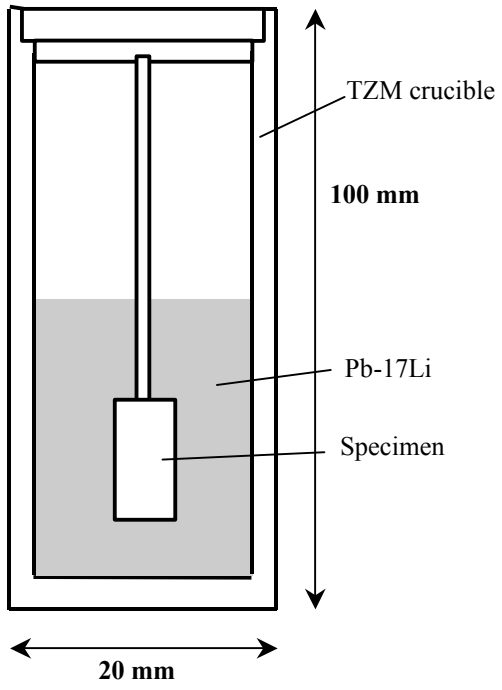

Figure 1 : Schematic drawing of the device for solubility measurements

The procedure to perform a test is the following: the container, the crucible, the cover and the holder are heated up to 500°C for 24 hours under vacuum. Moreover, a specimen is washed with an alcohol, acetone and tetrachloroethylene mixture and after with alcohol. Then, in a glove box with a purified argon atmosphere, the crucible is filled with liquid Pb-17Li. The holder with the sample is immersed in the liquid and the cover is mounted. The crucible is ready to be closed by welding the cover. After, the closed crucible is placed in the container which is also closed by welding. The container is then placed in the furnace and heated up to the experiment temperature. During the test, the container is periodically shacked in order to mix Pb-17Li.

At the end of the experiment, at the test temperature, the container is returned so that the liquid is no more in contact with the specimen. After, the container and the crucible are open. The Pb-17Li ingot is cut in four pieces which are each analysed by Inductively Coupler Plasma Mass Spectrometry (ICP-MS). The Pb-17Li adhering to the specimen surface is removed and then the specimen is weighted in order to determine its weight loss during the experiment.

Solubility tests and results

To test our experimental set up, iron and nickel, materials for which some solubility data exist, have been used. Three tests have been performed: two with iron and the third with nickel. The experimental conditions of the tests are given in table 1.

Table 1 : Experimental conditions of the solubility tests

Material	Duration (hours)	Temperature (°C)	Pb-17Li quantity (g)
Iron	1536	603 ± 3°C°C	39.4
Iron	1339	700 ± 3°C	35.3
Nickel	192	500 ± 3°C	42.1

Table 2 : Iron and nickel concentrations in Pb-17Li after the tests. Comparison with the iron and nickel solubilities in Pb-17Li available in the literature

	Fe – 600°C	Fe – 700°C	Ni –500°C
Concentration of dissolved species from ICP-MS measurements (4 measures)	< 5ppm (4 times)	< 5ppm (3 times) 11 ppm (1 time)	2700, 3800, 2400, 2100
Concentration of dissolved species from weight loss measurements (ppm)	80	292	3420
Solubility from Barker et al [4] (ppm)	59	71	3653
Iron solubility from Borgstedt et al [5] (ppm)	1.1	14	
Iron solubility from Feuerstein et al [1] (ppm)	1.0	1.7	

The experimental results are given in table 2. They are compared to the data available in the literature [1], [4], [5].

First, the results of Pb-17Li analyses, at least for the highest expected concentrations (Fe at 700°C and Ni at 500°C), are dispersed. It shows that it is necessary to analyse all the Pb-17Li.

Moreover, there is a discrepancy between the results obtained from Pb-17Li analyses and from the weight losses of the specimens: In all the cases, the quantities of Fe or Ni dissolved in Pb-17Li deduced from Pb-17Li analyses are smaller than those deduced from specimen weight measurements, especially for Fe. This difference could be due to:

- An attack of the specimens when Pb-17Li adhering to the surface has been removed: as the two Fe specimens have been cleaned in the same Li bath with the same procedure, they should be attacked in the same way. Their weight losses should be approximately the same whereas they differ by a 3.5 factor. Moreover, it has been controlled with Fe and Ni reference specimens, that in the same conditions they are not attacked by the bath used to remove Pb-17Li.

- A loss of Pb-17Li when the ingot was cut in four pieces, this part containing a significant part of dissolved species.

- A preferential deposition of the dissolved species at the crucible wall when Pb-17Li has been frozen. They should have only been partially recover when Pb-17Li has been dissolved for ICP-MS analysis.

It seems probable that all the dissolved species in Pb-17Li have not been taken into account in the analyses. For the future, in order to avoid to cut the Pb-17Li ingot, a system to sample the liquid Pb-17Li at the test temperature will be used.

However, from table 2, we can see that as Fe is concerned, the values we deduced from Pb-17Li analyses are compatible with the solubility values calculated by the equations given in [1] and [5] at 600°C and with [1] at 700°C. On the other hand, the values deduced from the weight loss measurements are closer to those of [4] but nevertheless larger, the difference increasing with the temperature: it could be due to the fact that the equation given by these authors has been deduced from experiments performed at lower temperatures (less than 500°C). As for Ni, the value we obtained differs from 7 % from the Barker's one, what can be considered as in good agreement.

In conclusion, the device we have built for the solubility determination of dissolved species in Pb-17Li, must be adapted in order to sample Pb-17Li in situ at the tested temperature in order to be able to analyse all the recovered Pb-17Li ingot. However, in addition to the Pb-17Li analyses, weight loss measurement of the sample must be performed.

CORROSION OF TUNGSTEN BY Pb-17Li IN THE PRESENCE OF A THERMAL GRADIENT

Experimental

Sintered polycrystalline tungsten has been supplied by Plansee. It has been used as small platelets 10mm x 15mm x1mm with the as received surface state.

Schematic drawings of the experimental device which has been built are given in figure 2. In a molybdenum cylindrical crucible, are located 4 W specimens: 2 at the bottom and 2 at the top. They are fixed with Mo wire to a Mo specimen holder. This crucible is 280 mm high, has a 51 mm diameter and contains 5 kg of Pb-17Li. The crucible is closed by a welded cover.

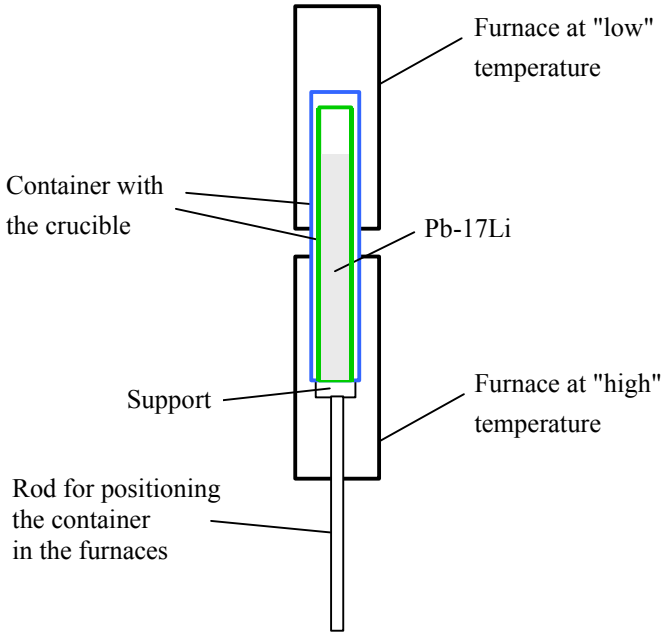

Figure 2 : Schematic view of the experimental device

In order to avoid a catastrophic Mo oxidation, the crucible is inside a nickel base alloy container closed by welding under vacuum a cover at which is fixed a finger for a thermocouple. This finger is between the container and the crucible walls. The container is placed in a thermal gradient obtained by using two furnaces. Two supports maintain the furnaces one above the other. The top of the crucible (including 2 of the specimens) is at the lowest temperature (740°C) and the bottom (including the 2 other specimens) at the highest temperature (800°C). Three baffle plates fixed at the specimen holder allow to reduce the thermal convection movements due to the thermal gradient. It was not possible to estimate the liquid velocity in such a device but it is likely that it was low because the temperature inside the container was easy to control. The container is maintained by a support allowing to move it in the furnaces. The test has been conducted in the following way: the crucible with the specimen holder and the container have been heated up to 500°C under vacuum for 48 hours.

Then, they have been placed in a glove box under an argon atmosphere with an oxygen and water control. The crucible has been filled with liquid Pb-17Li and the holder with the specimens and the baffles has been placed in its right position. After Pb-17Li has frozen, the crucible cover is welded under vacuum by electron beam. Then, the crucible is inserted in the container. This latter is closed under vacuum by welding the upper cover at which is fixed the finger for a thermocouple. Finally, the container is introduced in the furnaces and fixed to its support. During the test, the temperature at the top and bottom of the crucible were respectively 740°C and 800°C with a ± 4°C maximum variation.

The test has been interrupted after 1500 h running due to two consecutive stops of the lower furnace inducing a sharp temperature decrease at the bottom of the container and as a consequence a crack in the weld. The air inlet has led to a local excessive oxidation of the Mo crucible but without rupture of it.

a) **b)**

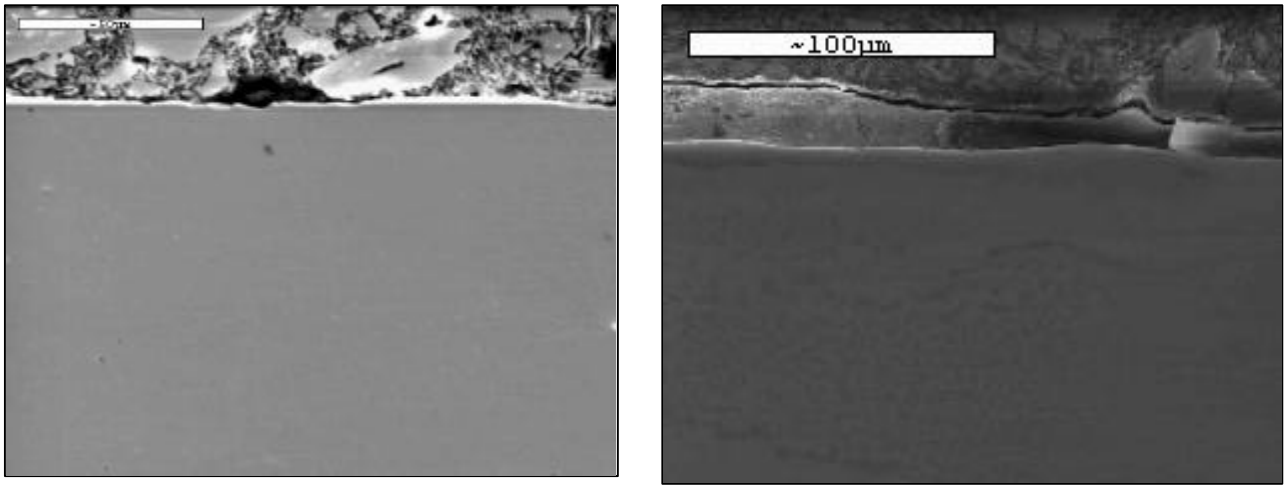

Figure 3 : SEM views of a specimen cross section:
a) Before test - b) After 1500 hours at 800°C in Pb-17Li

Results

As the alcohol, acetic acid and hydrogen peroxide mixture attacks tungsten, therefore weight measurements of the specimens after test are not valuable. Other ways to remove Pb-17Li adhering to a tungsten surface, such as specimen immersion in a nitric acid solution, are being tested.

Specimen cross sections have been polished and observations by means of a Scanning Electron Microscope (SEM) and analyses by Energy Dispersive Spectrometer (EDS) were performed. On figure 3, views of cross sections of the specimen before and after test.

The comparison of the specimen thickness before and after indicates no variation of the thickness during the test with a few tens micrometers uncertainty due to our method of measurement.

No significant change is observed between the specimen cross sections before and after the test. No reaction products are detected at the interface.

Another concern when solids are exposed to molten metals is the penetration of the liquid along the grain boundaries. The X-ray images do not show the presence of the Pb element in the solid or any grooving of the tungsten.

CONCLUSION

Compatibility of tungsten with liquid Pb-17Li has been conducted in 2001following two main guides:

- First, determination of the solubility of tungsten in order to delimit the temperature range in which significant dissolution can occur and therefore a large influence of liquid velocity can appear. In a first step we have designed and tested a device for determining solubility of metallic species in Pb-17Li. We have used Fe and Ni materials to check our procedure. The solubility is obtained by two ways: one from analysis of Pb-17Li after its contact with the metallic sample and a second from the specimen weight loss due to contact with Pb-17Li. It appears a discrepancy between these two methods and the data available in the literature are too scattered to allow to choose the right way. However, it seems that all the dissolved species are not taking into account in the Pb-17Li analysis with our procedure. Our device will be adapted in order to sample Pb-17Li in situ at the test temperature in order to be able to analyse all the recovered Pb-17Li ingot. However, in addition to the Pb-17Li analyses, weight loss measurement of the sample will be performed.

- Second, a first attempt has been made, by performing a test in a closed container, to evaluate if a thermal gradient and a Pb-17Li liquid flow at very low velocity can increase the corrosion of tungsten. A corrosion test of tungsten in anisothermal Pb-17Li (between 740°C and 800°C) at very low velocity has been performed. The observations and analyses of specimen cross-section don't show interaction between tungsten and Pb-17Li and no significant specimen thickness reduction has been observed.

REFERENCES

[1] H. FEUERSTEIN, H. GRÄBNER, J. OSCHINSKI, J. BEYER, S. HORN, L. HÖRNER, K. SANTO, Compatibility of 31 metals alloys and coatings with static Pb-17Li eutectic mixture, Forschungszentrum Karlsruhe, FZKA 5596 (1995).

[2] C. GUMINSKI, Solubility of metals in liquid low melting metals, Z. Metallkunde 81 (1119) 105-110.

[3] F. BARBIER, F. HERBERT, Corrosion Behaviour of W alloy in static liquid Pb-17Li, CEA Report, RT-SCECF (November 2001).

[4] M.G. BARKER, T. SAMPLE, The solubilities of Nickel Manganese and Chromium in Pb-17Li, Fusion Engineering and Design, 14 (1991) 219.

[5] H.U. BORGSTEDT, H. FEUERSTEIN, The solubility of metals in Pb-17Li liquid alloy, J. Nuc. Mat. 191-194 (1992) 988.

[6] G. BENAMATI, P. BUTTOL, V. IMBENI, C. MARTINI and G. PALOMBARINI, Behaviour of materials for accelerator driven systems in stagnant molten lead, J. of Nucl. Mater. 279 (2000) 308-316.

REPORT

T. DUFRENOY, T. DUFRENOY, V. LORENTZ, F. HERBERT, A. TERLAIN, Corrosion of tungsten by Pb-17Li, Rapport CEA RT-SCCME 595 (December 2001)

TASK LEADER

Thierry DUFRENOY

DEN/DPC/SCCME/LECNA
CEA Saclay
91191 Gif-sur-Yvette Cedex

Tél. : 33 1 69 08 16 16
Fax : 33 1 69 08 15 86

E-mail : thierry.dufrenoy@cea.fr

UT-TBM/MAT-LM/SiC

Task Title : COMPATIBILITY OF SiC_f/SiC COMPOSITES WITH LIQUID Pb-17Li

INTRODUCTION

Due to their high thermal conductivity, liquid metals and alloys are very efficient coolants. In the frame of fusion reactor development, the Pb-17Li eutectic alloy (17 at%Li) is the breeding and cooling candidate material for the self-cooled liquid metal breeding blanket (TAURO blanket) [1]. In this blanket concept, the SiC_f/SiC composite is proposed as the structural material. Moreover, with regard to the high heat flux components of fusion reactor, the Pb-17Li alloy is also considered to cool the divertor and SiC_f/SiC flow channel inserts (FCI) could be used as electrical insulators to avoid MHD pressure drops. Therefore, for these applications, the compatibility of the SiC_f/SiC composite with the liquid Pb-17Li alloy environment is a key issue.

A corrosion test of SiC_f/SiC composite with isothermal static liquid Pb-17Li has already been performed at 800°C for 3000 h and no damage was observed [1]. But, The thermal analysis of the TAURO blanket indicates that the breeder maximum temperature is about 900-990°C [2].Therefore, the compatibility of SiC_f/SiC composite with liquid Pb-17Li has to be investigated more in depth, taking into account higher temperatures and Pb-17Li velocity.

2001 ACTIVITIES

In the work performed in 2001, SiC_f/SiC composite specimens were exposed to isothermal static liquid Pb-17Li at 1000 °C up to 2500 h. Due to the high temperature of the test, a specific experimental procedure has been defined, in particular with regard to the container material and the possibility of sampling liquid alloy for chemical analysis (determination of the amount of dissolved elements in Pb-17Li).

Moreover, a specific device has been developed in order to study the influence of the liquid hydrodynamics on the corrosion of the composite. It is presented here together with the known corrosion models.

COMPATIBILITY OF SiCf/SiC COMPOSITE WITH ISOTHERMAL STATIC LIQUID Pb-17Li

Device

A specific experimental device was built (figure 1) and consists of various elements including a furnace (up to 1500°C), a nickel alloy 601 container and a TZM (a molybdenum alloy) test crucible. The furnace is such that it is possible to turn the container upside down inside the heated zone at the tested temperature.

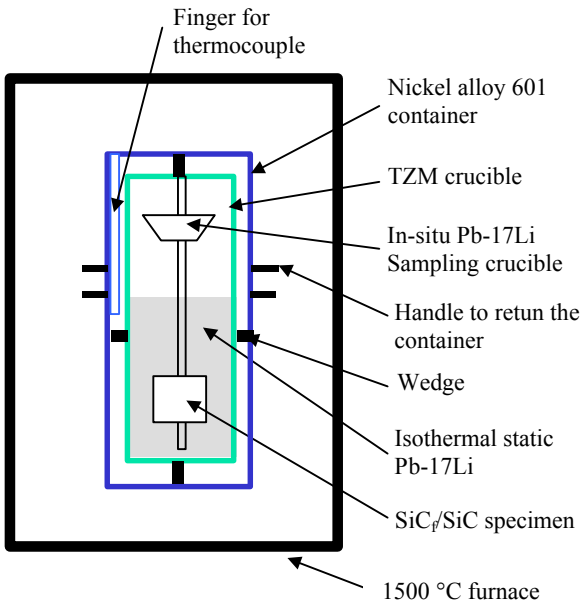

Figure 1 : Schematic drawing of the device

The alloy 601 container protects the TZM crucible from air oxidation during the experiment. The TZM crucible (∅ = 26 mm, h = 150 mm) has a TZM holder welded to the cover. On this holder are fixed at the bottom the sample and at the top a little TZM crucible to in-situ sample some Pb-17Li by turning upside down the container with the crucible.

This small Pb-17Li sample is used to perform a chemical analysis and determine the amount of dissolved elements.

Material

The SiC_f/SiC composite was provided by the SEP. The 3 dimensional composite CERASEP® N3-1 was used.

It is made of SiC fibers (Nicalon NL207) produced by Nippon Carbon and densified by chemical vapour infiltration process (CVI) and covered by a superficial layer.

The chemical composition (wt%) of the SiC fibers is 56.6 Si-31.7C-11.7O. The fiber content in the composite is of 40 % and its porosity is about 10%.

The SiC_f/SiC composite (density > 2.4 $g.cm^{-3}$) was delivered as sheets (25 x 25 x 3 mm^3).

For the corrosion test, the sheet was used as manufactured. Direct and cross-section views are shown in figure 2, where one can see the distribution of the fibers and some porosities.

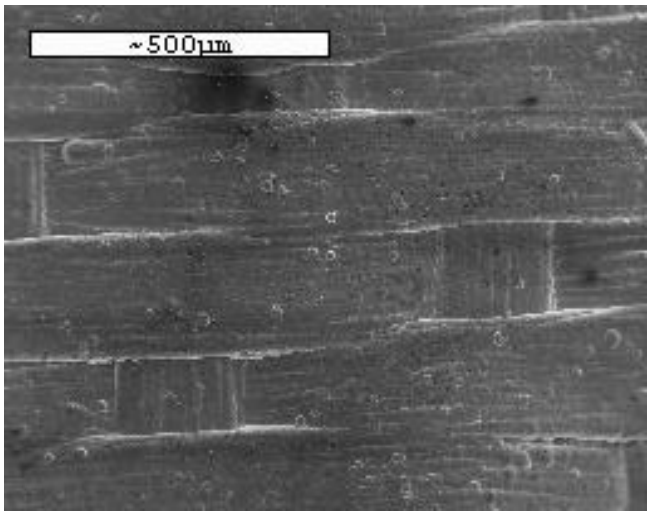

a) Surface of the as received specimen

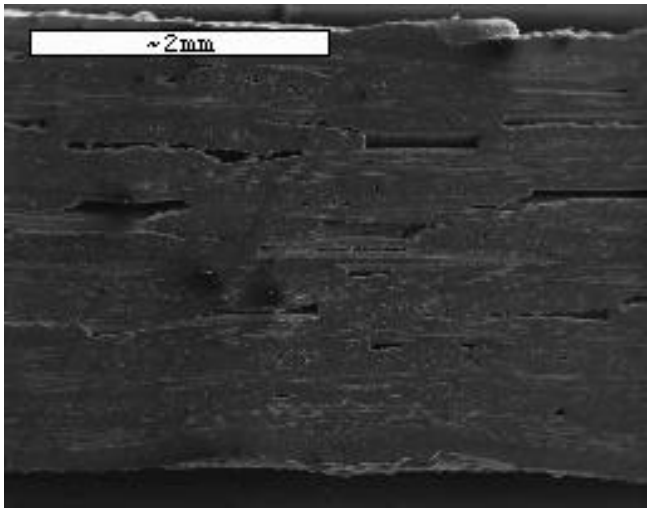

b) Cross section of the as received specimen

Figure 2 : SE images of SiC_f/SiC specimen before contact with liquid Pb-17Li

Experimental procedure

All the operations to introduce the specimen in the crucible with the molten Pb-17Li were carried out in a glove box under a purified argon atmosphere. About 600 g of Pb-17Li were introduced into the TZM crucible. One SiC_f/SiC specimen was mounted onto the specimen holder, which was immersed into the molten alloy in the crucible. After cooling, the TZM crucible with the specimen was welded by electron beam technique. The as-sealed crucible was placed into the alloy 601 container which was subsequently electron beam welded.

The corrosion test was performed at 1000 °C for 2500 h. At the end of the test, the container was turned upside down at 1000 °C (in-situ sample Pb-17Li) and cooled. The container and the crucible were open. In the glove box, the Pb-17Li sample was recovered and the rest of Pb-17Li was melted to recover the SiC_f/SiC specimen. It was not possible to measure the weight variation of the SiC_f/SiC specimen after test because it was not possible to remove the residual Pb-17Li adhering to the surface.

The effects of immersion in Pb-17Li were studied by Scanning Electron Microscopy (SEM) with analysis by Energy Dispersive Spectroscopy (EDS). Cross sections of the specimens were prepared using the usual metallographic techniques (diamond surface polishing).

Chemical analyses of the Pb-17Li alloy after corrosion test were performed by inductively coupled plasma mass spectrometry (ICP-MS).

Results and discussion

Chemical analyses of the Pb-17Li alloy before and after test indicated respectively 13 ± 2 ppm and 12 ± 2 ppm of Si. Taking into account the uncertainties on these values, no variation of the Si content in Pb-17Li has been observed. We can also notice that these values are about the same as the Si content in Pb-17Li after the 3000 h test at 800°C [1]: 8 ppm were measured.

These results suggest that no dissolution has occurred during the test perhaps due to a low Si solubility in Pb-17Li.

On the other hand, analysis of the Pb-17Li alloy showed an increase in the molybdenum concentration: from less than 1 ppm before test, it increased to 30 ± 5 ppm after test. This indicates that a small dissolution of the TZM crucible has occurred during the test.

Geometrical measurements of the SiC_f/SiC specimen thickness performed before test with a micrometer gauge and after test by means of a microscope on a specimen cross section indicate no specimen thickness variations at least higher than a few tens of microns which is the uncertainty on this evaluation by these techniques.

The specimen exposed to Pb-17Li was examined by SEM. The cross section view of the specimen (figure 3) shows neither morphologic evolution nor chemical attack of the composite. No penetration of Pb-17Li can be seen: Pb-17Li is only adhering to the surface.

Therefore, in the tested conditions, no corrosion damage of the SiC_f/SiC composite has been observed. This result has been obtained with a specimen with an as received surface state.

Other tests are in progress on specimens having faces that have been obtained by cutting an as received specimen in several pieces.

CONCEPTION OF A DEVICE TO STUDY THE INFLUENCE OF Pb-17Li VELOCITY ON CORROSION OF SiC_f/SiC COMPOSITE

We will first describe the experimental device we have designed and built and after we will present corrosion models which can be used when the corrosion mechanism is a dissolution controlled by the diffusion of the dissolved species in the liquid.

These models take into account the different specimen geometries.

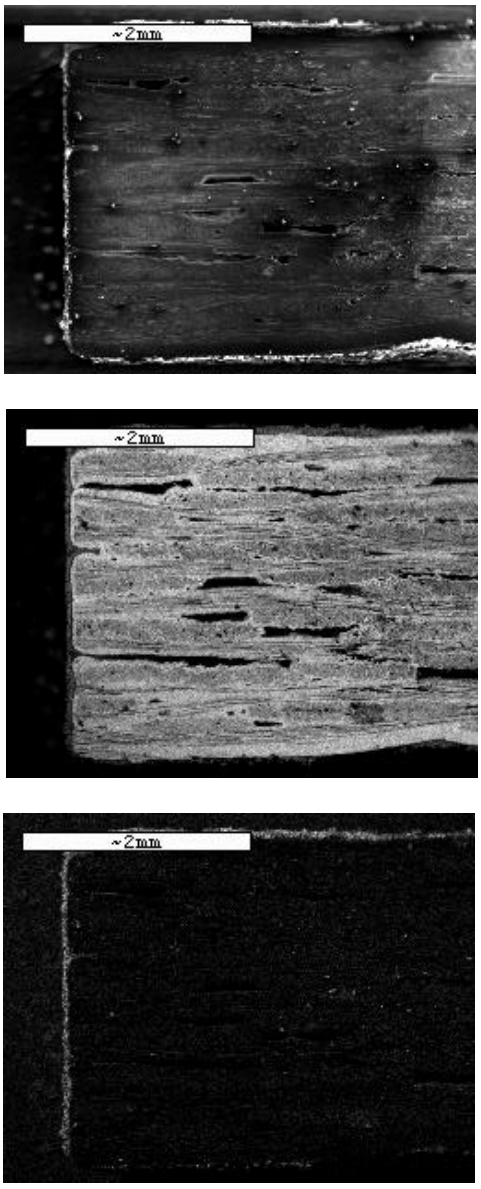

Figure 3 : X-ray images of the cross section of the specimen after 2500 h at 1000 °C in isothermal static liquid Pb-17Li (before removed Pb-17Li)

Device

As SiC_f/SiC composite material is available only as plates, we have considered the rotating disk technique to study the effect of Pb-17Li velocity on corrosion. A special device (figure 4) was designed with the following objectives:

- Temperature of the specimen: at least 600°C.
- Maximal temperature of the rotating system: 30°C.
- Rotational frequency of the specimen: at least 800 revolutions.min^{-1}.

A disk shape SiC_f/SiC specimen (20 mm diameter, 3.3 mm thick) is fixed at the bottom of an about 80 mm long TZM rod.

This rod is screwed to a nickel base alloy rod connected to the rotating system.

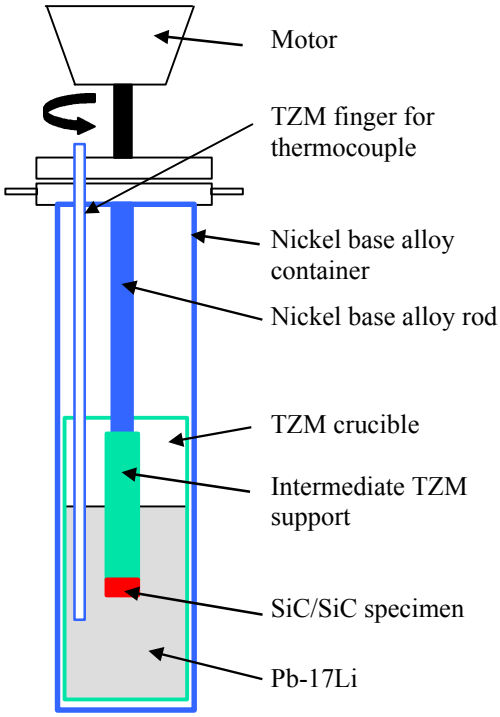

Figure 4 : Schematic diagram of the device to study the corrosion of a SiC_f/SiC rotating disk

All this system is in an airtight nickel base alloy container, which has its bottom part heated by an electrical furnace and its top part cooled by flowing water to maintain a temperature smaller than 35°C near the rotating system.

A TZM crucible containing the liquid Pb-17Li is in the container. It has a 47 mm diameter and is 300 mm high. It contains about 1000 g of Pb-17Li corresponding to an about 80 mm Pb-17Li height. A TZM finger for a thermocouple is fixed to the container cover and immersed in Pb-17Li.

Preliminary tests for very short times have shown that the specimen can be heated up to 800°C with a rotational frequency of 800 rev min^{-1}.

However, complementary tests must be performed to validate the use of this device for a long period.

Mass transfer coefficients when the mass transfer is limited by the dissolved species diffusion in the boundary layer

When dissolution is the corrosion mechanism and when the limiting step of this process is the diffusion of the dissolved species in the boundary layer, the corrosion rate of the specimen in the stationary state can be expressed by:

$$v_{corr} = K\,(C_i - C_0) \qquad \textbf{(1)}$$

With: v_{corr}: corrosion rate (g m^{-2} s^{-1})
K: mass transfer coefficient
C_I: concentration of the dissolved species at the solid /liquid interface
C_0: concentration of the dissolved species in the liquid.

Different expressions for the mass transfer coefficient K, in relation to the experimental conditions (pipe geometry, rotating disk or cylinder specimen…), can be found in the literature.

Case of the pipe geometry

Sannier et al [3] have analysed some results of martensitic steel corrosion at 500°C by Pb-17Li using the following expression for K:

$$K = 0.04\ v^{0.875}\ d_p^{-0.125}\ \nu^{-0.55}\ D^{0.545} \qquad \textbf{(2)}$$

Afterwards, Balbaud et al [4] have analysed the same results using another expression for K [8]:

$$K = 0.0096\ v^{0.86}\ d_p^{-0.087}\ \nu^{-0.530}\ D^{0.670} \qquad \textbf{(3)}$$

With: v: liquid velocity (m s^{-1})
d_p: hydraulical diameter of the pipe
D: diffusion coefficient of the dissolved species (m^2 s^{-1})
ν: kinematic viscosity of the liquid (m^2 s^{-1})

The corrosion results of martensitic steels in Pb-17Li at 500°C, available in the literature, indicate that the corrosion process is a dissolution process limited by the convective diffusion of Fe in Pb-17Li and that the mass transfer coefficient is well represented by equation 3.

Case of a rotating disk

The rotating disk is often used when a laminar flow is required in a large rotating frequency range. In the case of a rotating disk, the mass transfer coefficient is expressed by the Levich equation:

$$K_d = 0.620\ D^{2/3}\ \omega^{1/2}\ \nu^{-1/6} \qquad \textbf{(4)}$$

With: ω: rotating frequency of the specimen (rad s^{-1})

In these conditions, the corrosion rate can be expressed in the following way:

$$v_{corr} = 0.620\ D^{2/3}\ \omega^{1/2}\ \nu^{-1/6}\ C_i \qquad \textbf{(5)}$$

In that case, only a mean corrosion rate can be obtained by this equation. But, for large diameter disk, it can be observed a local corrosion rate, which varies with the distance to the disk centre.

Case of the cylindrical specimen

The cylindrical specimen is generally used for turbulent flow.

Only one empirical expression of K is available and has been obtained by Eisenberg [5] from data on nickel specimen rotating in alkaline solutions:

$$K_E = 0.0487\ d_c^{0.4}\ D^{0.644}\ \omega^{0.70}\ \nu^{-0.344} \qquad \textbf{(6)}$$

with: d_c: external diameter of the rotating specimen

Assuming that the concentration of the dissolved species in the liquid bulk is very low compare to their solubilities, it can therefore be deduced for v_{corr} the following expression:

$$v_{corr} = 0.0487\ d_c^{0.4}\ D^{0.644}\ \omega^{0.70}\ \nu^{-0.344}\ C_s \qquad \textbf{(7)}$$

This equation has been applied to some corrosion data on a rotating iron or martensitic steel cylinder in liquid Pb-17Li. In this case, the corrosion rate varies linearly with $\omega^{0.70}$, as it is expected from the Eisenberg equation, indicating that the hypothesis of a limitation of the dissolution process by the convective diffusion is correct.

In some cases, the mass transfer coefficients for a rotating specimen and for a pipe geometry can be the same. Therefore, the corrosion rate in a pipe geometry can be deduced from the results obtained with a rotating cylinder.

Discussion

When the corrosion proceeds by dissolution, the solubility of the dissolved species has a large influence on the corrosion rate. No reliable information on the solubility of Si in Pb-17Li exist and it will be very important to determine it: in fact, as long as the solubility is very small, no large dissolution of the material is expected and therefore no great influence of the liquid velocity on the dissolution rate will be observed. When corrosion proceeds by other mechanisms than dissolution, other corrosion models have to be developed.

However, depending on the liquid hydrodynamics, other phenomena can take place and lead to damages such as erosion phenomena. To determine the conditions in which they can occur, the hydrodynamics must be well characterized. For that purpose, small devices with a rotating specimen are well suited. Models exist to calculate the liquid velocity distribution near the surface of a rotating specimen and they have already been applied for similar experimental device.

In the present geometry of our SiC_f/SiC rotating disk, two different parts of the specimen will have to be considered: the radial surface (disk surface) and the lateral surface both having nearly the same area. At 800°C, with a rotating frequency of 800 rev min^{-1}, the corresponding Reynolds Number is about 10^5. It corresponds to a turbulent flow regime for the lateral surface and it is near the transition between laminar and turbulent regime for the radial surface. The lateral surface will have to be carefully observed in order to detect if damaging effects due to erosion have taken place or not.

CONCLUSION

The as-manufactured SiC_f/SiC composite (Cerasep® N3-1) was exposed to isothermal static liquid Pb-17Li at 1000 °C up to 2500 h. The experiments indicate that the material has not reacted with the liquid alloy in these experimental conditions. However, complementary tests will be necessary to investigate the liquid penetration in the open porosities.

Taking into account the avaibility of the SiC_f/SiC material, a disk shaped specimen rotating device has been designed and built. First short time tests have shown that it is possible to reach temperature up to 800°C with a specimen rotating frequency of 800 rev min^{-1}.

Different expressions of the mass transfer coefficient have been established from various data obtained with aqueous liquids when the corrosion process is dissolution of the material and when the limiting step of the process is the diffusive transport of the dissolved species. Data on martensitic steel corrosion by Pb-17Li liquid obtained in loops (pipe geometry) or with a rotating cylinder device have shown that the available equations of mass transfer can be applied and used to determine the corrosion rate from one geometry to another. In the case of the SiC_f/SiC composite, no dissolution has been observed in the tested conditions but it is very important to determine the Si solubility because dissolution is very dependent of this latter parameter. As long as solubility is very small no large dissolution and therefore no great influence of the liquid hydrodynamics are expected. However, other damaging effects such as erosion can take place.

REFERENCES

[1] F. Barbier, F. Herbert, Compatibility of SiC/SiC composite with static liquid Pb-17Li alloy, CEA report, DTA/DEN/SCECF/LECNA/00-133 (November 2000).

[2] H. Golfier, G. Aiello and L. Giancarli , Sensitivity analysis to the design parameters of the TAURO blanket, CEA report, SERMA/LCA/RT/99-2694/A (November 1999).

[3] J. Sannier, T. Flament, A. Terlain, Corrosion of martensitic stainless steels in flowing Pb-17 Li, Fusion Technology (1990), 901.

[4] F. Balbaud-Célérier, F. Barbier, Investigation of models to predict the corrosion of steels in flowing liquid lead alloys, Journal of Nuclear Materials, 289 (2001) 227.

[5] M. Eisenberg, C. W. Tobias, C. R. Wilke, Ionic mass transfer and concentration polarization at rotating electrodes, J. Electrochem. Soc., 101 (1954) 306.

REPORT AND PUBLICATION

Ph. Deloffre, A. Terlain, T. Dufrenoy, F. Herbert, V. Lorentz, Compatibility of SiCf/SiC composite with liquid Pb-17Li alloy at high temperature, RT-SCCME 586 (Décembre 2001).

Ph. Deloffre, A. Terlain, F. Herbert , F. Barbier, Compatibility with Pb-17Li of material for fusion reactor, 10th International Conference on Fusion Reactor Materials, 14-19 October 2001, Baden-Baden, Germany.

TASK LEADER

Philippe DELOFFRE

DEN/DPC/SCCME/LECNA
CEA Saclay
91191 Gif-sur-Yvette Cedex

Tél. : 33 1 69 08 16 18
Fax : 33 1 69 08 15 86

E-mail : deloffre.philippe@cea.fr

UT-TBM/MAT-LM/WET

Task Title : WETTING OF MATERIALS BY LIQUID METALS

INTRODUCTION

OBJECTIVE

In a fusion reactor, the plasma-facing region is submitted to a high particle flux generated in the plasma and thus High Heat Flux Components (HHFC) operate in conditions of high thermal stresses, neutron flux and heat flux.

Solutions must be found to extract such high heat fluxes (> 5 MW/m^2), especially on the divertor which is a key component of a fusion power plant. Several divertor concepts based on different coolants are proposed. Liquid metals, in particular Pb-17Li, have been identified as attractive coolants due to their high thermal conductivity.

Concerning the potential materials for the divertor, W-alloys appear to be the best choice as armor material. Several designs were evaluated and whatever the concept, the coolant liquid metal is in contact with W-alloy surfaces and therefore wetting and reactivity of the liquid with the solid have to be known to assess the efficiency and lifetime of the system.

This report is focused on the wetting of tungsten by Pb and Pb-17Li. The work performed in 1999 and 2000 [1], [2] has shown that the sessile drop and transferred drop techniques are well suited to study the wetting of Pb/Fe and Pb/Fe-7Cr systems, even if some specific adaptations were developed.

The wetting of tungsten by Pb and Pb-17Li has been studied by means of these techniques and we report here the results which have been obtained.

2001 ACTIVITIES

EXPERIMENTAL

Sintered polycrystalline tungsten has been supplied by Goodfellows. It has been used as small platelets which have been polished successively with 15 µm, 6 µm, 3 µm and 1 µm size grading diamond paste for 40 minutes each. The mean surface roughness, equal to 10 nm, is very small.

Wetting of tungsten by liquids Pb and Pb-17Li has been studied by means of the sessile drop and the dispensed drop techniques which have already been described elsewhere [1], [2].

We only would like to recall that the dispensed drop technique allows to break the natural oxide films which are present at the liquid and solid surfaces.

RESULTS

Seven experiments have been carried out.

The objective of experiment 1 was to study the wetting of tungsten by liquid Pb. Two drops have been deposited on two different tungsten platelets at 400°C under a high vacuum (10^{-5} Pa).

The observations of the two drops lead to the same result: the contact angle is constant for at least 2000s and is equal to $\vartheta = 106° \pm 2°$. This value is far from the one corresponding to a liquid metal/ solid metal contact but rather indicates that an oxide film covers the tungsten surface.

The aim of experiment 2 was to determine the non wetting/wetting transition of Pb on tungsten.

A Pb drop has been deposited on a tungsten plate under high vacuum at 400°C. The vacuum has been replaced by a He+ 8vol.% H_2 gas mixture and the temperature has been increased up to 804°C and maintained constant for 25 minutes. The temperature has been then quickly increased up to 914°C for a short time (temperature peak) before lowering it.

As the temperature increases, a non wetting ($\vartheta > 90°$) / wetting ($\vartheta < 90°$) transition is observed at 570°C (Figure 1). At higher temperatures ϑ is constant up to 670°C, temperature from which ϑ continuously decreases to reach 60° at 804°C. As the temperature was maintained at 804°C, a second drop was deposited on a tungsten plate and a 60° stationary contact angle value has been observed. During a rapid temperature increase up to 910°C, ϑ seemed to decrease: this effect can be attributed, at least partially, to Pb evaporation because the volume drop decreases. Consequently, it can be considered that the contact angle value of Pb on tungsten at 800°C in an $He+H_2$ atmosphere is $\vartheta = 60°$. This value is in the upper limit range of contact angles corresponding to non reactive metal/metal systems. Tungsten surface observations by means of a scanning electron microscope do not show any trace of reactivity at the 0.1 µm scale.

In experiment 3, the wettability of Pb on tungsten substrate after a high temperature heat treatment has been studied. The aim of this preliminary heat treatment is to modify the surface state of tungsten.

The tungsten substrate was first heated up to 400°C under high vacuum, then heated up again from 400°C to 900°C under a $He+H_2$ atmosphere and finally cooled down to 400°C. Once it was at this temperature, a Pb drop was deposited on its surface.

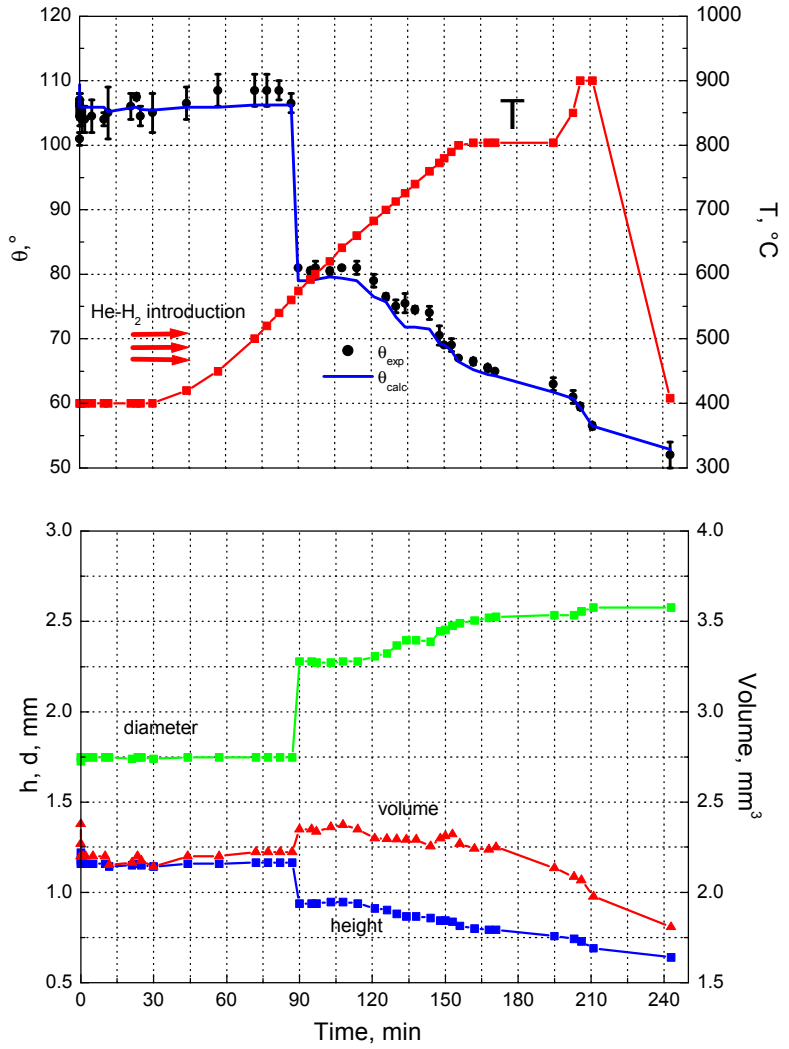

Figure 1 : Experiment 2 : pure Pb wetting curves at 400°C on tungsten under high vacuum as a function of the time and temperature
(J: contact angle, d: diameter of the drop at its basis, h: drop height, V: drop volume)

The initial contact angle value, $\vartheta = 59°$, is basically the same as the value obtained at 800°C under a $He+H_2$ atmosphere in experiment 2 ($\vartheta = 60°$).

However, after 30 seconds, this value increases to 64°±2° (Figure 1), indicating that the tungsten surface is polluted during the experiment.

The experiments 4 and 5 were performed with the same objective than the experiment 3 but under high vacuum.

The tungsten substrate was heated up to 870°C (experiment 4) or 930°C (experiment 5) under high vacuum and then the temperature was lowered to 400°C and three drops were successively deposited in situ on the tungsten surface for each experiment.

The contact angles of the Pb drops observed during experiments 4 and 5 were stationary for 2000s and respectively equal to 70°, 69°, 68° and 70°, 66°, 66°. The increase of the heat treatment temperature from 870°C to 930°C induces practically no change in the contact angle value. The 66° value is not far from those obtained under an $He+H_2$ atmosphere at 800°C ($\vartheta \approx 60°$) and 400°C ($\vartheta = 64°$).

It can be concluded that these values characterise the contact angle of a Pb drop on a metallic (non oxidised) tungsten surface though it is possible or even likely that this surface is polluted by adsorbed oxygen.

With the experiment 6t, it has been tried to evidence the effect of Li in Pb by studying the wetting of tungsten by Pb-17Li.

Three Pb-17Li drops were deposited on a tungsten substrate at 400°C under high vacuum.

The stationary contact angle is reached after less than 40 ms which corresponds to the CCD camera temporary resolution. No contact angle variations have been observed for 6000s. From the observations of the three drops, it has been deduced the following ϑ values: 86°, 88°, 86° which corresponds to a 87°±2° mean value. This value is less by about 20° than the one obtained with Pb on oxidised tungsten.

No trace of reactivity at the 0.1 µm scale is observed. However, near the triple line, it is observed a 50 µm large and ≈ 100 nm deep mark.

This depression near the triple line has been attributed to a lithium oxide film (or a Li-W oxide) formed by Li from the drop and oxygen from the tungsten surface (and to a less extent from oxygen in vapour phase). The semi-quantitative EDAX analysis of oxygen at the tungsten surface shows an oxygen concentration increase near the triple line. Such an oxygen enrichment is not observed in the case of Pb/W system. For this latter system, the few oxygen % measured can be considered as some noise which is relatively important when a light element (O) is analysed in the presence of a heavy element (tungsten).

Why the formation of an oxide film can induce such a depression ? We can imagine that while the oxide film thickness, stresses grow within this latter and finally result in its rupture and detachment. It can also be envisaged that a volatile Li-W oxide is formed.

In the experiment 7, it was investigated the effect of Li on the wetting of Pb on tungsten preliminary deoxidised by a heat treatment at high temperature.

At 400°C under a high vacuum, four Pb-17Li drops were successively put on tungsten first heat treated at 930°C. The contact angle values as a function of the contact time of the drop with tungsten are given in the table 1 (t=0 corresponds to the time when the substrate temperature was stabilised at 400°C).

The first two drops have a contact angle near 50°, which corresponds to 15° less than the contact angle of pure Pb deposited on tungsten in the same conditions. It is observed that the contact angle increases with the time at which the drop has been deposited and reaches for the drop 4 a value near 65°, as in the case of pure Pb.

Table 1 : Contact angles at 400°C under high vacuum of Pb and Pb-17Li drops on tungsten with (deoxidised) and without (oxidised) a first heat treatment at 900°C under high vacuum

	θ(deg)	
Liquid	$W_{oxidised}$	$W_{desoxidised}$
Pb	106 ± 2	67 ± 2
Pb-17Li	87 ± 2	49 ± 3*

As in the case of Pb-17Li/oxidised W system, a depression is observed near the triple line. It is slightly smaller than for oxidised tungsten.

CONCLUSION

The tungsten surface, heated directly at 400°C is not wetted by Pb (107° contact angle), whatever the atmosphere (high vacuum or an $He+H_2$ gas mixture). A non wetting / wetting transition is observed at 570°C in $He+H_2$ atmosphere and leads to a 60° contact angle value up to 800°C.

After a high temperature heat treatment of tungsten under vacuum or $He+H_2$ atmosphere, the contact angle of Pb at 400°C is near 65°.

At 400°C, the addition of 17%at. Li to Pb induces a contact angle decrease of 15° on tungsten with a prior high temperature heat treatment and of 20° without this heat treatment. When the tungsten surface is oxidised, this effect can be explained by the chemisorption of Li (Li has a very high affinity for oxygen) at the Pb/oxide film interface.

When tungsten has been heat treated at high temperature in order to remove at least partially (some chemisorbed oxygen is always present at the surface) the native oxide layer, the ϑ variations could result from the local P_{O2} decrease at the triple line due to the $2\ Li + 1/2\ O_2 \rightarrow Li_2O$ chemical reaction.

No reactivity between Pb (or Pb-17Li) and tungsten oxidised or not has been observed by means of SEM (0.1 µm resolution) even when the tungsten substrate has been heat treated at 900°C.

As for Pb-17Li, and for long time experiences (several thousand seconds) a reaction has been observed outside the drop but near the triple line between Li and oxygen from the surface.

This study shows that to have a good wetting of tungsten by Pb-17Li (contact angle characteristic of a liquid metal/solid metal contact) its is necessary to perform a preliminary heat treatment of tungsten at high temperature and under vacuum or an atmosphere with a very low oxygen activity.

It is different from what it has been observed with Fe and Fe-7Cr: the Li activity in the Pb-17Li liquid is sufficient to modify or even suppress the native oxide film at the surface of these materials and therefore to insure a good wetting.

REFERENCES

[1] P. PROTSENKO, N. EUSTATHOPOULOS, A.TERLAIN - Wetting of materials by liquid lead, CEA Report, RT SCECF 518 (November1999).

[2] P. PROTSENKO, M. JEYMOND, N. EUSTATHOPOULOS, A.TERLAIN - Wetting and reactivity in the Pb-17Li/Fe and Pb-17Li/Fe-7Cr systems, CEA Report, RT SCECF 550 (November 2000).

REPORT

P. PROTSENKO, M. JEYMOND, N. EUSTATHOPOULOS, A. TERLAIN - Wetting of tungsten by Pb and Pb-17Li, CEA Report, RT SCCME 588 (December 2001).

TASK LEADER

Anne TERLAIN

DEN/DPC/SCCME/LECNA
CEA Saclay
91191 Gif-sur-Yvette Cedex

Tél. : 33 1 69 08 16 18
Fax : 33 1 69 08 15 86

E-mail : anne.terlain@cea.fr